國立交通大學

統計學研究所

碩士論文

利用藥物化學特徵和統計學習建構藥物負向事件預測模型

Prediction for Adverse Drug Events by Chemical Descriptors and Statistical Learning

研 究 生：吳宜靜

指導教授：盧鴻興 教授

中華名國一百零一年六月

利用藥物化學特徵和統計學習建構藥物負向事件預測模型

Prediction for Adverse Drug Events by Chemical Descriptors and Statistical Learning

研究生：吳宜靜　　Student：Yi-Jing Wu

指導教授：盧鴻興 博士　　Advisor：Dr. Henry Horng-Shing Lu

國 立 交 通 大 學

統 計 學 研 究 所

碩　士　論　文

A Thesis

Submitted to Institute of Statistics

College of Science

National Chiao Tung University

In Partial Fulfillment of the Requirements

For the Degree of

Master

in

Statistics

June 2012

Hsinchu, Taiwan, Republic of China

中華民國一百零一年六月

利用藥物化學特徵和統計學習建構藥物負向事件預測模型

研究生：吳宜靜　　指導教授：盧鴻興 教授

國立交通大學統計學研究所

摘　要

當藥物成分進入人體後，產生複雜的擾動效應稱為藥效。藥效可分為主要治療藥效和額外的效果，而藥物不良反應事件是額外效果的一部分。每個藥物成分都是一種化合物，由其化學式可以得到化學資訊特徵。基於藥物在人體系統中產生的生物擾動與其化學結構有關的假設，我們檢視上市藥物的藥物不良反應事件與其化學資訊特徵之間的關聯。在本研究中，我們使用決策樹方法指認出與 1384 個藥物不良反應事件的相關化學資訊特徵，並設計一套自動分析流程。針對我們選定的 35 個有興趣的藥物不良反應事件可以得到模型十折交叉驗證正確率高於 80%，例如：糖尿病（87.1%），急性腎功能衰竭（91.0%）和腎功能不全（94.6%）。

Prediction for Adverse Drug Events by Chemical Descriptors and Statistical Learning

Student：Yi-Jing Wu

Advisor：Dr. Henry Horng-Shing Lu

Institute of Statistics

National Chiao Tung University

Hsinchu, Taiwan

Abstract

In addition to the medicine treatment effect, side effects are complex undesired phenomena due to the bio-activity of pharmaceutical compound. For each compound, the chemistry informatics can delineate its intrinsic chemical formula into chemistry informatics features. Based on the assumption that the chemical structure is critical to the biological perturbation in the human system, we investigate different adverse drug events with associated chemistry informatics features of marketed drugs. In this research, we identify 1,384 ADEs with corresponding associated chemistry informatics features by decision tree. With an automatic analysis workflow, we can obtain a concordant drug subset with satisfying 10-fold cross-validation accuracy. The accuracy of selected 35 ADEs in the test experiment is higher than 80%. For example, there are three ADEs of interest and their accuracy: Diabetes Mellitus (0.871), Renal Failure Acute (0. 910) and Renal Impairment (0. 946).

誌　　謝

兩年碩士生涯雖然短暫但是收穫卻不少。這兩年能夠有所成果，首先必須感謝我的指導教授—盧鴻興教授，感謝您在論文上、課業上以及生活上不厭其煩地指導與幫助。其次，感謝口試委員許文郁教授、王秀瑛教授以及謝文萍教授辛苦審查，並給指導和建議使論文更加完善。

也必須感謝交大統計所所有的老師、郭姐和劉小姐，除了提供我們良好的學習環境，讓我在碩士兩年學到了許多知識外，平日給予的關懷與幫助讓我們能夠無憂無慮地學習。

再來要感謝所有交大統計所 99 級的同學們，因為有你們的一同努力與分享，在兩年碩士生活中一起歡笑一起哭，讓我這兩年的學習過程多了更多的調味劑。

最後，我要感謝我的家人，謝謝他們在我學習生涯中無論是遇到挫折或是難過都給予我百分百的支持，使我能夠在學習過程中完全無後顧之憂。

吳宜靜　　謹誌于

國立交通大學統計學研究所

中華名國一百零一年六月

Contents

List of Figures

List of Tables

List of Notation and Abbreviations

Abbreviation	Terminology
ADE	Adverse Drug Event
FDA	Food and Drug Administration
AERS	Adverse Event Reporting System
HIV	
MedDRA	Medical Dictionary for Regulatory Activities
CDK	Chemistry Development Kit
ISR	
CV	Cross-Validation
IDT	Initial Decision Tree
SGDT	Similarity Guide Decision Tree

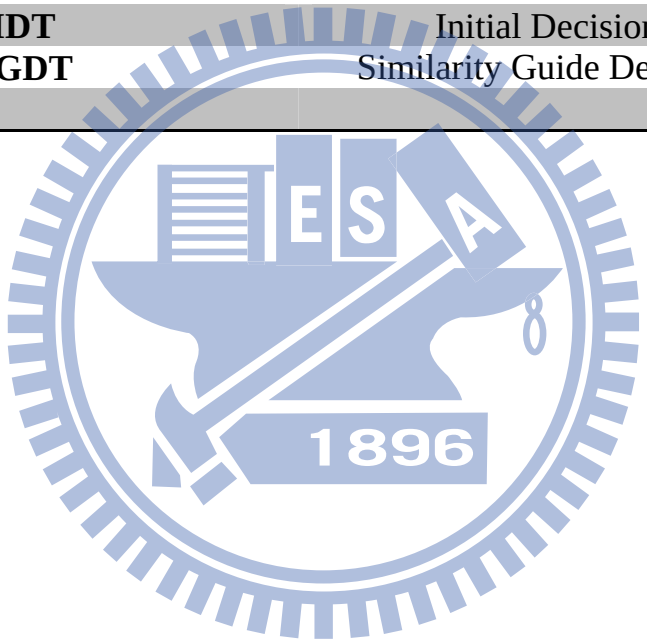

1. Introduction

1.1. Background

Modern medicine provides more sanative treatment due to the improvement in pharmaceutical equipment. However, this achievement gives rise to some potential danger in drug usage. An UK national analysis indicates that each year adverse drug reactions are responsible for 5% hospital admission which cost approximately 0.5 billion pounds per year. Besides, fatal adverse drug reactions account for approximately 3% of all death in the general population [1]. The research of drug monitoring reveals that adverse drug reactions can turn into social cost.

The market drugs are required to show indications on the package or in the instructions leaflet. If the pharmacists want drugs to be approved for sale, they must report clinical results to the Food and Drug Administration (FDA). The clinical trial should control some of the confounding variable effect, such as, age, gender, or changes in hormone level. Subjects of the clinical trial are randomly assigned into two groups in double blind procedure. Subjects in the experiment group are given the drug, and the others in control group are receiving placebo. The main purpose of the clinical trial is to confirm the principal treatment effect and the secondary purpose is to find possible adverse reactions.

Side effect is a usual term for the negative consequence of adverse drug reaction. And the medical record about side effect or adverse drug reaction is a report of adverse drug event (ADE). Since 2004, the FDA set up a Pharmacovigilance system to collect the negative consequence of market drug reports from the health professionals and patients. All the information about adverse drug events is recorded in adverse effect reporting system (AERS).

Besides, FDA is asked to do some analysis related to adverse drug effects and provides these results to the public. If FDA find some adverse drug effects are not listed on the package or in the instructions leaflet, FDA will ask pharmaceutical company to provide inspection reports, and may have three possible procedures:

i. The pharmaceutical company should list “new” adverse effects on the package or in the instructions leaflet.

ii. The pharmaceutical company should indicate the eligibility of patients on the package or in the instructions leaflet.

iii. In the worst case, the drugs will be removed from the shelves.

We notice the importance to investigate adverse drug events. In consequence, we search the literatures about the hidden risk of approval drugs and start the following research in this thesis for the drug safety issue.

“The occurrence of drug side effect” is one of the most popular topics in the field of modern medicine. Nowadays, experts and scholars have proposed the possible causes of adverse drug effects into four categories [2]:

(1) Adverse events related to the therapeutic effects of drugs:

The first category of adverse drug effects occurs when the therapeutic effects have other additional negative consequences. Generally, these drug side effects occur as the concentration of medication is higher than required for beneficial drug effects. The drug metabolism variation is related to several enzyme activities. The required dose of drug might be different among people due to the individual genomic factor.

In general case, drugs are catalyzed by some enzymes in the liver. The drug effects in human system will become vanished as the time passed. After enzymatic reaction, the catalyzed drug waste will be transported to the kidney and then excreted into urine. However, the enzyme activity is diverse among people. If the enzyme activity is higher; that is, the rate of metabolism increases, then the time of drugs functioning in vivo is shorter than average. Therefore, it can result in less treatment effect. However, if the enzyme activity is lower; that is, the rate of metabolism decreases, then the time of drugs

functioning in vivo is longer than average. Thus, it results in higher treatment effect and adverse drug effect (Figure 1.1).

For example, anticoagulant (Warfarin) is to inhibit vitamin K epoxide reductase (VKOR). However, if the concentration of medication in vivo is higher than that required for beneficial drug effect, this will result in over-inhibited clotting, which may lead to hemorrhagic stroke.

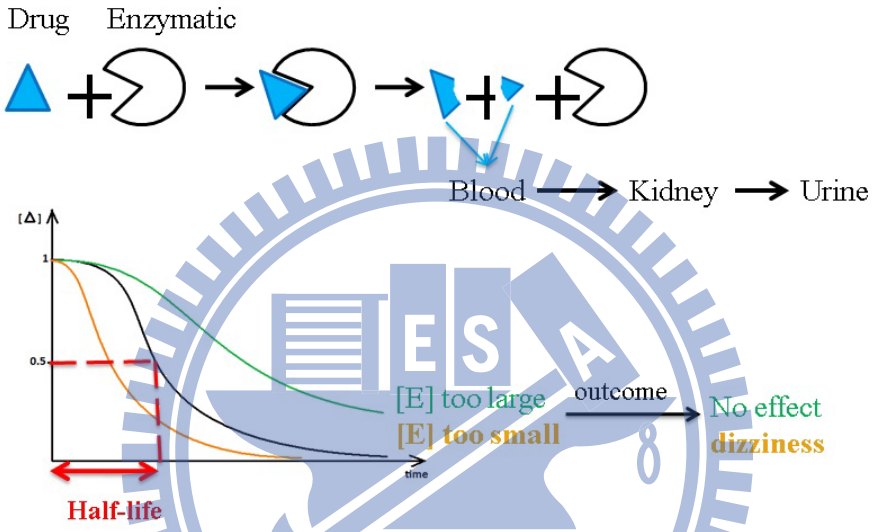

Figure 1.1: This figure shows that the drug-metabolizing capability. The black curve denotes the general case, the orange curve denotes the lower enzyme activity, and the green curve denotes the higher enzyme activity.

(2) The therapeutic drug targets existing in multiple cell and tissue types:

The second category of adverse drug events occurs when a drug's target (a specific protein) serves multiple functions in different tissues of the body.

For illustration, given three different tissues, A, B, and C, all of them contain two proteins x and y and their corresponding expression level in normal case. If the expression of protein y in tissue C is higher, tissue C becomes cancerous. And the design a chemical compound, which can hydrolyze protein y or block its bio-activity, aims to shrink the function of y in cancerous tissue C. Under this consideration, the anti-cancer

drug inhibits protein y in tissue C, as well as in tissue A and tissue B. Thus, it causes the function of protein y in tissue A and tissue B becomes less than normal, which we consider as a possible scenario of the cause of adverse drug effect (Figure 1.2).

In real case, Morphine is designed to achieve analgesia by binding with μ-opioid receptors in the brain. However, it may affect the same type of opiate receptors in the intestines, which inhibits peristalsis.

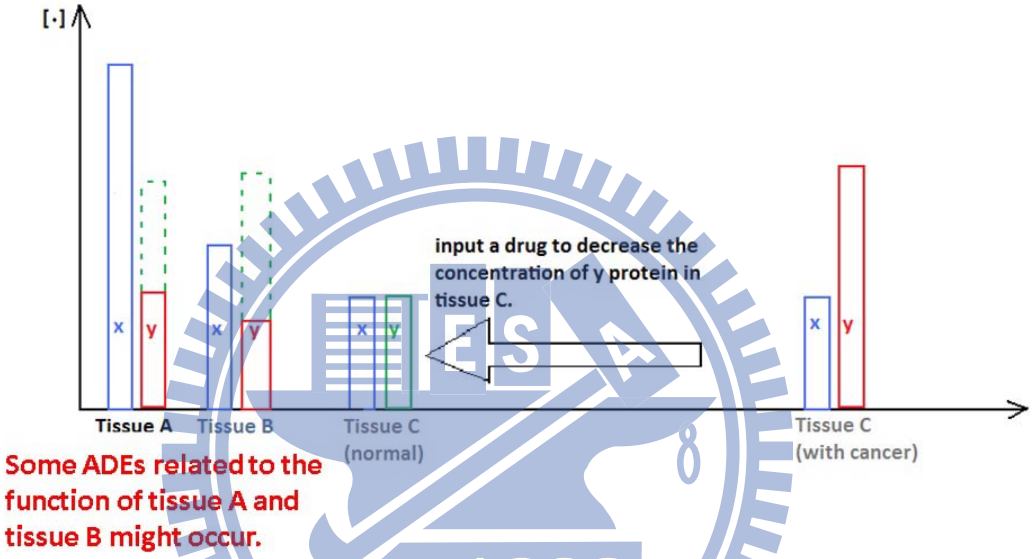

Figure 1.2: Initially, we want to regulate tissue C by inputting an anti-cancer drug. The function of the anti-cancer drug inhibits the protein y in tissue C. It as well as inhibits protein y in tissue A and tissue B at the same time. Thus, ADEs will be resulted.

(3) Adverse drug events mediated by off-targets of a drug:

The third category of adverse drug events occurs when one drug interferes with other unexpected proteins or pathways. This category is different from the second category. The former considers that one drug affects single protein among more than one tissue. The protein or pathway that the drug intends to function is called “drug-target”, and the drug affecting unexpected proteins or pathway is called “off-target”. It should be mentioned that the off-target will be another scenario of side effects.

For example, Delavirdine, HIV reverse transcriptase inhibitor, not only inhibits the reverse transcriptase of HIV, but also interacts with histamine H4 receptor, which will result in severe rash.

(4) Mixture of several drug side effects:

The fourth category is a mixture of the adverse drug events in above three categories. For example, Domperidone is designed to promote gastrointestinal motility, but also inhibits the human *Ether-à-go-go*-Related Gene K+ channels (HERG K+ channels), which will result in cardiac arrhythmias.

1.2. Literature Review

Hammann *et.al* has reported a set of ADE prediction models with high prediction accuracy in chemistry and pharmaceutical field [3]. This research has been published in a journal of nature group (Clinical Pharmacology & Therapeutics, with impact factor 6.961*). In this article, they state the relation between the drug chemical features and the ADE as the perturbed "human body functioning mechanism".

In the study, they used decision tree to establish the association between drugs' chemical features and ADEs. They analyzed four kinds of ADEs, allergy, central nervous system (CNS), hepatotoxicity and nephrotoxicity. The importance of drug chemical descriptors can be revealed, because the proposed the four ADE prediction models achieved high prediction accuracy rate, 89.74%, 90.22%, 88.68%, and 78.94%, respectively.

However, in the four ADE models, only few market drugs are considered. The number of market drugs of each ADE is 164, 286, 334, and 338 respectively. In addition, they do not clearly explain how to select the "drug subset" from the initial drug set (507 drugs) for each ADE by using the reporting frequency threshold.

1.3. Purpose of Research

Although a majority of patients can reach the most of efficacy after taking medicine, still some patients will experience some particular side effects or adverse events. Furthermore, some side effects will result in serious injury in patients, such as hepatotoxicity and rhabdomyolysis which lead to acute cardiac death. In our study, we want to predict more ADEs based on Adverse Event Reporting System (AERS) and more market drugs. Our goals of the present study are to expand the chemical descriptors database, and to develop an automatic concordant analysis to obtain an explainable drug subset in the feature space. In this research, we aim to determine the chemical, physical, and structural properties of compounds that are associated with certain ADE.

The impact of this research is profound, for patients' safety related to prescription medicine is an important issue in public health. In this study, we propose a new approach for investigate more adverse drug events of market drugs based on the current chemistry informatics. The new approach can help researchers and clinicians to have an estimated ADE propensity for a new designed drug. (Figure 1.3)

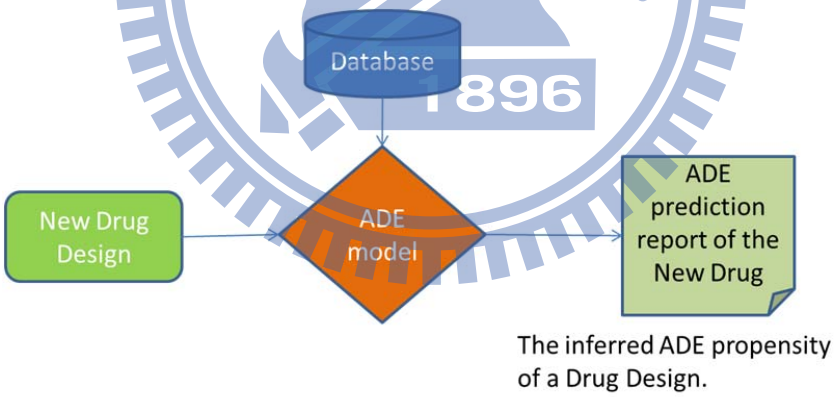

Figure 1.3: The main purpose of our research is to build a set of ADE prediction models.

2. Method

2.1. Materials

Adverse drug report

AERS is a computerized information database [4]. It is a monitoring program designed to support the safety of drugs on the shelf. When we download the AERS database, we can get two kinds of formats, one is SGML and the other is ASCII. ASCII data files contain seven different types of folders and each folder contains the relative information of adverse drug events. For example, the “REAC” folder contains several data files (notated: REACyyQq.txt), and each file contains the adverse events of each drug. Table 2.1 lists each folder in detail. We use the ASCII data files which are collected from the first quarter of 2004 to the fourth quarter of 2010 to get the number of reports for each drug and each ADE.

In order to get the ADE list, we download the pt.asc file from the Medical Dictionary for Regulatory Activities (MedDRA). MedDRA is a medical dictionary and is used to classify the information about adverse event associated with the use of biopharmaceuticals and other medical products. Because the drugs’ names which recorded in the AERS database are not always generic names, we need a comprehensive list of drugs’ names. Therefore, we find the corresponded generic name, brand names, and synonyms of each approval drug in the DrugBank database. The DrugBank database combines the complete information about drug target and detailed drug [5].

Table 2.1: In the ASCII format, file names have the format <file-descriptor>yyQq, where <file-descriptor> is a 4-letter abbreviation of the data source, "yy" is a 2-digit identifier for the year, "Q" stands for the quarter, and "q" is a 1-digit identifier for the ordinal of quarter. As an example, the ASCII Reaction file for the 4th quarter of 2004 is represented as DEAC04Q4.txt.

File names	Description
DEMOyyQq.txt (DEMOGRAPHIC file)	Contains patient demographic and administrative information, a single record for each event report.
DRUGyyQq.txt (DRUG file)	Contains drug/biologic information for as many medications as were reported for the event. (1 or more per event)
REACyyQq.txt (REACTION file)	Contains all "Medical Dictionary for Regulatory Activities" (MedDRA) term coded for the adverse event (1 or more).
QUTyyQq.txt (OUTCOME file)	Contains patient outcomes for the event (0 or more).
RPSRyyQq.txt (REPORT SOURCE file)	Contains report sources for event (0 or more).
THERyyQq.txt (THERAPY dates file)	Contains drug therapy start dates and end dates for the reported drugs (0 or more per drug per event).
INDIyyQq.txt (INDICATIONS for us file)	Contains all MedDRA terms codes for the indications for use (diagnoses) for the reported drugs (0 or more per drug per event)

Chemical descriptor

Chemical descriptors are numerical attributes for computing a chemical compound's structure. These include elemental analysis, charge analysis, geometry, partitioning coefficient and other characteristics. Some of chemical descriptors include large information about measures of molecular connectivity, connectivity indexes.

There are two sources to get chemical descriptors, one is ChemAxon, and the other is Chemistry Development Kit (CDK). ChemAxon is a providing chemical software development platform for characterizing chemical structures and substructures [6]. Additional chemical descriptors are calculated by using the open-source cheminformatics package, CDK [7]. This package allows users to access functionality by a Java framework for cheminformatics including load molecules, evaluate fingerprints, and calculate molecular descriptors, etc.

A list of chemical descriptors used in our study is given in Table 2.2. It is worth noting that for some chemical descriptors they do not have only one chemical feature. A comprehensive list of chemical features used in this study is given in Appendix A.

Table 2.2: This is a comprehensive list of chemical descriptors we used in this study. There are two sources of chemical descriptors, one is ChemAxon and the other is CDK.

Software	**ChemAxon**	**CDK**
User Interface	Excel; JAVA	R
Chemical Descriptors	• Elemental Analysis • Charge • Conformation • Geometry • Isomers • Markush Enumerations • Partitioning • Predictor • Protonation • Other	• Electronic • Protein • Topological • Geometrical • Constitutional • Hybrid

2.2. Data Analysis

Pre-processing work

The purpose of our study is to explain the association between drugs' chemical features and ADEs through a set of ADE prediction models. In order to build an ADE prediction model, we need to get the risk-index (High-risk/Low-risk) for each drug. We believe that it exist the relation between drug-risk and the number of ADE reports. In order to know the number of reports for every drug and every ADE, we use the ASCII data files to build the DRUG-ADE table. In this table, each column shows what kind of ADEs, each row shows what kind of drugs, and each cell denotes the number of reports for each drug and each ADE. Figure 2.1 shows the flow chart of the pre-processing work and Table 2.3 introduces these files used in the work. The following are the procedure of the pre-processing work:

(1) Define the columns and rows of DRUG-ADE table:

We work for the union of the adverse reaction names in the REACyyQq.txt and the adverse reaction names in pt.asc file. The union becomes the columns of DRUG-ADE table. Then, we use the Drug_ATC.txt data file to get the generic name of each drug. The drugs' generic names become the rows of DRUG-ADE table.

(2) The reported code-ISR for each quarter and each year:

ISR denotes the number uniquely representing an adverse event report and is the primary link field between data files. We work for the union of the ISR in DRUGyyQq.txt data file and the ISR in the REACyyQq.txt data file. The file name of output file is called ISRyyQq.txt.

(3) Get used drugs' codes of each ISR for each drug's role in event:

There are four types of drug's reported role in event, primary suspect drug (PS), secondary suspect drug (SS), concomitant (C), and interacting (I). For each type of drug's reported role, we use DRUGyyQq.txt and the rows of DRUG-ADE table to list the code of used drug for each ISR. (The details of each output data are: ISR ij$k…, where i, j, and k denotes the i^{th}, j^{th}, and k^{th} rows in the Drug-ADE table; "$" is a delimiter.)

(4) Get the codes of adverse events for each ISR, where the code represents which column adverse events is in the DRUG-ADE table:

For each ISR in the REACyyQq.txt, we can get the corresponded adverse reactions, and then we use the columns of DRUG-ADE table to get which column matches the adverse reaction. The output file is called "Out_REACyyQq.txt" which records the code of adverse reactions for each ISR.

(5) Get the number of reports for each drug and each ADE:

Use these output files in step (2), (3), and (4) to compute the number of adverse reports for each drug and each ADE

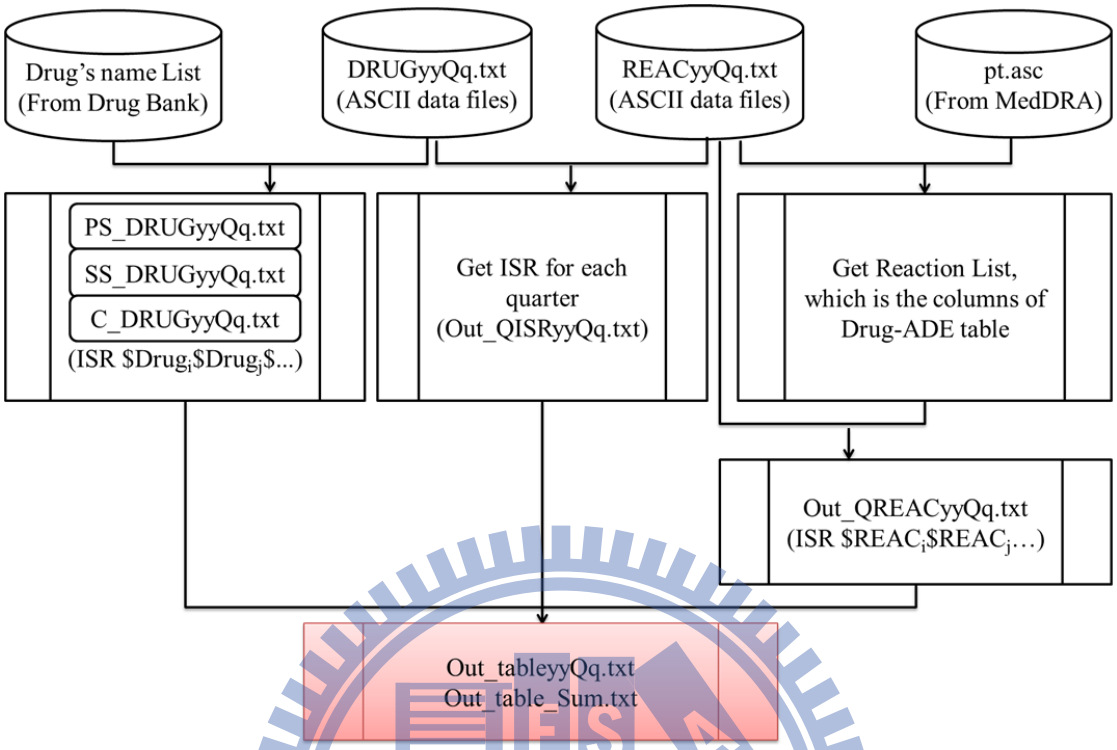

Figure2.1: This is a flow chart about pre-processing work. The finally output file is the DRUG-ADE table. Each cell of the table denotes the number of reports per drug per ADE.

Table 2.3(a): This data file contains 1,411 approval drugs' information. We can download these information in the DrugBank.

Drug_ATC.txt	
DB Name	Accession number of drug in Drug Bank.
Generic Name	Drug's name.
ATC Code	The Anatomical Therapeutic Chemical Classification System is used for the classification of drugs

Table 2.3(b): The DRUGyyQq.TXT contains drug/biologic information about medications reported for the event (1 or more per event).

DRUGyyQq.txt	
Name	Description
ISR	The number uniquely identifies an adverse event report and is the primary link field between data files.
ROLE_COD	It is a code for drug's reported role in event. (See table below.) CODE / MEANING_TEXT PS / Primary Suspect Drug SS / Secondary Suspect Drug C / Concomitant I / Interacting
DRUGNAME	Name of medicinal product. If a "Valid Trade Name" is populated for this ISR, then DRUGNAME = Valid Trade Name; If not, then DRUGNAME = "Verbatim" name, exactly as entered on the report. For the great majority of reports, there is a "Valid Trade Name."

Table 2.3(c): The REACyyQq.TXT contains all MedDRA term coded for the adverse event (1 or more).

REACyyQq.txt	
Name	Description
ISR	The number uniquely identifies an adverse event report and is the primary link field between data files.
PT	"Preferred Term" is a level of medical terminology in the Medical Dictionary for Regulatory Activities (MedDRA) to, which describe the adverse event.

Risk-index

After the pre-processing work, we want to give a risk-index to each drug and each ADE by the DRUG-ADE table. In order to determine the risk-index for each drug and each ADE, we define some criteria:

If the number of reports is zero, then we define that the risk-index is low risk. Otherwise, we compare the average ADE reports with a cut value. If the average ADE repots is larger than the cut value, we define the ADE as high risk. Otherwise, the ADE is not deterministic.

$$Drug\ Risk \begin{cases} low-risk & \frac{The\ number\ of\ the\ ADE\ report\ for\ the\ drug}{The\ total\ number\ of\ the\ drug\ is\ complained} = 0. \\ high-risk & \frac{The\ number\ of\ the\ ADE\ report\ for\ the\ drug}{The\ total\ number\ of\ the\ drug\ is\ complained} \geq cut\ value. \\ undetermined & 0 < \frac{The\ number\ of\ the\ ADE\ report\ for\ the\ drug}{The\ total\ number\ of\ the\ drug\ is\ complained} < cut\ value \end{cases}$$

For deciding which cut value is appropriate, we try different quantile, such as 0.05, 0.1, 0.15, etc. And then, we choose a cut-value which makes the ratio between the number of high risk and low risk closed to 1.

Classification rule- decision tree [8] [9]

Generally, a decision tree is built by a root at the top and several leaves at the bottom. Both the root and the leaves are called "node", but there is only one special node which is called "root". We start a decision tree at the root node, and for each node, there is a test applied to determine what the next node will be. This process is repeated until all the data points arrive at a terminal node (leaf). The terminal node gives what group the data point belongs to. The data points that end up at the same leaf of the tree are classified as one group. It should be mentioned that there are a lot of ways to grow a tree, but this does not mean the types of all of leaves in each tree are different. Therefore, it needs some trim after growing up one tree.

Suppose that Y is an indicator variable and there is a single feature X. First, we choose a split point t that partitions the feature X into two disjoint sets $A_1 = (-\infty, t]$ and $A_2 = (t, \infty)$:

Let $\hat{P}_s(j)$ be the proportion of observation in A_s such as $Y_i = j$:

$$\hat{P}_s(j) = \frac{\sum_{i=1}^{n} I(Y_i = j, X_i \in A_s)}{\sum_{i=1}^{n} I(X_i \in A_s)},$$

$$where\ i\ means\ ith\ data\ point, s = 1, 2\ and\ j = 0, 1.$$

The impurity of the split t is defined to be

$$I(t) = \sum_{s=1}^{2} \gamma_s,$$

$$where\ \gamma_s = 1 - \sum_{j=0}^{1} \hat{P}_s(j)^2.$$

This particular measure of impurity is known as the Gini index. We choose the split point t to minimize the impurity. We decide split points that bring about the smallest impurity among features. This process is continued until some stopping criterion is met.

Use 10-fold cross validation to estimate accuracy rate [9]

The basic idea of cross-validation is to partition randomly the observed data into two groups: the training set and the testing set. The training set is used to produce an estimated classifier $\hat{k}$, and the testing set to obtain an estimate $\hat{\mathrm{A}}$ of the accuracy rate of $\hat{k}$. The accuracy rate is defined by

$$\hat{A}(k) = \frac{1}{m} \sum_{X_i \in testing\ set} 1(\hat{k}(X_i) = Y_i),$$

$$where\ m\ is\ the\ number\ of\ data\ points\ in\ the\ testing\ set.$$

The algorithm of 10-fold cross-validation is listed as following:

(1) The data are randomly partitioned into 10 subsets of approximately equal sizes.

(2) For $k = 1,2, \ldots, 10$, do the following steps:

(2.1) Take subset k as the testing set and take the others as the training set.

(2.2) Use the training set to compute the classifier $\hat{h}(k)$.

(2.3) Use $\hat{h}(k)$ to predict the data in subset k. Let $\hat{A}(k)$ denote the observed accuracy rate.

(3) The average accuracy rate, $\hat{A}(h)$, would be $\hat{A}(h) = \frac{1}{10}\sum_{k=1}^{10} \hat{A}(k)$

Find concordant drug subset determined by ADE risk-index and chemical features

We build an automatic work flow to find concordant drug subset for each ADE. The drug subset contains two types of ADE risk-index (high-risk or low-risk). For drugs in each type, they are more similar in drugs' chemical feature set.

The workflow is described as the following, and Figure 2.2 shows the flow chart of it:

(1) Given an ADE, we separate the drug set into two groups (Notation:$[H_0,\ L_0]$), one is collected low-risk drugs (L_0), and the other group is collected high-risk drugs (H_0).

(2) Use Kendall rank correlation coefficient to evaluate the concordance between each two drugs on feature space.

– For L_0 group with n_1 high-risk drugs, we build an $n_1 \times n_1$ Kendall table notated as $\text{TABLE}_{Kendall}$:

$$[\text{TABLE}_{Kendall}]_{ij} = the\ Kenall\ rank\ correlation\ coefficent\ between\ drug_i\ and\ drug_j$$

– For H_0 group with n_2 high-risk drugs, we build an $n_2 \times n_2$ Kendall table notated as $\text{TABLE}_{Kendall}$.

(3) Use divisive analysis to divide items into two clusters.

— For H_0 group, we take the $1 - \text{TABLE}_{Kendall}$ as a distance matrix. Then, we divide n_2 items into two clusters (Notation: H_1 and H_2).

— For L_0 group, we take the $1 - \text{TABLE}_{Kendall}$ as a distance matrix. Then, we divide n_1 items into two clusters (Notation: L_1 and L_2).

(4) We consider these eight possibilities of drug subset:

$$[H_0,\ L_1], [H_0,\ L_2], [H_1,\ L_0], [H_1,\ L_1], [H_1,\ L_2], [H_2,\ L_0], [H_2,\ L_1], [H_2,\ L_1]$$

(5) If the drug subset, $[H_i,\ L_j], for\ i,j = 0,1,2,$ satisfy the number of drugs lager than 500 and

$$\frac{\max\{\#\ of\ high\ risk\ drug, \#\ of\ low\ risk\ drug\}}{\min\{\#\ of\ high\ risk\ drug, \#\ of\ low\ risk\ drug\}} < 2.5,$$

then the drug subset $[H_i, L_j]$ is the possibility of concordant drug subset. We take this drug subset as $[H_0, L_0]$ and repeat the steps from (1) to (4).

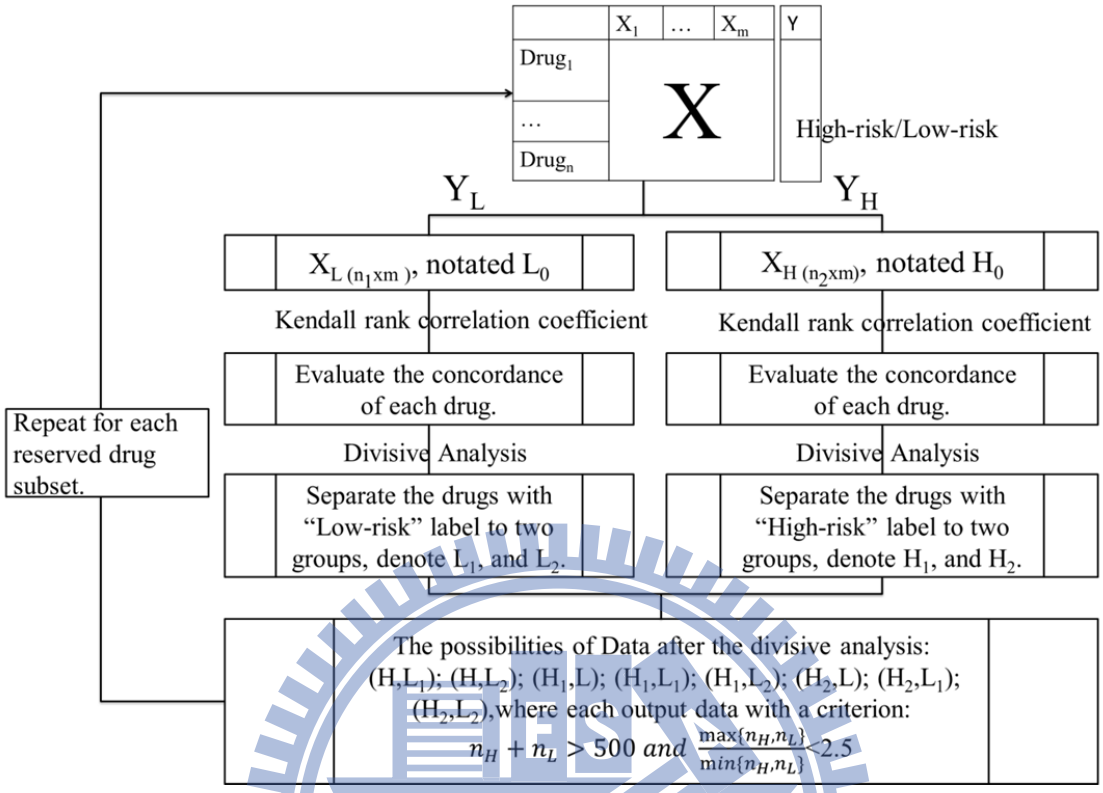

Figure 2.2: The automatic clustering analysis method is designed to select some concordant drugs for each ADE. The remainder is called "drug subset". Finally, we can use the drug subset to analyze the relation between chemical compounds and ADE under general condition.

2.3. Research Design

In our study, there are two stages to explore the drug injuries, ADEs.

In the first stage, we extract chemical features to be the covariates and take ADE record to be the drugs' risk-index as the response variable. C4.5 Decision tree is used to obtain the mapping function from chemical feature space onto the binary risk-index space. Then, we use 10-fold cross-validation to estimate the prediction model accuracy. The resulted decision tree is the build ADE prediction model with associated chemical features. The ADE prediction models on the first stage are called Initial Decision Trees (IDTs). It serves as feature selection for each ADE. We use "rpart" package of statistical software **R** to obtain the IDTs for each ADE. Finally we compare the prediction accuracy among three chemical feature sets for each ADE. The aim of the

first stage is to compare the performance of different chemical feature sets and obtain the associated chemical features for each ADE.

The performance of IDT implies that there exists an instance subset that is relatively more separable in the associated feature space. We call this instance subset as concordant drug subset. It is illustrated in Figure 2.3.

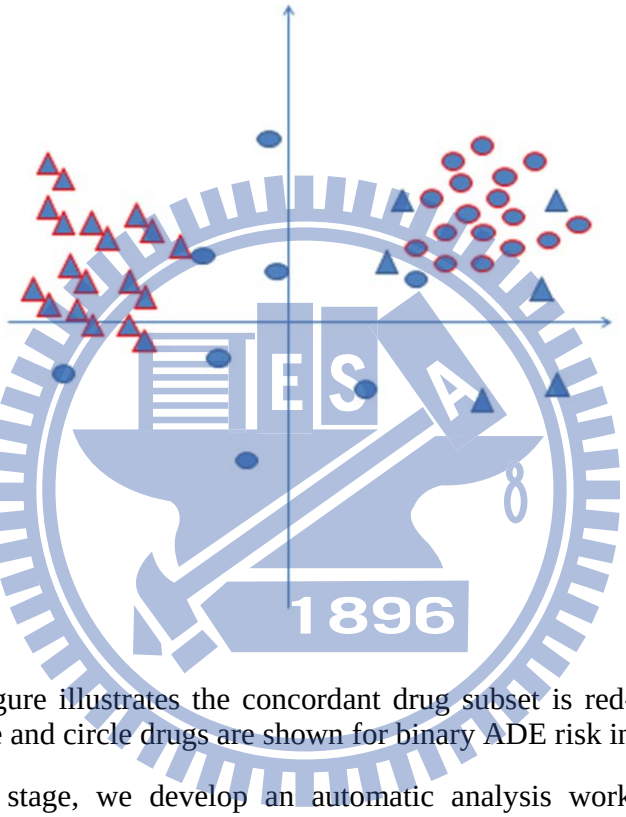

Figure 2.3: This figure illustrates the concordant drug subset is red-surrounded. The triangle and circle drugs are shown for binary ADE risk index.

In the second stage, we develop an automatic analysis work flow to obtain concordant drug subset on each ADE of interest. After divisive clustering, we can get several drug subsets which are candidate concordant drug subsets of a particular ADE. Finally, we take the drug subset as the data set and use 10-fold CV and decision tree to build a set of candidate models for the fixed ADE. Among all of candidate models, we choose the optimal model with the highest prediction accuracy. For instance, we have 29 drug subsets as illustrated in Figure 2.3. The 29 drug subset is obtained by divisive clustering analysis. Each node stands for a drug set with binary risk index. The high risk drugs can be divided into two groups, H_1 and H_2. H_0 represents all the high risk drugs. And the low risk drugs can also be divided to two groups, L_1 and L_2. L_0 represents all

the low risk drugs. There can be 8 children of each node at most due to the combination illustrated in the first level in Figure 2.3. Among 29 drug subset, each has a candidate model and each model represents a decision tree with its own 10-fold CV accuracy. The model with the highest 10-fold CV accuracy is the final ADE prediction model. The optimal prediction models of ADEs are called “Similarity Guided Decision Tree” (SGDT). Figure 2.4 gives an overall view of our research.

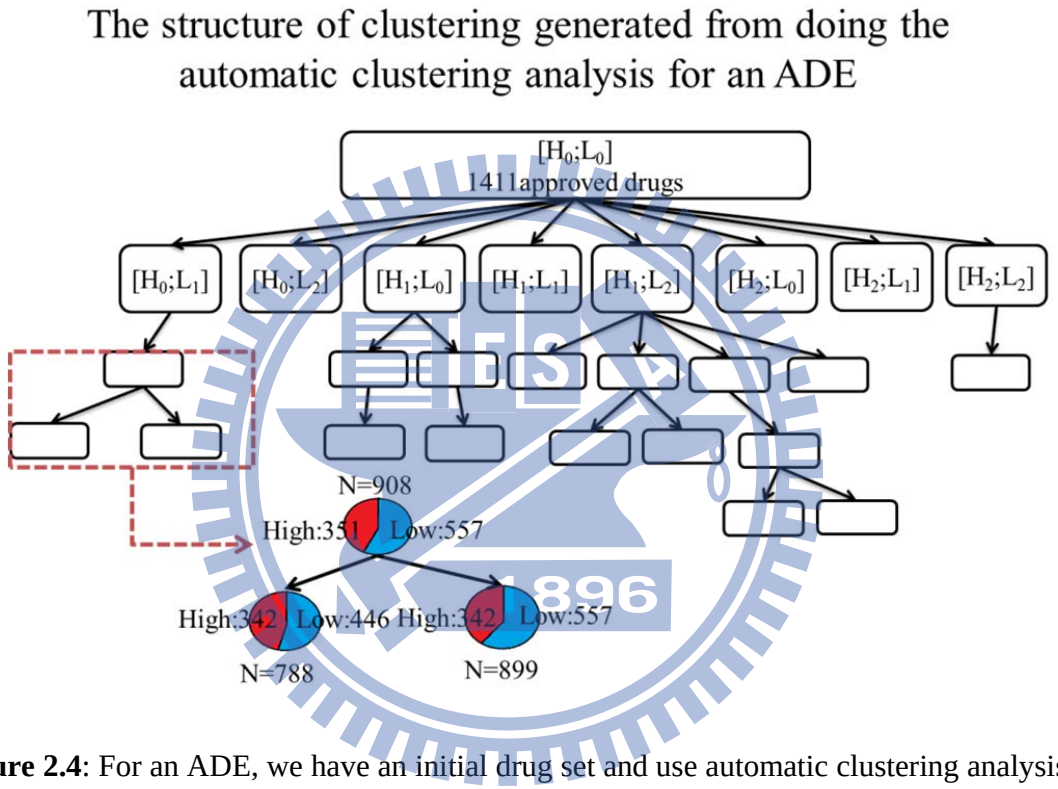

Figure 2.4: For an ADE, we have an initial drug set and use automatic clustering analysis to get numerous drug subsets which contain concordant drugs. Put the initial drug set into automatic clustering analysis, then we can get several drug subsets which satisfy the condition we set. Each drug subset could be another initial drug set in the next level, and iteratively execute the automatic clustering analysis. The iteration stops until none of output file satisfies the criteria we set.

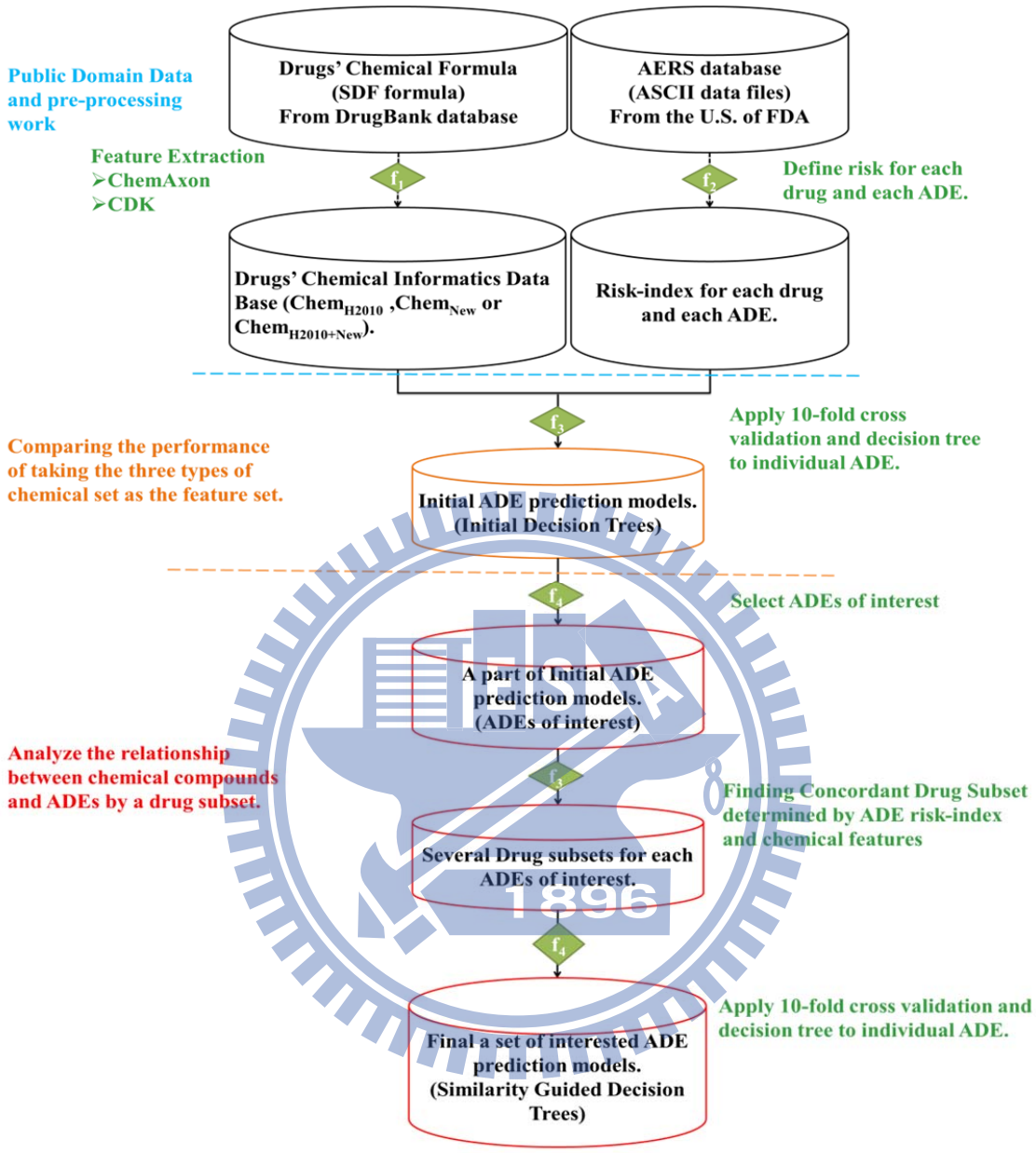

Figure 2.5: The flow chart of our research. The first step is material collection and pre-processing work. The pre-processing work is to get the risk-index for each drug and each ADE. The second step is to compare the performance of ADE prediction models which generate by taking three types of chemical sets as the feature set, such as, $Chem_{H2010}$, $Chem_{New}$, and $Chem_{H2010+New}$. The most important of our research is the part which locates below the orange dashed line. This step is to analyze the relation between chemical compounds and ADEs of interest under some regular condition.

3. Results

The most important of our research is that we build an automatic concordant analytic method. We use automatic clustering analysis, 10-fold cross-validation and decision tree to analyze the relation between chemical compounds and ADEs under some regular condition. We define the prediction accuracy and the ratio of $\frac{Accuracy}{Guess\ rate}$ to evaluate the performance of ADE prediction.

3.1. Compare the performance by using different types of chemical feature sets.

There are three issues to compare the performance of prediction model by using three different types of chemical feature sets, $Chem_{H2010}$, $Chem_{New}$, and $Chem_{H2010+New}$:

Q 1. Can we find some ADEs (Y^* s), satisfying $X[Chem_{H2010}] \xrightarrow{f} Y^*$, with a good prediction function?

Q 2. Given those Y^* s, can we verify if the performance of $X[Chem_{New}] \xrightarrow{g} Y^*$ is better than that of $X[Chem_{H2010}] \xrightarrow{f} Y^*$?

Q 3. If we get the negative answer in Q 2, can we verify if the performance of $X[Chem_{H2010+New}] \xrightarrow{h} Y^*$ is better than that of $X[Chem_{H2010}] \xrightarrow{f} Y^*$?

In the first question, we define some criterion to judge the performance of ADE prediction models. Let the upper bound of 95% C.I. of $\mu_{\frac{accuracy}{guess\ rate}}$ be the threshold. If $\frac{prediction\ accuracy}{random\ guess}$ of an ADE model is larger than the threshold, then we consider this ADE model as an acceptable prediction model. We find 642 out of 1,483 ADEs that has the prediction accuracy higher than the threshold, shown in Figure 3.1(a). Considering the second question, we can find 121 ADEs whose prediction accuracy of using Chem_{New} as the feature set is higher than using Chem_{H2010}, shown in Figure 3.1(b). For answering the third question, we use 841 ADEs which have negative response in the second question. Then, we test whether the prediction accuracy of using $\text{Chem}_{H2010+New}$

as the feature set is higher than using Chem_{H2010}. The result shows that there are only 44 ADEs which indicate that the prediction accuracy of using $\text{Chem}_{H2010+New}$ is better than using Chem_{H2010}, shown in Figure 3.1(c).

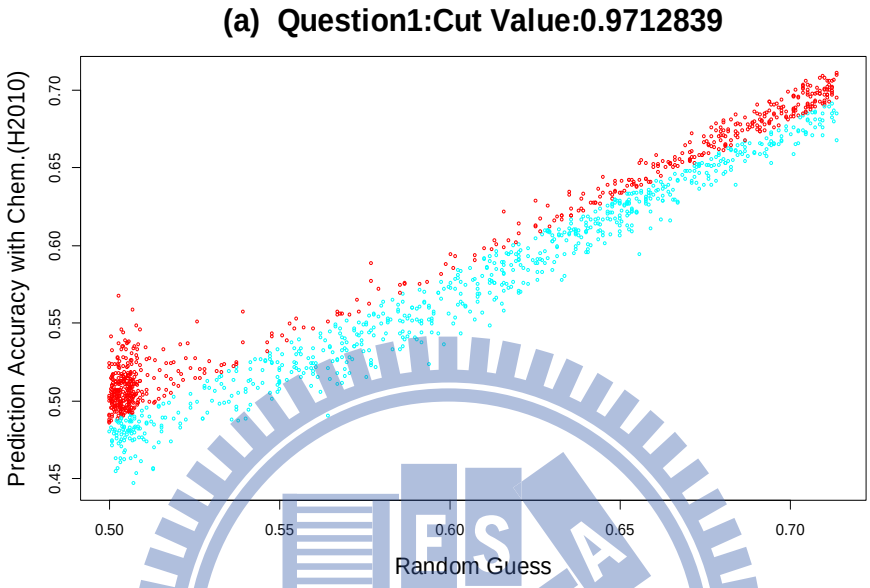

Figure 3.1(a): Each red point denotes that the ADE model's $\frac{accuracy}{guess\ rate}$ is higher than the threshold. And each blue point denotes that the ADE model's $\frac{accuracy}{guess\ rate}$ is not higher than the threshold.

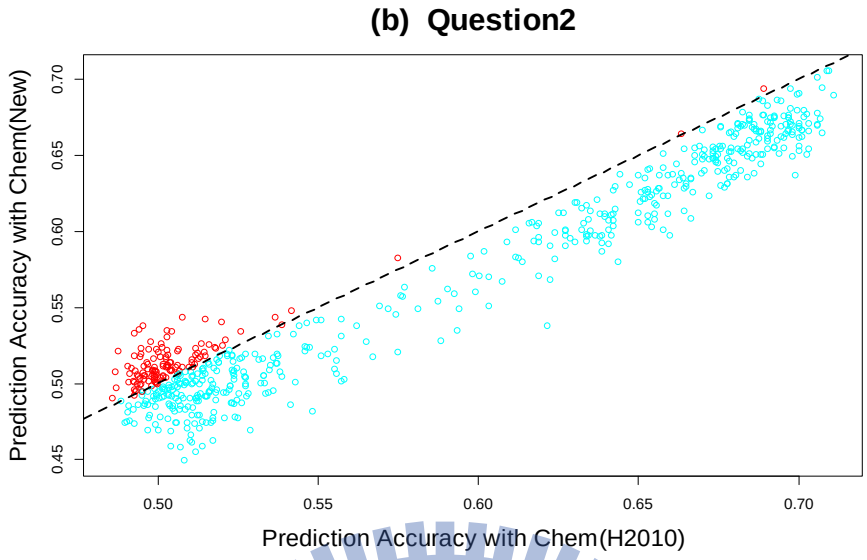

Figure 3.1(b): In the scatter plot, the red points (121 points) denote that the performance of using the $Chem_{New}$ feature set to build an ADE model is better than using the $Chem_{H2010}$ feature set. The blue points denoted that the performance of using the $Chem_{New}$ feature set to build model is not better than using $Chem_{H2010}$.

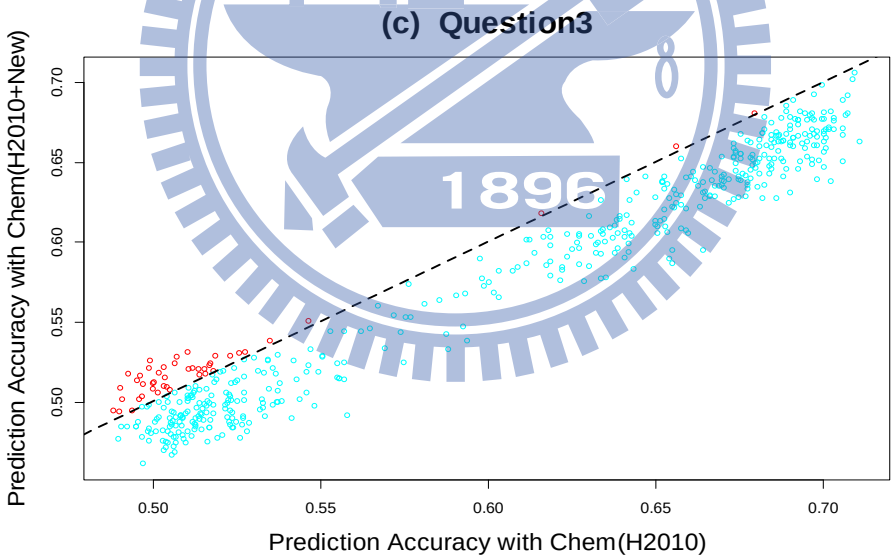

Figure 3.1(c): Among 841 ADEs have a negative answer in Q 2; there are only 44 ADEs (red points) which satisfy that the performance of using $Chem_{H2010+New}$ is better than using $Chem_{H2010}$.

After comparing the performance of using different types chemical feature sets, we find that no matter which feature set we take to build ADE models, the prediction accuracy of each ADE is not higher than 0.8. The accuracy rate will decrease rapidly if we consider multiple ADEs. For illustration, suppose we are interested in a new drug is high-risk or low-risk drug corresponding to 3 specific ADEs and of each ADEs, the prediction rate is 0.8. Then the total prediction accuracy would be reduced to $(0.8)^3 \approx 0.512$. Therefore, we need to increase the prediction accuracy of ADE models as higher as possible.

3.2. Select concordant drugs and then analyze the relation between chemical compounds and ADE under some regular condition

We build an automatic concordant analysis to select concordant drugs. Then, we take the remaining drugs as data set to build prediction models by decision tree. Finally, we use 10-fold cross-validation to estimate the prediction accuracy of each ADE model.

3.2.1. ADEs of interest filtering.

In order to check the feasibility of this automatic concordant analysis, we need to construct testing data. There are a lot of ADEs in our study (1,483 ADEs), so we select some ADEs to be the testing data. In this thesis, we filter out the ADE of interest by considering the 10-fold CV accuracy to the guess rate:

$$guess\ rate = \frac{max\{\#\ of\ high\ ris\ drugs, \#\ of\ low\ risk\ drugs\}}{\#\ of\ drugs}.$$

We use the ADEs' prediction accuracy as the response variable and the guess rate as the covariate to build a simple linear regression, where the prediction accuracy is generated by taking $\text{Chem}_{H2010+New}$ as the feature set and the prediction model is called "Initial Decision Tree" (IDT). If the accuracy of an ADE model is higher than the upper bound of 95% prediction interval of accuracy, then the ADE is one of the "ADEs of interest". Among 1,384 ADEs, we obtain 35 ADEs which satisfy that the accuracy is higher than the upper bound.

3.2.2. Similarity Guided Decision Tree (SGDT) for each ADEs of interest.

Now we use these ADEs of interest to analyze the relationship between drugs' chemical compounds and ADEs under some regular condition. These prediction models are called "Similarity Guided Decision Tree" (SGDT). In Figure 3.2 (a), we compare the prediction accuracy between IDT (blue bars) and SGDT (red bars) for each "ADEs of interest", where the drug subset contains the remaining drugs after doing automatic clustering analysis. Obviously, the prediction accuracy of SGDT is higher than IDT for each ADEs of interest.

What we are most interested in is the ratio between prediction accuracy and guess rate, for the guess rate has a significant effect on the prediction accuracy. The high random guess shows that the majority of drugs belong to one kind of drug-risk level (high-risk or low-risk). As a result, we just guess all of drugs are belong to this drug-risk level, and then the prediction accuracy rate is naturally high. In order to avoid this situation, we need to consider the ratio, $\frac{prediction\ accuracy}{guess\ rate}$. The higher ratio illustrates that the prediction model is more reliable. In Figure 3.2(b), we compare the ratio, $\frac{prediction\ accuracy}{guess\ rate}$ between IDT and SGDT for each ADEs of interest. Since the red bar (SGDT) is higher than the blue bar (IDT) of each interest ADEs. Consequently, we conclude that the performance of using an appropriate drug subset is better than using a fixed drug set for these ADEs of interest.

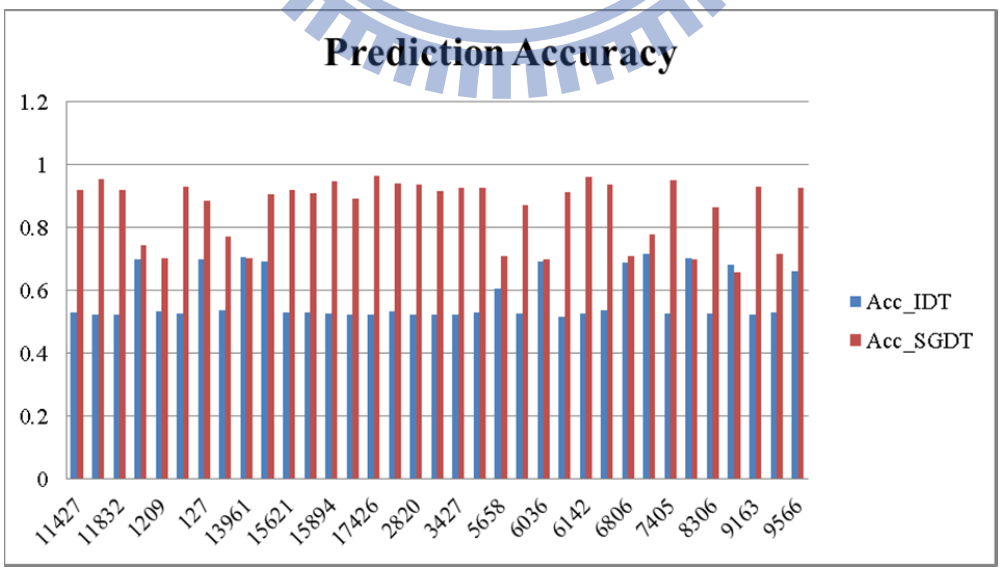

Figure 3.2(a): In this bar plot, each red bar denotes that the performance of an ADE prediction model after doing the automatic clustering analysis, and each blue bar denotes the performance of ADE model by using initial drug set.

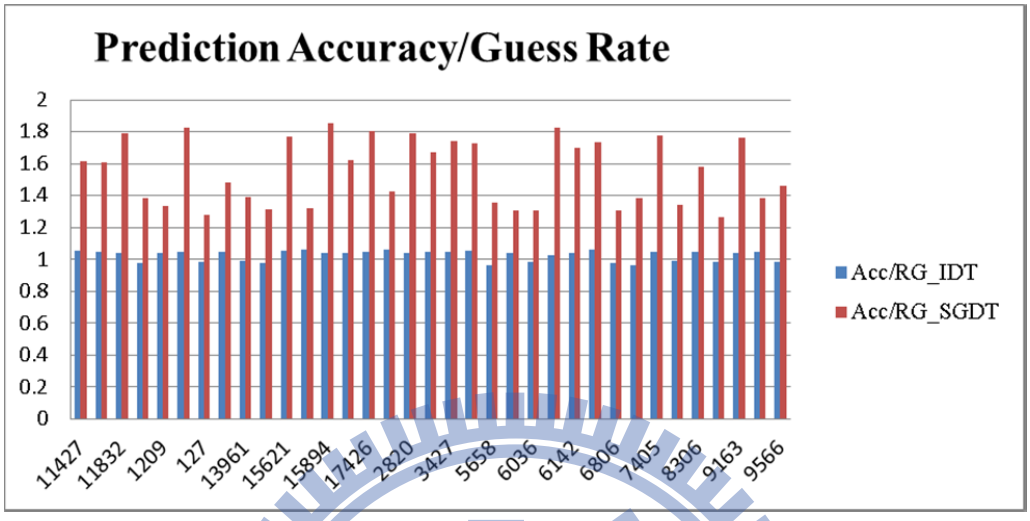

Figure 3.2(b): For each ADEs of interest, the ratio, $\frac{Prediction\ Accuracy}{Random\ Guess}$ by using a drug subset (red bar) is higher than using a fixed drug set (blue bar).

In summary, the results of interested ADEs' prediction models show that 24 ADEs have the prediction accuracy greater than 80%. However, if we consider the ratio between prediction accuracy and guess rate, we can find 33 ADEs of interest have $\frac{prediction\ accuracy}{guess\ rate} > 1.3$ among 35 ADEs of interest.

Among these 35 ADEs of interest, there are three more serious ADEs: Diabetes Mellitus (PT_{5768}), Renal Failure Acute (PT_{15877}) and Renal Impairment (PT_{15894}).

(1) DIABETES MELLITUS (PT_{5768}):

Feature Set:$Chem_{H2010+New}$

Drug Size: 1,411 approval drugs

By automatic clustering analysis (the second stage), the prediction accuracy is listed as following:

	Cut Value	High	Low	N	Guess Rate	Accuracy

IDT	≒0.0085	524	538	1062	≒0.493	≒0.527
SGDT		489	244	733	≒0.667	≒0.871

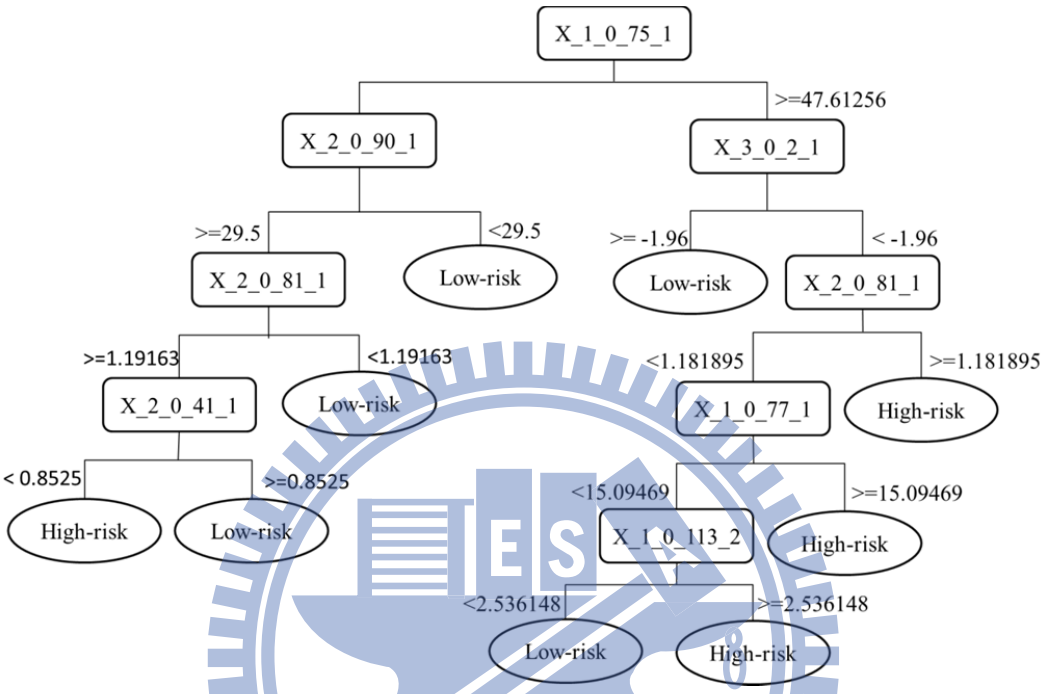

Figure 3.3: The SGDT of the ADE-DIABETES MELLITUS for 489 high-risk drugs and 244 low-risk drugs ($N = 733$), with a prediction accuracy of 0.871.

Table 3.1: The chemical description of features we used in the ADE model.

Feature Code	Feature Name	Parameter/ Discriptive Statistic
X1_0_113_2	JCStericEffectIndex	Atom=false
X1_0_75_1	JCMinimalProjectionArea	None
X1_0_77_1	JCMinZ	None
X2_0_41_1	JAR_hmoelectrophiliclocalizationenergy_Localization energy L(+)	IQR
X2_0_81_1	JAR_sterichindrance	None
X2_0_90_1	JAR_wienerpolarity	None
X3_0_2_1	SDF_ALOGPS_LOGS	None

Table 3.1 (Continue)

Feature Code	Descriptor	Definition
X1_0_113_2	JCStericEffectIndex	Steric effect index
X1_0_75_1	JCMinimalProjectionArea	Calculates the minimal projection area
X1_0_77_1	JCMinZ	Returns the minimum z coordinate of the bounding box.
X2_0_41_1	JAR_hmoelectrophilicloc-alizationenergy	HMO Electrophilic localization energy L(+).
X2_0_81_1	JAR_sterichindrance	Steric hindrance
X2_0_90_1	JAR_wienerpolarity	Wiener polarity
X3_0_2_1	SDF_ALOGPS_LOGS	"The extent to which a compound will dissolve in water. The log of solubility is generally inversely related to molecular weight."- U.S. Environmental Protection Agency, 2009

(2) RENAL FAILURE ACUTE (PT_{15877})

Feature Set: $Chem_{H2010+New}$

Drug Size: 1,411 approval drugs

By divisive analysis (the second stage), the prediction accuracy is listed as following:

	Cut Value	High	Low	N	Guess Rate	Accuracy
IDT	≒0.027	539	438	977	≒0.552	≒0.531
SGDT		508	231	739	≒0.687	≒0.910

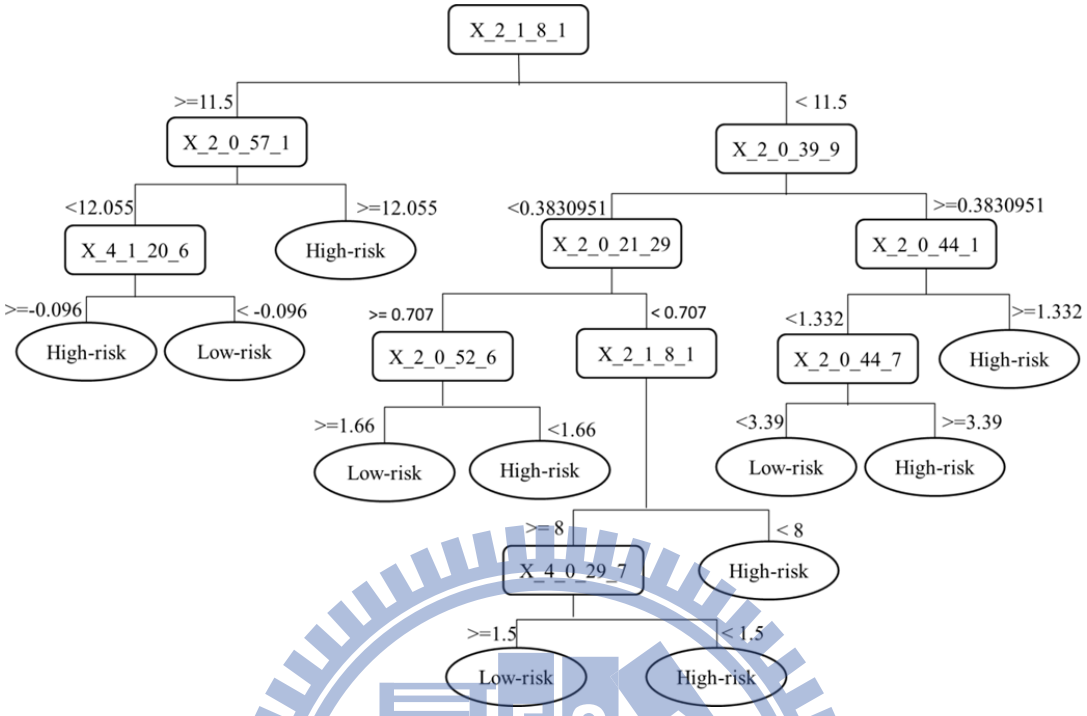

Figure 3.4: The SGDT of the ADE- RENAL FAILURE ACUTE for 508 high-risk drugs and 231 low-risk drugs ($N = 739$), with a prediction accuracy of 0.910.

Table 3.2: The description of features we used in the ADE model.

Feature Code	Feature Name	Parameter/ Discriptive Statistic
X2_0_21_29	JAR_composition	Carbon
X2_0_39_9	JAR_hmoelectrondensity_Electron density	Standard deviation
X2_0_44_1	JAR_hmolocalizationenergy_L_minus	Standard deviation
X2_0_52_6	JAR_localizationenergy_L_minus	0.25 quantile
X2_0_57_1	JAR_msacc	pH=0
X2_1_8_1	JAR_aromaticbondcount	None
X4_0_29_7	RCDK_khs.tCH	None
X4_1_20_6	RCDK_FNSA.3	None

Table 3.2 (*Continue*)

Feature Code	Descriptor	Definition
X2_0_21_29	JAR_composition	Elemental composition calculation (w/w%).
X2_0_39_9	JAR_hmoelectro-ndensity	HMO Electron density.
X2_0_44_1	JAR_hmolocalizat-ionenergy	HMO Electrophilic localization energy L(+).
X2_0_52_6	JAR_localization-energy	Localization energy L(+)/L(-).
X2_0_57_1	JAR_msacc	Hydrogen bond acceptor average multiplicity over microspecies by pH.
X2_1_8_1	JAR_aromatic-bondcount	Aromatic bond count.
X4_0_29_7	RCDK_KierHall-SmartsDescriptor	A fragment count descriptor that uses e-state fragments
X4_1_20_6	RCDK_CPSA-Descriptor	Calculates 29 Charged Partial Surface Area (CPSA) descriptors. One of them is FNSA.3. FNSA.3=the ratio between charge weighted partial negative surface area and total molecular surface area.

(3) RENAL IMPAIRMENT (PT_{15894})

Feature Set:$Chem_{H2010+New}$

Drug Size: 1,411 approval drugs

By divisive analysis (the second stage), the prediction accuracy is listed as following:

	Cut Value	High	Low	N	Guess Rate	Accuracy
IDT	≒0.006	561	548	1109	≒0.506	≒0.526
SGDT		247	257	504	≒0.510	≒0.946

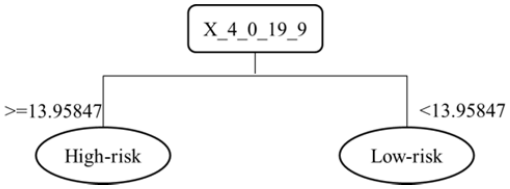

Figure 3.5: The SGDT of the ADE- Renal Impairment for 247 high-risk drugs and 257 low-risk drugs (N=504), with a prediction accuracy of 0.946.

Table 3.3: The description of features we used in the ADE model.

Feature Code	Feature Name	Parameter/ Discriptive Statistic	Descriptor	Definition
X4_0_19_9	RCDK_VP.0	None	RCDK_ChiPathDescriptor	Evaluates chi path descriptors

4. Discussion and Conclusions

4.1. Discussion

In our research, we find that the size of drug subset is smaller for each ADEs after conducting automatic concordant analysis. Therefore, we do some check-up on these "unselected drugs".

Given an ADE, we can examine the Kendall τ rank correlation coefficient between "unselected drugs" and "selected drugs" in the chemical feature space. For each "unselected drug", we choose a most similar "selected drug" which has the maximum τ value. Then, we compare the corresponding risk-indices.

If the risk-indices are different between some unselected drug and some most similar selected drug, the unselected drug is called "mislabel" drug. Otherwise, if the drug-risk of some unselected drug and some most similar selected drug are the same, the unselected drug is called "concordant" drug. For example, we can get results for Renal Failure Acute and Diabetes Mellitus as the following table:

Table 4.1 Show the number of unselected drugs and selected drugs for the two ADEs of interest.

ADE_i	Name	FileName	Unselected	Selected	Concordant	Mislabel
15877	Renal Failure Acute	PT15877_iPRO_3_2.csv	672	739	156	516
5768	Diabetes Mellitus	PT5768_iPRO_6_1.csv	678	733	305	373

We list out the possible speculations for mislabel and concordant as the following:

(1) Mislabel:

Mislabel drugs can be separated into two cases:

(1.1) The unselected drug is a low-risk drug, and the most similar selected drug is a high-risk drug. There are several possible reasons of this case:

(1.1.1) The drug is used for particular patients. The patient population size for each drug is not available.

(1.1.2) Incomplete documentation

(1.1.2.1) AERS does not cover all adverse event occurrences globally.

(1.1.2.2) The newly marketing drugs documented in shorter history tend to have less observation.

(1.2) The other case is that the unselected drug is a high-risk drug, and the most similar selected drug is a low-risk drug. The possible reason of this case is that the drug may be a concomitant drug, such as, second suspect drug, concomitant drug, and interacting drug. This kind of drugs tends to have higher reports.

For example, in Renal Failure Acute prediction model, the approval history duration of the two low-risk drugs (DB01193, DB00488) are at least less than ten years comparing to the most similar selected drugs (DB00190, DB01168). Therefore, the observed ADE report frequency may lead us to underestimate their risk propensity.

Table4.2 Show the approval date of the two unselected drugs and two "the most similar" selected drugs.

Unselected Drug	Approval date	Risk-index	Most similar selected drug	Approval date	Risk Index
DB01193	1999/12/30	Low-risk	DB00190	Approved Prior to jan 1, 1982	High-risk
DB00488	1990/12/26	Low-risk	DB01168	Approved Prior to jan 1, 1982	High-risk

(2) Concordant

Given an ADE risk-index (high or low), some unselected drugs are actually relatively closer to the selected drug group. For instance, drug A, drug B and other four drugs are the same ADE risk-indexed. However, drug A and drug B are determined as unselected by our automatic analysis method. As shown in Figure 4.1, drug B are actually closer to the four selected drugs.

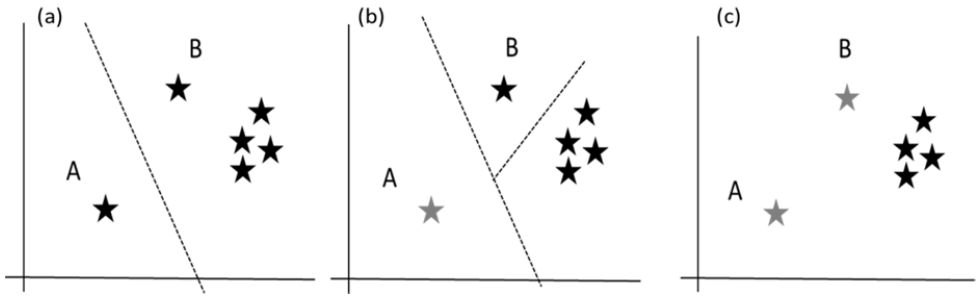

Figure 4.1: (a) The first division separates drug A from the other five drugs. (b) The second division separates drug B from the other four drugs. (c) The remained four drugs are determined as selected drugs. Drug A is relatively far from the four selected drugs in chemical feature space, while drug B is relatively closer to the four selected drugs.

4.2. Conclusion

In our research, we identify 1,384 ADEs with corresponding associated chemistry informatics features by decision tree. With an automatic analysis work flow, we can obtain a concordant drug subset with satisfying 10-fold cross-validation accuracy. The test experiment about selected 35 ADEs of interest results in accuracy higher than 80%. Three observations from the results are worth emphasizing:

(1) After conducting the automatic analytic method, these drugs give a significant drug-risk level. This leads to significant results of decision tree.

(2) Compared with the research of Hammann *et al.*, we consider more ADEs, chemical features and approval drugs to build a set of ADE prediction models.

(3) There are 35 ADE models with the prediction accuracy higher than 0.8.

The practical benefits of our experimental results are of great interest both for the R&D in medicine industry and in public health. We can apply the trained model to forecast the new designed drugs (potential compounds) for its ADE. In addition, we can recognize the probability of some ADE occurrence when some chemical compound exits. Our models can not only guide future clinical trials, but also run monitoring and test during such trials. Moreover, they allow pharmacists for more advanced and efficient drug design.

4.3. Recommendation for Future Research

Our analysis is focused on the relation between chemical compounds and ADEs. In fact, the process of drug-related injuries resulted in some adverse reaction is still a “black box”. After years of study, many experts believe that the types of elements which result in drug-related injuries are not only chemical compounds, but also target gene. Some scholars have proposed some other view about the causes of adverse reactions (Berger, 2011). In their approach, they believe that drug side effect is mediated by complex cellular networks. In response to a drug, the variations in cellular networks can expose silent phenotypes. This type of adverse drug event is caused by inheritance. Namely, if we only use chemistry features, we cannot thoroughly explain this type of adverse drug events.

In the future studies, to break the limitation of ADEs’ study, we can consider other factors which may result in drug-related injuries, such as, drugs’ target gene and ADME mechanism. Thus, it may be of interest for future research that we combine the systems biology and drugs' chemistry to build ADE prediction model. The ADE models not only have higher prediction accuracy but also contain more "selected drugs". That means the "concordant drug" are really dissimilar to a "selected drug" on the "new" feature space (combine chemistry and system biology), where the two drugs have the same risk-index.

Reference:

[1] Ritter, J. M. (2008). Minimising Harm: Human Variation and Adverse Drug Reactions (ADRs). *British Journal of Clinical Pharmacology*.

[2] Berger, S. I., and Iyengar R. (2011). Role of systems pharmacology in understanding drug adverse events. *WIREs Systems Biology and Medicine.*

[3] Hammann, F., and Gutmann, H. (2010). Prediction of Adverse Drug Reactions Using Decision Tree Modeling. *Clinical Pharmacology & Therapeutics*, 88 (1), 52–59.

[4] U.S. Food and Drug Administration. (2012). *Adverse Event Reporting System (AERS)*. Retrieved July 01, 2011, from http://www.fda.gov/Drugs/default.htm

[5] Departments of Computing Science & Biological Sciences, University of Alberta. (2012). DrugBank. Retrieved July 5, 2011, from http://www.drugbank.ca/

[6] Marvin was used for drawing, displaying and characterizing chemical structures, substructures and reactions, Marvin 5.9.3 (version number), 201n (insert year of version release), ChemAxon (http://www.chemaxon.com)

[7] Guha, R. (2007). 'Chemical Informatics Functionality in R'. Journal of Statistical Software 6(18)

[8] Michael J. A. (1997). *Data Mining Techniques*. New York: WILEY

[9] Wasserman, L. (2004). *All of statistics a concise course in statistical inference*. New York: Springer.

[10] Keiser M. J., and Setola V. (2009). Predicting new molecular targets for known drugs. *Nature*, 462:175–181.

[11] Campillos M., and Kuhn M. (2008). Drug target identification using side-effect similarity. *Science*, 321:263–266.

[12] Pouliot, Y., and Chiang, A.P. (2011). Predicting Adverse Drug Reactions Using Publicly Available PubChem BioAssay Data. *Nature*, 90(1):90-99.

[13] Huang, L.C., and Wu, X. (2011). Predicting adverse side effects of drugs. *BMC Genomics*

[14] Kuhn, M., and Campillos, M. (2009). A side effect resource to capture phenotypic effects of drugs. *Molecular Systems Biology*, 6 (343).

Appendix A

No.	Feature Name	Chemcial Descriptors	#ofNA	Source	v5.1Code
1	JCChainAtomCount	JCChainAtomCount	0	ChemAxonByExcel	1_1_27_1
2	JCCarboRingCount	JCCarboRingCount	0	ChemAxonByExcel	1_1_25_1
3	JClogP	JClogP	0	ChemAxonByExcel	1_1_68_1
4	JCFusedAromaticRingCount	JCFusedAromaticRingCount	0	ChemAxonByExcel	1_1_50_1
5	JCFusedRingCount	JCFusedRingCount	0	ChemAxonByExcel	1_0_51_1
6	JClogD(9)	JClogD	0	ChemAxonByExcel	1_1_67_5
7	JClogD(5)	JClogD	0	ChemAxonByExcel	1_1_67_3
8	JCChainBondCount	JCChainBondCount	0	ChemAxonByExcel	1_1_28_1
9	JCIsoelectricPoint	JCIsoelectricPoint	0	ChemAxonByExcel	1_0_60_1
10	JCSmallestRingSize	JCSmallestRingSize	0	ChemAxonByExcel	1_1_111_1
11	JCBalabanIndex	JCBalabanIndex	0	ChemAxonByExcel	1_1_19_1
12	JClogD(11)	JClogD	0	ChemAxonByExcel	1_1_67_2
13	JCDonorCount	JCDonorCount	0	ChemAxonByExcel	1_1_41_1
14	JCResonantCount	JCResonantCount	2	ChemAxonByExcel	1_1_100_1
15	JCAcceptorSiteCount	JCAcceptorSiteCount	0	ChemAxonByExcel	1_1_3_1
16	JCAromaticAtomCount	JCAromaticAtomCount	0	ChemAxonByExcel	1_1_12_1
17	JCBasicpKa(strongness=1)	JCBasicpKa	87	ChemAxonByExcel	1_1_20_1
18	JCBasicpKa(strongness=2)	JCBasicpKa	292	ChemAxonByExcel	1_1_20_2
19	JCAcidicpKa(strongness=1)	JCAcidicpKa	306	ChemAxonByExcel	1_1_4_1
20	JCAcidicpKa(strongness=2)	JCAcidicpKa	732	ChemAxonByExcel	1_1_4_2
21	JCRingCount	JCRingCount	0	ChemAxonByExcel	1_1_104_1
22	JCAliphaticBondCount	JCAliphaticBondCount	0	ChemAxonByExcel	1_1_7_1
23	JClogD(7.4)	JClogD	0	ChemAxonByExcel	1_1_67_4
24	JCDonorSiteCount	JCDonorSiteCount	0	ChemAxonByExcel	1_1_42_1
25	JCPSA(PH=12)	JCPSA	0	ChemAxonByExcel	1_0_83_1
26	JCQ_N	JCQ_N	0	ChemAxonByExcel	1_1_93_1
27	JCQ_O	JCQ_O	0	ChemAxonByExcel	1_1_95_1
28	JCQ_C	JCQ_C	0	ChemAxonByExcel	1_1_87_1
29	JCQ_halogen	JCQ_halogen	0	ChemAxonByExcel	1_1_90_1
30	JCQ_azole	JCQ_azole	0	ChemAxonByExcel	1_1_85_1
31	JCQ_phenol	JCQ_phenol	0	ChemAxonByExcel	1_1_96_1
32	JCQ_ketone	JCQ_ketone	0	ChemAxonByExcel	1_1_91_1
33	JCQ_amine	JCQ_amine	0	ChemAxonByExcel	1_1_84_1
34	JCQ_COOH	JCQ_COOH	0	ChemAxonByExcel	1_1_88_1
35	JCQ_benzene	JCQ_benzene	0	ChemAxonByExcel	1_1_86_1
36	JCQ_ester	JCQ_ester	0	ChemAxonByExcel	1_1_89_1
37	JCQ_nitro	JCQ_nitro	0	ChemAxonByExcel	1_1_94_1
38	JCQ_methyl	JCQ_methyl	0	ChemAxonByExcel	1_1_92_1
39	JCQ_S	JCQ_S	0	ChemAxonByExcel	1_0_97_1
40	JCAcceptorCount	JCAcceptorCount	0	ChemAxonByExcel	1_0_2_1
41	JClogD(0)	JClogD	4	ChemAxonByExcel	1_1_67_1
42	JCMolecularPolarizability	JCMolecularPolarizability	4	ChemAxonByExcel	1_0_78_1
43	JCAliphaticAtomCount	JCAliphaticAtomCount	0	ChemAxonByExcel	1_1_6_1
44	JCBondCount	JCBondCount	0	ChemAxonByExcel	1_1_23_1
45	JCFusedAliphaticRingCount	JCFusedAliphaticRingCount	0	ChemAxonByExcel	1_1_49_1
46	JCHeteroRingCount	JCHeteroRingCount	0	ChemAxonByExcel	1_1_58_1
47	JCHyperWienerIndex	JCHyperWienerIndex	0	ChemAxonByExcel	1_1_59_1
48	JCRandicIndex	JCRandicIndex	0	ChemAxonByExcel	1_1_98_1
49	JCAcceptor(PH=0)	JCAcceptor	0	ChemAxonByExcel	1_0_1_1
50	JCAcceptor(PH=1)	JCAcceptor	4	ChemAxonByExcel	1_0_1_2
51	JCAcceptor(PH=2)	JCAcceptor	9	ChemAxonByExcel	1_0_1_8
52	JCAcceptor(PH=3)	JCAcceptor	10	ChemAxonByExcel	1_0_1_9
53	JCAcceptor(PH=4)	JCAcceptor	10	ChemAxonByExcel	1_0_1_10
54	JCAcceptor(PH=5)	JCAcceptor	11	ChemAxonByExcel	1_0_1_11
55	JCAcceptor(PH=6)	JCAcceptor	13	ChemAxonByExcel	1_0_1_12
56	JCAcceptor(PH=7)	JCAcceptor	13	ChemAxonByExcel	1_0_1_13
57	JCAcceptor(PH=8)	JCAcceptor	15	ChemAxonByExcel	1_0_1_14
58	JCAcceptor(PH=9)	JCAcceptor	18	ChemAxonByExcel	1_0_1_15
59	JCAcceptor(PH=10)	JCAcceptor	23	ChemAxonByExcel	1_0_1_3
60	JCAcceptor(PH=11)	JCAcceptor	27	ChemAxonByExcel	1_0_1_4
61	JCAcceptor(PH=12)	JCAcceptor	33	ChemAxonByExcel	1_0_1_5
62	JCAcceptor(PH=13)	JCAcceptor	39	ChemAxonByExcel	1_0_1_6
63	JCAcceptor(PH=14)	JCAcceptor	48	ChemAxonByExcel	1_0_1_7
64	JCAcidicpKaLargeModel(strongness=1)	JCAcidicpKaLargeModel	303	ChemAxonByExcel	1_0_5_1
65	JCAcidicpKaLargeModel(strongness=2)	JCAcidicpKaLargeModel	723	ChemAxonByExcel	1_0_5_2
66	JCAcidicpKaLargeModel(strongness=3)	JCAcidicpKaLargeModel	1006	ChemAxonByExcel	1_0_5_3
67	JCAcidicpKaLargeModel(strongness=4)	JCAcidicpKaLargeModel	1150	ChemAxonByExcel	1_0_5_4
68	JCAcidicpKaLargeModel(strongness=5)	JCAcidicpKaLargeModel	1209	ChemAxonByExcel	1_0_5_5
69	JCAcidicpKaLargeModel(strongness=6)	JCAcidicpKaLargeModel	1222	ChemAxonByExcel	1_0_5_6
70	JCAcidicpKaLargeModel(strongness=7)	JCAcidicpKaLargeModel	1224	ChemAxonByExcel	1_0_5_7
71	JCAcidicpKaLargeModel(strongness=8)	JCAcidicpKaLargeModel	1226	ChemAxonByExcel	1_0_5_8
72	JCAliphaticRingCount	JCAliphaticRingCount	0	ChemAxonByExcel	1_0_8_1
73	JCAliphaticRingCountOfSize(size=5)	JCAliphaticRingCountOfSize	0	ChemAxonByExcel	1_0_9_1
74	JCAngle	JCAngle	20	ChemAxonByExcel	1_0_10_1
75	JCAromaticAtom	JCAromaticAtom	9	ChemAxonByExcel	1_0_11_1
76	JCAromaticBondCount	JCAromaticBondCount	0	ChemAxonByExcel	1_0_13_1

No.	Feature Name	Chemcial Descriptors	#ofNA	Source	v5.1Code
77	JCAromaticRingCount	JCAromaticRingCount	0	ChemAxonByExcel	1_1_14_1
78	JCAromaticRingCountOfSize(Size=6)	JCAromaticRingCountOfSize	0	ChemAxonByExcel	1_0_15_1
79	JCAsymmetricAtomCount	JCAsymmetricAtomCount	0	ChemAxonByExcel	1_1_16_1
80	JCAtomCount	JCAtomCount	0	ChemAxonByExcel	1_1_17_1
81	JCAtomicPolarizability(PH=0)	JCAtomicPolarizability	28	ChemAxonByExcel	1_0_18_1
82	JCAtomicPolarizability(PH=1)	JCAtomicPolarizability	24	ChemAxonByExcel	1_0_18_2
83	JCAtomicPolarizability(PH=2)	JCAtomicPolarizability	23	ChemAxonByExcel	1_0_18_8
84	JCAtomicPolarizability(PH=3)	JCAtomicPolarizability	29	ChemAxonByExcel	1_0_18_9
85	JCAtomicPolarizability(PH=4)	JCAtomicPolarizability	26	ChemAxonByExcel	1_0_18_10
86	JCAtomicPolarizability(PH=5)	JCAtomicPolarizability	26	ChemAxonByExcel	1_0_18_11
87	JCAtomicPolarizability(PH=6)	JCAtomicPolarizability	31	ChemAxonByExcel	1_0_18_12
88	JCAtomicPolarizability(PH=7)	JCAtomicPolarizability	31	ChemAxonByExcel	1_0_18_13
89	JCAtomicPolarizability(PH=8)	JCAtomicPolarizability	35	ChemAxonByExcel	1_0_18_14
90	JCAtomicPolarizability(PH=9)	JCAtomicPolarizability	37	ChemAxonByExcel	1_0_18_15
91	JCAtomicPolarizability(PH=10)	JCAtomicPolarizability	41	ChemAxonByExcel	1_0_18_3
92	JCAtomicPolarizability(PH=11)	JCAtomicPolarizability	41	ChemAxonByExcel	1_0_18_4
93	JCAtomicPolarizability(PH=12)	JCAtomicPolarizability	49	ChemAxonByExcel	1_0_18_5
94	JCAtomicPolarizability(PH=13)	JCAtomicPolarizability	51	ChemAxonByExcel	1_0_18_6
95	JCAtomicPolarizability(PH=14)	JCAtomicPolarizability	60	ChemAxonByExcel	1_0_18_7
96	JCBasicpKaLargeModel(strongness=1)	JCBasicpKaLargeModel	81	ChemAxonByExcel	1_0_21_1
97	JCBasicpKaLargeModel(strongness=2)	JCBasicpKaLargeModel	285	ChemAxonByExcel	1_0_21_2
98	JCBasicpKaLargeModel(strongness=3)	JCBasicpKaLargeModel	640	ChemAxonByExcel	1_0_21_3
99	JCBasicpKaLargeModel(strongness=4)	JCBasicpKaLargeModel	916	ChemAxonByExcel	1_0_21_4
100	JCBasicpKaLargeModel(strongness=5)	JCBasicpKaLargeModel	1078	ChemAxonByExcel	1_0_21_5
101	JCBasicpKaLargeModel(strongness=6)	JCBasicpKaLargeModel	1170	ChemAxonByExcel	1_0_21_6
102	JCBasicpKaLargeModel(strongness=7)	JCBasicpKaLargeModel	1233	ChemAxonByExcel	1_0_21_7
103	JCBasicpKaLargeModel(strongness=8)	JCBasicpKaLargeModel	1266	ChemAxonByExcel	1_0_21_8
104	JCBioavailability	JCBioavailability	0	ChemAxonByExcel	1_0_22_1
105	JCCarboAromaticRingCount	JCCarboAromaticRingCount	0	ChemAxonByExcel	1_1_24_1
106	JCChainAtom(Atom=false)	JCChainAtom	0	ChemAxonByExcel	1_0_26_11
107	JCChainAtom(Atom=1)	JCChainAtom	4	ChemAxonByExcel	1_0_26_1
108	JCChainAtom(Atom=2)	JCChainAtom	9	ChemAxonByExcel	1_0_26_3
109	JCChainAtom(Atom=3)	JCChainAtom	10	ChemAxonByExcel	1_0_26_4
110	JCChainAtom(Atom=4)	JCChainAtom	10	ChemAxonByExcel	1_0_26_5
111	JCChainAtom(Atom=5)	JCChainAtom	11	ChemAxonByExcel	1_0_26_6
112	JCChainAtom(Atom=6)	JCChainAtom	13	ChemAxonByExcel	1_0_26_7
113	JCChainAtom(Atom=7)	JCChainAtom	13	ChemAxonByExcel	1_0_26_8
114	JCChainAtom(Atom=8)	JCChainAtom	15	ChemAxonByExcel	1_0_26_9
115	JCChainAtom(Atom=9)	JCChainAtom	18	ChemAxonByExcel	1_0_26_10
116	JCChainAtom(Atom=10)	JCChainAtom	23	ChemAxonByExcel	1_0_26_2
117	JCChiralCenter(Expression=FALSE)	JCChiralCenter	0	ChemAxonByExcel	1_0_29_1
118	JCChiralCenterCount	JCChiralCenterCount	0	ChemAxonByExcel	1_1_30_1
119	JCConformerCount	JCConformerCount	0	ChemAxonByExcel	1_0_32_1
120	JCConnected(atom1=2,atom2=3)	JCConnected	10	ChemAxonByExcel	1_0_33_1
121	JCConnectedGraph	JCConnectedGraph	0	ChemAxonByExcel	1_0_34_1
122	JCCyclomaticNumber	JCCyclomaticNumber	0	ChemAxonByExcel	1_0_35_1
123	JCDihedral(atom1=1,atom2=2,atom3=4,atom4=6)	JCDihedral	16	ChemAxonByExcel	1_0_36_1
124	JCDistance(atom1=2,atom2=4)	JCDistance	16	ChemAxonByExcel	1_0_37_1
125	JCDistanceDegree(Atom=FALSE)	JCDistanceDegree	0	ChemAxonByExcel	1_0_38_1
126	JCDominantTautomerCount	JCDominantTautomerCount	4	ChemAxonByExcel	1_0_39_1
127	JCDoubleBondStereoisomerCount	JCDoubleBondStereoisomerCount	4	ChemAxonByExcel	1_0_43_1
128	JCDreidingEnergy	JCDreidingEnergy	5	ChemAxonByExcel	1_0_44_1
129	JCEccentricity(Atom=FALSE)	JCEccentricity	0	ChemAxonByExcel	1_0_45_1
130	JCExactMass	JCExactMass	0	ChemAxonByExcel	1_0_46_1
131	JCFragmentCount	JCFragmentCount	0	ChemAxonByExcel	1_0_48_1
132	JCGhoseFilter	JCGhoseFilter	0	ChemAxonByExcel	1_0_52_1
133	JCHararyIndex	JCHararyIndex	55	ChemAxonByExcel	1_1_53_1
134	JCHasValenceError	JCHasValenceError	0	ChemAxonByExcel	1_0_54_1
135	JCHasValidConformer	JCHasValidConformer	1	ChemAxonByExcel	1_0_55_1
136	JCHeavyAtomCount	JCHeavyAtomCount	0	ChemAxonByExcel	1_0_56_1
137	JCHeteroAromaticRingCount	JCHeteroAromaticRingCount	0	ChemAxonByExcel	1_1_57_1
138	JCLargestAtomRingSize(Atom=false)	JCLargestAtomRingSize	0	ChemAxonByExcel	1_0_61_11
139	JCLargestAtomRingSize(Atom=1)	JCLargestAtomRingSize	0	ChemAxonByExcel	1_0_61_1
140	JCLargestAtomRingSize(Atom=2)	JCLargestAtomRingSize	0	ChemAxonByExcel	1_0_61_3
141	JCLargestAtomRingSize(Atom=3)	JCLargestAtomRingSize	0	ChemAxonByExcel	1_0_61_4
142	JCLargestAtomRingSize(Atom=4)	JCLargestAtomRingSize	0	ChemAxonByExcel	1_0_61_5
143	JCLargestAtomRingSize(Atom=5)	JCLargestAtomRingSize	0	ChemAxonByExcel	1_0_61_6
144	JCLargestAtomRingSize(Atom=6)	JCLargestAtomRingSize	0	ChemAxonByExcel	1_0_61_7
145	JCLargestAtomRingSize(Atom=7)	JCLargestAtomRingSize	0	ChemAxonByExcel	1_0_61_8
146	JCLargestAtomRingSize(Atom=8)	JCLargestAtomRingSize	0	ChemAxonByExcel	1_0_61_9
147	JCLargestAtomRingSize(Atom=9)	JCLargestAtomRingSize	0	ChemAxonByExcel	1_0_61_10
148	JCLargestAtomRingSize(Atom=10)	JCLargestAtomRingSize	0	ChemAxonByExcel	1_0_61_2
149	JCLargestRingSize	JCLargestRingSize	0	ChemAxonByExcel	1_1_62_1
150	JCLargestRingSystemSize	JCLargestRingSystemSize	0	ChemAxonByExcel	1_0_63_1
151	JCLeadLikeness	JCLeadLikeness	0	ChemAxonByExcel	1_0_64_1
152	JCLipinskiRuleof53of4	JCLipinskiRuleof53of4	0	ChemAxonByExcel	1_0_65_1
153	JCLipinskiRuleof54of4	JCLipinskiRuleof54of4	0	ChemAxonByExcel	1_0_66_1
154	JCMarkushMatch	JCMarkushMatch	0	ChemAxonByExcel	1_0_69_1
155	JCMass	JCMass	0	ChemAxonByExcel	1_0_70_1

No.	Feature Name	Chemcial Descriptors	#ofNA	Source	v5.1Code
156	JCMaximalProjectionArea	JCMaximalProjectionArea	0	ChemAxonByExcel	1_0_71_1
157	JCMaximalProjectionRadius	JCMaximalProjectionRadius	0	ChemAxonByExcel	1_0_72_1
158	JCMaxZ	JCMaxZ	0	ChemAxonByExcel	1_0_73_1
159	JCMicrospeciesCount	JCMicrospeciesCount	0	ChemAxonByExcel	1_0_74_1
160	JCMinimalProjectionArea	JCMinimalProjectionArea	0	ChemAxonByExcel	1_0_75_1
161	JCMinimalProjectionRadius	JCMinimalProjectionRadius	0	ChemAxonByExcel	1_0_76_1
162	JCMinZ	JCMinZ	0	ChemAxonByExcel	1_0_77_1
163	JCMolFormat	JCMolFormat	0	ChemAxonByExcel	1_0_79_1
164	JCMueggeFilter	JCMueggeFilter	0	ChemAxonByExcel	1_0_80_1
165	JCOrbitalElectroNegativityImage	JCOrbitalElectroNegativityImage	0	ChemAxonByExcel	1_0_81_1
166	JCPlattIndex	JCPlattIndex	0	ChemAxonByExcel	1_1_82_1
167	JCRefractivity	JCRefractivity	0	ChemAxonByExcel	1_1_99_1
168	JCRingAtom(Atom=false)	JCRingAtom	0	ChemAxonByExcel	1_0_101_11
169	JCRingAtom(Atom=1)	JCRingAtom	4	ChemAxonByExcel	1_0_101_1
170	JCRingAtom(Atom=2)	JCRingAtom	9	ChemAxonByExcel	1_0_101_3
171	JCRingAtom(Atom=3)	JCRingAtom	10	ChemAxonByExcel	1_0_101_4
172	JCRingAtom(Atom=4)	JCRingAtom	10	ChemAxonByExcel	1_0_101_5
173	JCRingAtom(Atom=5)	JCRingAtom	11	ChemAxonByExcel	1_0_101_6
174	JCRingAtom(Atom=6)	JCRingAtom	13	ChemAxonByExcel	1_0_101_7
175	JCRingAtom(Atom=7)	JCRingAtom	13	ChemAxonByExcel	1_0_101_8
176	JCRingAtom(Atom=8)	JCRingAtom	15	ChemAxonByExcel	1_0_101_9
177	JCRingAtom(Atom=9)	JCRingAtom	18	ChemAxonByExcel	1_0_101_10
178	JCRingAtom(Atom=10)	JCRingAtom	23	ChemAxonByExcel	1_0_101_2
179	JCRingAtomCount	JCRingAtomCount	0	ChemAxonByExcel	1_1_102_1
180	JCRingBondCount	JCRingBondCount	0	ChemAxonByExcel	1_1_103_1
181	JCRingCountOfAtom(Atom=false)	JCRingCountOfAtom	0	ChemAxonByExcel	1_0_105_11
182	JCRingCountOfAtom(Atom=1)	JCRingCountOfAtom	0	ChemAxonByExcel	1_0_105_1
183	JCRingCountOfAtom(Atom=2)	JCRingCountOfAtom	0	ChemAxonByExcel	1_0_105_3
184	JCRingCountOfAtom(Atom=3)	JCRingCountOfAtom	0	ChemAxonByExcel	1_0_105_4
185	JCRingCountOfAtom(Atom=4)	JCRingCountOfAtom	0	ChemAxonByExcel	1_0_105_5
186	JCRingCountOfAtom(Atom=5)	JCRingCountOfAtom	0	ChemAxonByExcel	1_0_105_6
187	JCRingCountOfAtom(Atom=6)	JCRingCountOfAtom	0	ChemAxonByExcel	1_0_105_7
188	JCRingCountOfAtom(Atom=7)	JCRingCountOfAtom	0	ChemAxonByExcel	1_0_105_8
189	JCRingCountOfAtom(Atom=8)	JCRingCountOfAtom	0	ChemAxonByExcel	1_0_105_9
190	JCRingCountOfAtom(Atom=9)	JCRingCountOfAtom	0	ChemAxonByExcel	1_0_105_10
191	JCRingCountOfAtom(Atom=10)	JCRingCountOfAtom	0	ChemAxonByExcel	1_0_105_2
192	JCRingCountOfSize(Size=5)	JCRingCountOfSize	0	ChemAxonByExcel	1_0_106_1
193	JCRingSystemCount	JCRingSystemCount	0	ChemAxonByExcel	1_0_107_1
194	JCRingSystemCountOfSize(Size=3)	JCRingSystemCountOfSize	0	ChemAxonByExcel	1_0_108_1
195	JCRotatableBondCount	JCRotatableBondCount	0	ChemAxonByExcel	1_1_109_1
196	JCSmallestAtomRingSize(Atom=true)	JCSmallestAtomRingSize	0	ChemAxonByExcel	1_0_110_2
197	JCSmallestAtomRingSize(Atom=false)	JCSmallestAtomRingSize	0	ChemAxonByExcel	1_0_110_1
198	JCStereoIsomerCount	JCStereoIsomerCount	40	ChemAxonByExcel	1_0_112_1
199	JCStericEffectIndex(Atom=false)	JCStericEffectIndex	0	ChemAxonByExcel	1_0_113_2
200	JCStericEffectIndex(Atom=2)	JCStericEffectIndex	9	ChemAxonByExcel	1_0_113_1
201	JCSzegedIndex	JCSzegedIndex	0	ChemAxonByExcel	1_1_114_1
202	JCTautomerCount	JCTautomerCount	2	ChemAxonByExcel	1_0_115_1
203	JCTetrahedralStereoisomerCount	JCTetrahedralStereoisomerCount	35	ChemAxonByExcel	1_0_116_1
204	JCValence(atom=false)	JCValence	0	ChemAxonByExcel	1_0_117_11
205	JCValence(atom=1)	JCValence	4	ChemAxonByExcel	1_0_117_1
206	JCValence(atom=2)	JCValence	9	ChemAxonByExcel	1_0_117_3
207	JCValence(atom=3)	JCValence	10	ChemAxonByExcel	1_0_117_4
208	JCValence(atom=4)	JCValence	10	ChemAxonByExcel	1_0_117_5
209	JCValence(atom=5)	JCValence	11	ChemAxonByExcel	1_0_117_6
210	JCValence(atom=6)	JCValence	13	ChemAxonByExcel	1_0_117_7
211	JCValence(atom=7)	JCValence	13	ChemAxonByExcel	1_0_117_8
212	JCValence(atom=8)	JCValence	15	ChemAxonByExcel	1_0_117_9
213	JCValence(atom=9)	JCValence	18	ChemAxonByExcel	1_0_117_10
214	JCValence(atom=10)	JCValence	23	ChemAxonByExcel	1_0_117_2
215	JCVeberFilter	JCVeberFilter	0	ChemAxonByExcel	1_0_118_1
216	JCWienerIndex	JCWienerIndex	0	ChemAxonByExcel	1_0_119_1
217	JCComposition(Precision=FALSE)_ Ag	JCComposition	1410	ChemAxonByExcel	1_0_31_26
218	JCComposition(Precision=FALSE)_ Al	JCComposition	1409	ChemAxonByExcel	1_0_31_1
219	JCComposition(Precision=FALSE)_ Au	JCComposition	1410	ChemAxonByExcel	1_0_31_2
220	JCComposition(Precision=FALSE)_ B	JCComposition	1410	ChemAxonByExcel	1_0_31_3
221	JCComposition(Precision=FALSE)_ Bi	JCComposition	1410	ChemAxonByExcel	1_0_31_8
222	JCComposition(Precision=FALSE)_ Br	JCComposition	1395	ChemAxonByExcel	1_0_31_9
223	JCComposition(Precision=FALSE)_ Ca	JCComposition	1409	ChemAxonByExcel	1_0_31_10
224	JCComposition(Precision=FALSE)_ Cl	JCComposition	1213	ChemAxonByExcel	1_0_31_4
225	JCComposition(Precision=FALSE)_ Co	JCComposition	1409	ChemAxonByExcel	1_0_31_5
226	JCComposition(Precision=FALSE)_ F	JCComposition	1279	ChemAxonByExcel	1_0_31_6
227	JCComposition(Precision=FALSE)_ Fe	JCComposition	1410	ChemAxonByExcel	1_0_31_11
228	JCComposition(Precision=FALSE)_ Gd	JCComposition	1404	ChemAxonByExcel	1_0_31_7
229	JCComposition(Precision=FALSE)_ H	JCComposition	15	ChemAxonByExcel	1_0_31_12
230	JCComposition(Precision=FALSE)_ Hg	JCComposition	1410	ChemAxonByExcel	1_0_31_13
231	JCComposition(Precision=FALSE)_ I	JCComposition	1397	ChemAxonByExcel	1_0_31_14
232	JCComposition(Precision=FALSE)_ K	JCComposition	1409	ChemAxonByExcel	1_0_31_15
233	JCComposition(Precision=FALSE)_ Mg	JCComposition	1409	ChemAxonByExcel	1_0_31_16
234	JCComposition(Precision=FALSE)_ N	JCComposition	235	ChemAxonByExcel	1_0_31_17

No.	Feature Name	Chemcial Descriptors	#ofNA	Source	v5.1Code
235	JCComposition(Precision=FALSE)_ Na	JCComposition	1400	ChemAxonByExcel	1_0_31_18
236	JCComposition(Precision=FALSE)_ O	JCComposition	159	ChemAxonByExcel	1_0_31_19
237	JCComposition(Precision=FALSE)_ P	JCComposition	1376	ChemAxonByExcel	1_0_31_20
238	JCComposition(Precision=FALSE)_ Pt	JCComposition	1408	ChemAxonByExcel	1_0_31_21
239	JCComposition(Precision=FALSE)_ S	JCComposition	1090	ChemAxonByExcel	1_0_31_22
240	JCComposition(Precision=FALSE)_ Sb	JCComposition	1410	ChemAxonByExcel	1_0_31_23
241	JCComposition(Precision=FALSE)_ Se	JCComposition	1410	ChemAxonByExcel	1_0_31_24
242	JCComposition(Precision=FALSE)_ Si	JCComposition	1410	ChemAxonByExcel	1_0_31_25
243	JCComposition(Precision=FALSE)_ Al	JCComposition	1409	ChemAxonByExcel	1_0_31_27
244	JCComposition(Precision=FALSE)_ As	JCComposition	1410	ChemAxonByExcel	1_0_31_28
245	JCComposition(Precision=FALSE)_ C	JCComposition	15	ChemAxonByExcel	1_0_31_29
246	JCComposition(Precision=FALSE)_ Ca	JCComposition	1410	ChemAxonByExcel	1_0_31_30
247	JCComposition(Precision=FALSE)_ Cl	JCComposition	1409	ChemAxonByExcel	1_0_31_31
248	JCComposition(Precision=FALSE)_ Fe	JCComposition	1410	ChemAxonByExcel	1_0_31_32
249	JCComposition(Precision=FALSE)_ Ga	JCComposition	1410	ChemAxonByExcel	1_0_31_33
250	JCComposition(Precision=FALSE)_ I	JCComposition	1410	ChemAxonByExcel	1_0_31_34
251	JCComposition(Precision=FALSE)_ Li	JCComposition	1410	ChemAxonByExcel	1_0_31_35
252	JCComposition(Precision=FALSE)_ Mg	JCComposition	1409	ChemAxonByExcel	1_0_31_36
253	JCComposition(Precision=FALSE)_ N	JCComposition	1410	ChemAxonByExcel	1_0_31_37
254	JCComposition(Precision=FALSE)_ S	JCComposition	1410	ChemAxonByExcel	1_0_31_38
255	JCComposition(Precision=FALSE)_ Zn	JCComposition	1410	ChemAxonByExcel	1_0_31_39
256	JCDonor(PH=0)	JCDonor	0	ChemAxonByExcel	1_0_40_1
257	JCDonor(PH=1)	JCDonor	4	ChemAxonByExcel	1_0_40_2
258	JCDonor(PH=2)	JCDonor	9	ChemAxonByExcel	1_0_40_8
259	JCDonor(PH=7)	JCDonor	13	ChemAxonByExcel	1_0_40_9
260	JCDonor(PH=8)	JCDonor	15	ChemAxonByExcel	1_0_40_10
261	JCDonor(PH=9)	JCDonor	18	ChemAxonByExcel	1_0_40_11
262	JCDonor(PH=10)	JCDonor	23	ChemAxonByExcel	1_0_40_3
263	JCDonor(PH=11)	JCDonor	27	ChemAxonByExcel	1_0_40_4
264	JCDonor(PH=12)	JCDonor	33	ChemAxonByExcel	1_0_40_5
265	JCDonor(PH=13)	JCDonor	39	ChemAxonByExcel	1_0_40_6
266	JCDonor(PH=14)	JCDonor	48	ChemAxonByExcel	1_0_40_7
267	JCFormalCharge(pH=0)	JCFormalCharge	0	ChemAxonByExcel	1_0_47_1
268	JCFormalCharge(pH=1)	JCFormalCharge	4	ChemAxonByExcel	1_0_47_2
269	JCFormalCharge(pH=2)	JCFormalCharge	9	ChemAxonByExcel	1_0_47_8
270	JCFormalCharge(pH=3)	JCFormalCharge	10	ChemAxonByExcel	1_0_47_9
271	JCFormalCharge(pH=4)	JCFormalCharge	10	ChemAxonByExcel	1_0_47_10
272	JCFormalCharge(pH=5)	JCFormalCharge	11	ChemAxonByExcel	1_0_47_11
273	JCFormalCharge(pH=6)	JCFormalCharge	13	ChemAxonByExcel	1_0_47_12
274	JCFormalCharge(pH=7)	JCFormalCharge	13	ChemAxonByExcel	1_0_47_13
275	JCFormalCharge(pH=8)	JCFormalCharge	15	ChemAxonByExcel	1_0_47_14
276	JCFormalCharge(pH=9)	JCFormalCharge	18	ChemAxonByExcel	1_0_47_15
277	JCFormalCharge(pH=10)	JCFormalCharge	23	ChemAxonByExcel	1_0_47_3
278	JCFormalCharge(pH=11)	JCFormalCharge	27	ChemAxonByExcel	1_0_47_4
279	JCFormalCharge(pH=12)	JCFormalCharge	33	ChemAxonByExcel	1_0_47_5
280	JCFormalCharge(pH=13)	JCFormalCharge	39	ChemAxonByExcel	1_0_47_6
281	JCFormalCharge(pH=14)	JCFormalCharge	48	ChemAxonByExcel	1_0_47_7
282	JAR_acceptorsitecount	JAR_acceptorsitecount	8	ChemAxonByJAR	2_1_3_1
283	JAR_aliphaticbondcount	JAR_aliphaticbondcount	4	ChemAxonByJAR	2_1_5_1
284	JAR_aliphaticringcount	JAR_aliphaticringcount	4	ChemAxonByJAR	2_0_6_1
285	JAR_aromaticatomcount	JAR_aromaticatomcount	4	ChemAxonByJAR	2_0_7_1
286	JAR_aromaticbondcount	JAR_aromaticbondcount	0	ChemAxonByJAR	2_1_8_1
287	JAR_aromaticringcount	JAR_aromaticringcount	0	ChemAxonByJAR	2_0_10_1
288	JAR_asymmetricatomcount	JAR_asymmetricatomcount	0	ChemAxonByJAR	2_1_11_1
289	JAR_atomcount	JAR_atomcount	4	ChemAxonByJAR	2_1_12_1
290	JAR_balabaiIndex	JAR_balabaiIndex	55	ChemAxonByJAR	2_0_14_1
291	JAR_carboaromaticringcount	JAR_carboaromaticringcount	0	ChemAxonByJAR	2_1_15_1
292	JAR_carboringcount	JAR_carboringcount	4	ChemAxonByJAR	2_1_16_1
293	JAR_chainatomcount	JAR_chainatomcount	4	ChemAxonByJAR	2_1_17_1
294	JAR_chainbondcount	JAR_chainbondcount	4	ChemAxonByJAR	2_1_18_1
295	JAR_chiralcentercount	JAR_chiralcentercount	0	ChemAxonByJAR	2_1_20_1
296	JAR_donorcount	JAR_donorcount	8	ChemAxonByJAR	2_1_24_1
297	JAR_donorsitecount	JAR_donorsitcount	8	ChemAxonByJAR	2_1_25_1
298	JAR_dreidingenergy	JAR_dreidingenergy	61	ChemAxonByJAR	2_0_27_1
299	JAR_fusedaliphaticringcount	JAR_fusedaliphaticringcount	4	ChemAxonByJAR	2_1_32_1
300	JAR_fusedaromaticringcount	JAR_fusedaromaticringcount	4	ChemAxonByJAR	2_1_33_1
301	JAR_fusedringcount	JAR_fusedringcount	4	ChemAxonByJAR	2_0_34_1
302	JAR_hararyindex	JAR_hararyindex	55	ChemAxonByJAR	2_1_35_1
303	JAR_heteroaromaticringcount	JAR_heteroaromaticringcount	0	ChemAxonByJAR	2_1_36_1
304	JAR_heteroringcount	JAR_heteroringcount	4	ChemAxonByJAR	2_1_37_1
305	JAR_hyperwienerindex	JAR_hyperwienerind	0	ChemAxonByJAR	2_1_49_1
306	JAR_isoelectricpoint	JAR_isoelectricpoint	476	ChemAxonByJAR	2_0_50_1
307	JAR_largestringsize	JAR_largestringsize	0	ChemAxonByJAR	2_1_51_1
308	JAR_logp	JAR_logp	8	ChemAxonByJAR	2_0_54_1
309	JAR_molpol	JAR_molpol	8	ChemAxonByJAR	2_1_55_1
310	JAR_plattindex	JAR_plattindex	0	ChemAxonByJAR	2_1_64_1
311	JAR_psa	JAR_psa	4	ChemAxonByJAR	2_0_66_1
312	JAR_randicindex	JAR_randicind	4	ChemAxonByJAR	2_1_67_1
313	JAR_ringatomcount	JAR_ringatomcount	0	ChemAxonByJAR	2_1_70_1

No.	Feature Name	Chemcial Descriptors	#ofNA	Source	v5.1Code
314	JAR_ringbondcount	JAR_ringbondcount	0	ChemAxonByJAR	2_1_71_1
315	JAR_ringcount	JAR_ringcount	4	ChemAxonByJAR	2_1_72_1
316	JAR_rotatablebondcount	JAR_rotatablebondcount	0	ChemAxonByJAR	2_1_76_1
317	JAR_sterichindrance	JAR_sterichindrance	61	ChemAxonByJAR	2_0_81_1
318	JAR_szegedindex	JAR_szegedindex	0	ChemAxonByJAR	2_1_82_1
319	JAR_vdwsa	JAR_vdwsa	12	ChemAxonByJAR	2_1_86_1
320	JAR_acc_RationOfNA	JAR_acc	0	ChemAxonByJAR	2_0_1_8
321	JAR_acc_Mean	JAR_acc	8	ChemAxonByJAR	2_0_1_3
322	JAR_acc_Min	JAR_acc	8	ChemAxonByJAR	2_0_1_4
323	JAR_acc_Max	JAR_acc	8	ChemAxonByJAR	2_0_1_2
324	JAR_acc_Range	JAR_acc	8	ChemAxonByJAR	2_0_1_7
325	JAR_acc_Q1	JAR_acc	8	ChemAxonByJAR	2_0_1_5
326	JAR_acc_Q3	JAR_acc	8	ChemAxonByJAR	2_0_1_6
327	JAR_acc_IQR	JAR_acc	8	ChemAxonByJAR	2_0_1_1
328	JAR_acc_Std	JAR_acc	8	ChemAxonByJAR	2_0_1_9
329	JAR_acceptorcount	JAR_acceptorcount	8	ChemAxonByJAR	2_1_2_1
330	JAR_accsitecount	JAR_accsitecount	8	ChemAxonByJAR	2_0_4_1
331	JAR_aromaticelectrophilicityorder_Aromatic E(+) order_RationOfNA	JAR_aromaticelectrophilicityorder	14	ChemAxonByJAR	2_0_9_8
332	JAR_aromaticelectrophilicityorder_Aromatic E(+) order_Mean	JAR_aromaticelectrophilicityorder	14	ChemAxonByJAR	2_0_9_3
333	JAR_aromaticelectrophilicityorder_Aromatic E(+) order_Min	JAR_aromaticelectrophilicityorder	14	ChemAxonByJAR	2_0_9_4
334	JAR_aromaticelectrophilicityorder_Aromatic E(+) order_Max	JAR_aromaticelectrophilicityorder	14	ChemAxonByJAR	2_0_9_2
335	JAR_aromaticelectrophilicityorder_Aromatic E(+) order_Range	JAR_aromaticelectrophilicityorder	14	ChemAxonByJAR	2_0_9_7
336	JAR_aromaticelectrophilicityorder_Aromatic E(+) order_Q1	JAR_aromaticelectrophilicityorder	14	ChemAxonByJAR	2_0_9_5
337	JAR_aromaticelectrophilicityorder_Aromatic E(+) order_Q3	JAR_aromaticelectrophilicityorder	14	ChemAxonByJAR	2_0_9_6
338	JAR_aromaticelectrophilicityorder_Aromatic E(+) order_IQR	JAR_aromaticelectrophilicityorder	29	ChemAxonByJAR	2_0_9_1
339	JAR_aromaticelectrophilicityorder_Aromatic E(+) order_Std	JAR_aromaticelectrophilicityorder	8	ChemAxonByJAR	2_0_9_9
340	JAR_averagemicrospeciescharge_Charge	JAR_averagemicrospeciescharge	8	ChemAxonByJAR	2_0_13_1
341	JAR_chargedensity_Charge density_RationOfNA	JAR_chargedensity	0	ChemAxonByJAR	2_0_19_8
342	JAR_chargedensity_Charge density_Mean	JAR_chargedensity	58	ChemAxonByJAR	2_0_19_3
343	JAR_chargedensity_Charge density_Min	JAR_chargedensity	58	ChemAxonByJAR	2_0_19_4
344	JAR_chargedensity_Charge density_Max	JAR_chargedensity	58	ChemAxonByJAR	2_0_19_2
345	JAR_chargedensity_Charge density_Range	JAR_chargedensity	58	ChemAxonByJAR	2_0_19_7
346	JAR_chargedensity_Charge density_Q1	JAR_chargedensity	58	ChemAxonByJAR	2_0_19_5
347	JAR_chargedensity_Charge density_Q3	JAR_chargedensity	58	ChemAxonByJAR	2_0_19_6
348	JAR_chargedensity_Charge density_IQR	JAR_chargedensity	58	ChemAxonByJAR	2_0_19_1
349	JAR_chargedensity_Charge density_Std	JAR_chargedensity	58	ChemAxonByJAR	2_0_19_9
350	JAR_composition_ Ag	JAR_composition	1410	ChemAxonByJAR	2_0_21_10
351	JAR_composition_ Al	JAR_composition	1409	ChemAxonByJAR	2_0_21_11
352	JAR_composition_ Au	JAR_composition	1410	ChemAxonByJAR	2_0_21_12
353	JAR_composition_ B	JAR_composition	1410	ChemAxonByJAR	2_0_21_13
354	JAR_composition_ Bi	JAR_composition	1410	ChemAxonByJAR	2_0_21_14
355	JAR_composition_Br	JAR_composition	1395	ChemAxonByJAR	2_0_21_1
356	JAR_composition_Ca	JAR_composition	1409	ChemAxonByJAR	2_0_21_2
357	JAR_composition_Cl	JAR_composition	1214	ChemAxonByJAR	2_0_21_3
358	JAR_composition_Co	JAR_composition	1409	ChemAxonByJAR	2_0_21_4
359	JAR_composition_ F	JAR_composition	1279	ChemAxonByJAR	2_0_21_15
360	JAR_composition_ Fe	JAR_composition	1410	ChemAxonByJAR	2_0_21_16
361	JAR_composition_ Gd	JAR_composition	1404	ChemAxonByJAR	2_0_21_17
362	JAR_composition_ H	JAR_composition	19	ChemAxonByJAR	2_0_21_18
363	JAR_composition_Hg	JAR_composition	1410	ChemAxonByJAR	2_0_21_5
364	JAR_composition_ I	JAR_composition	1397	ChemAxonByJAR	2_0_21_19
365	JAR_composition_ K	JAR_composition	1409	ChemAxonByJAR	2_0_21_20
366	JAR_composition_ Mg	JAR_composition	1409	ChemAxonByJAR	2_0_21_21
367	JAR_composition_ N	JAR_composition	237	ChemAxonByJAR	2_0_21_22
368	JAR_composition_Na	JAR_composition	1400	ChemAxonByJAR	2_0_21_6
369	JAR_composition_ O	JAR_composition	163	ChemAxonByJAR	2_0_21_23
370	JAR_composition_P	JAR_composition	1377	ChemAxonByJAR	2_0_21_7
371	JAR_composition_ Pt	JAR_composition	1408	ChemAxonByJAR	2_0_21_24
372	JAR_composition_ S	JAR_composition	1096	ChemAxonByJAR	2_0_21_25
373	JAR_composition_Sb	JAR_composition	1410	ChemAxonByJAR	2_0_21_8
374	JAR_composition_Se	JAR_composition	1410	ChemAxonByJAR	2_0_21_9
375	JAR_composition_ Si	JAR_composition	1410	ChemAxonByJAR	2_0_21_26
376	JAR_composition_Al	JAR_composition	1409	ChemAxonByJAR	2_0_21_27
377	JAR_composition_As	JAR_composition	1410	ChemAxonByJAR	2_0_21_28
378	JAR_composition_C	JAR_composition	19	ChemAxonByJAR	2_0_21_29
379	JAR_composition_Ca	JAR_composition	1410	ChemAxonByJAR	2_0_21_30
380	JAR_composition_Cl	JAR_composition	1409	ChemAxonByJAR	2_0_21_31
381	JAR_composition_Fe	JAR_composition	1410	ChemAxonByJAR	2_0_21_32
382	JAR_composition_Ga	JAR_composition	1410	ChemAxonByJAR	2_0_21_33
383	JAR_composition_I	JAR_composition	1410	ChemAxonByJAR	2_0_21_34
384	JAR_composition_Li	JAR_composition	1410	ChemAxonByJAR	2_0_21_35
385	JAR_composition_Mg	JAR_composition	1409	ChemAxonByJAR	2_0_21_36
386	JAR_composition_N	JAR_composition	1410	ChemAxonByJAR	2_0_21_37
387	JAR_composition_S	JAR_composition	1410	ChemAxonByJAR	2_0_21_38
388	JAR_composition_Zn	JAR_composition	1410	ChemAxonByJAR	2_0_21_39
389	JAR_don_RationOfNA	JAR_don	0	ChemAxonByJAR	2_0_22_7
390	JAR_don_Mean	JAR_don	8	ChemAxonByJAR	2_0_22_3
391	JAR_don_Min	JAR_don	8	ChemAxonByJAR	2_0_22_4
392	JAR_don_Max	JAR_don	8	ChemAxonByJAR	2_0_22_2

No.	Feature Name	Chemcial Descriptors	#ofNA	Source	v5.1Code
393	JAR_don_Range	JAR_don	8	ChemAxonByJAR	2_0_22_6
394	JAR_don_Q3	JAR_don	8	ChemAxonByJAR	2_0_22_5
395	JAR_don_IQR	JAR_don	8	ChemAxonByJAR	2_0_22_1
396	JAR_don_Std	JAR_don	15	ChemAxonByJAR	2_0_22_8
397	JAR_donor_donorcount	JAR_donor	8	ChemAxonByJAR	2_1_23_1
398	JAR_donor_donsitecount	JAR_donor	8	ChemAxonByJAR	2_0_23_2
399	JAR_doublebondstereoisomercount_Stereoisomer count	JAR_doublebondstereoisomercount	0	ChemAxonByJAR	2_0_26_1
400	JAR_exactmass_Exact Mass	JAR_exactmass	0	ChemAxonByJAR	2_0_31_1
401	JAR_electrophiliclocalizationenergy_RationOfNA	JAR_electrophiliclocalizationenergy	0	ChemAxonByJAR	2_0_29_8
402	JAR_electrophiliclocalizationenergy_Mean	JAR_electrophiliclocalizationenergy	14	ChemAxonByJAR	2_0_29_3
403	JAR_electrophiliclocalizationenergy_Min	JAR_electrophiliclocalizationenergy	14	ChemAxonByJAR	2_0_29_4
404	JAR_electrophiliclocalizationenergy_Max	JAR_electrophiliclocalizationenergy	14	ChemAxonByJAR	2_0_29_2
405	JAR_electrophiliclocalizationenergy_Range	JAR_electrophiliclocalizationenergy	14	ChemAxonByJAR	2_0_29_7
406	JAR_electrophiliclocalizationenergy_Q1	JAR_electrophiliclocalizationenergy	14	ChemAxonByJAR	2_0_29_5
407	JAR_electrophiliclocalizationenergy_Q3	JAR_electrophiliclocalizationenergy	14	ChemAxonByJAR	2_0_29_6
408	JAR_electrophiliclocalizationenergy_IQR	JAR_electrophiliclocalizationenergy	14	ChemAxonByJAR	2_0_29_1
409	JAR_electrophiliclocalizationenergy_Std	JAR_electrophiliclocalizationenergy	29	ChemAxonByJAR	2_0_29_9
410	JAR_hmochargedensity_Charge density_RationOfNA	JAR_hmochargedensity	0	ChemAxonByJAR	2_0_38_8
411	JAR_hmochargedensity_Charge density_Mean	JAR_hmochargedensity	62	ChemAxonByJAR	2_0_38_3
412	JAR_hmochargedensity_Charge density_Min	JAR_hmochargedensity	62	ChemAxonByJAR	2_0_38_4
413	JAR_hmochargedensity_Charge density_Max	JAR_hmochargedensity	62	ChemAxonByJAR	2_0_38_2
414	JAR_hmochargedensity_Charge density_Range	JAR_hmochargedensity	62	ChemAxonByJAR	2_0_38_7
415	JAR_hmochargedensity_Charge density_Q1	JAR_hmochargedensity	62	ChemAxonByJAR	2_0_38_5
416	JAR_hmochargedensity_Charge density_Q3	JAR_hmochargedensity	62	ChemAxonByJAR	2_0_38_6
417	JAR_hmochargedensity_Charge density_IQR	JAR_hmochargedensity	62	ChemAxonByJAR	2_0_38_1
418	JAR_hmochargedensity_Charge density_Std	JAR_hmochargedensity	62	ChemAxonByJAR	2_0_38_9
419	JAR_hmoelectrondensity_Electron density_RationOfNA	JAR_hmoelectrondensity	0	ChemAxonByJAR	2_0_39_8
420	JAR_hmoelectrondensity_Electron density_Mean	JAR_hmoelectrondensity	62	ChemAxonByJAR	2_0_39_3
421	JAR_hmoelectrondensity_Electron density_Min	JAR_hmoelectrondensity	62	ChemAxonByJAR	2_0_39_4
422	JAR_hmoelectrondensity_Electron density_Max	JAR_hmoelectrondensity	62	ChemAxonByJAR	2_0_39_2
423	JAR_hmoelectrondensity_Electron density_Range	JAR_hmoelectrondensity	62	ChemAxonByJAR	2_0_39_7
424	JAR_hmoelectrondensity_Electron density_Q1	JAR_hmoelectrondensity	62	ChemAxonByJAR	2_0_39_5
425	JAR_hmoelectrondensity_Electron density_Q3	JAR_hmoelectrondensity	62	ChemAxonByJAR	2_0_39_6
426	JAR_hmoelectrondensity_Electron density_IQR	JAR_hmoelectrondensity	62	ChemAxonByJAR	2_0_39_1
427	JAR_hmoelectrondensity_Electron density_Std	JAR_hmoelectrondensity	62	ChemAxonByJAR	2_0_39_9
428	JAR_hmoelectrophilicityorder_Aromatic E(+) order_RationOfNA	JAR_hmoelectrophilicityorder	0	ChemAxonByJAR	2_0_40_8
429	JAR_hmoelectrophilicityorder_Aromatic E(+) order_Mean	JAR_hmoelectrophilicityorder	17	ChemAxonByJAR	2_0_40_3
430	JAR_hmoelectrophilicityorder_Aromatic E(+) order_Min	JAR_hmoelectrophilicityorder	17	ChemAxonByJAR	2_0_40_4
431	JAR_hmoelectrophilicityorder_Aromatic E(+) order_Max	JAR_hmoelectrophilicityorder	17	ChemAxonByJAR	2_0_40_2
432	JAR_hmoelectrophilicityorder_Aromatic E(+) order_Range	JAR_hmoelectrophilicityorder	17	ChemAxonByJAR	2_0_40_7
433	JAR_hmoelectrophilicityorder_Aromatic E(+) order_Q1	JAR_hmoelectrophilicityorder	17	ChemAxonByJAR	2_0_40_5
434	JAR_hmoelectrophilicityorder_Aromatic E(+) order_Q3	JAR_hmoelectrophilicityorder	17	ChemAxonByJAR	2_0_40_6
435	JAR_hmoelectrophilicityorder_Aromatic E(+) order_IQR	JAR_hmoelectrophilicityorder	17	ChemAxonByJAR	2_0_40_1
436	JAR_hmoelectrophilicityorder_Aromatic E(+) order_Std	JAR_hmoelectrophilicityorder	31	ChemAxonByJAR	2_0_40_9
437	JAR_hmoelectrophiliclocalizationenergy_Localization energy L(+)_RationOfNA	JAR_hmoelectrophiliclocalizationenergy	0	ChemAxonByJAR	2_0_41_8
438	JAR_hmoelectrophiliclocalizationenergy_Localization energy L(+)_Mean	JAR_hmoelectrophiliclocalizationenergy	17	ChemAxonByJAR	2_0_41_3
439	JAR_hmoelectrophiliclocalizationenergy_Localization energy L(+)_Min	JAR_hmoelectrophiliclocalizationenergy	17	ChemAxonByJAR	2_0_41_4
440	JAR_hmoelectrophiliclocalizationenergy_Localization energy L(+)_Max	JAR_hmoelectrophiliclocalizationenergy	17	ChemAxonByJAR	2_0_41_2
441	JAR_hmoelectrophiliclocalizationenergy_Localization energy L(+)_Range	JAR_hmoelectrophiliclocalizationenergy	17	ChemAxonByJAR	2_0_41_7
442	JAR_hmoelectrophiliclocalizationenergy_Localization energy L(+)_Q1	JAR_hmoelectrophiliclocalizationenergy	17	ChemAxonByJAR	2_0_41_5
443	JAR_hmoelectrophiliclocalizationenergy_Localization energy L(+)_Q3	JAR_hmoelectrophiliclocalizationenergy	17	ChemAxonByJAR	2_0_41_6
444	JAR_hmoelectrophiliclocalizationenergy_Localization energy L(+)_IQR	JAR_hmoelectrophiliclocalizationenergy	17	ChemAxonByJAR	2_0_41_1
445	JAR_hmoelectrophiliclocalizationenergy_Localization energy L(+)_Std	JAR_hmoelectrophiliclocalizationenergy	31	ChemAxonByJAR	2_0_41_9
446	JAR_elemanal_Mass	JAR_elemanal	0	ChemAxonByJAR	2_0_30_2
447	JAR_elemanal_Atom count	JAR_elemanal	0	ChemAxonByJAR	2_0_30_1
448	JAR_huckeleigenvalue_Eigenvalue_RationOfNA	JAR_huckeleigenvalue	0	ChemAxonByJAR	2_0_47_8
449	JAR_huckeleigenvalue_Eigenvalue_Mean	JAR_huckeleigenvalue	8	ChemAxonByJAR	2_0_47_3
450	JAR_huckeleigenvalue_Eigenvalue_Min	JAR_huckeleigenvalue	8	ChemAxonByJAR	2_0_47_4
451	JAR_huckeleigenvalue_Eigenvalue_Max	JAR_huckeleigenvalue	8	ChemAxonByJAR	2_0_47_2
452	JAR_huckeleigenvalue_Eigenvalue_Range	JAR_huckeleigenvalue	8	ChemAxonByJAR	2_0_47_7
453	JAR_huckeleigenvalue_Eigenvalue_Q1	JAR_huckeleigenvalue	8	ChemAxonByJAR	2_0_47_5
454	JAR_huckeleigenvalue_Eigenvalue_Q3	JAR_huckeleigenvalue	8	ChemAxonByJAR	2_0_47_6
455	JAR_huckeleigenvalue_Eigenvalue_IQR	JAR_huckeleigenvalue	8	ChemAxonByJAR	2_0_47_1
456	JAR_huckeleigenvalue_Eigenvalue_Std	JAR_huckeleigenvalue	563	ChemAxonByJAR	2_0_47_9
457	JAR_hmohuckeleigenvalue_Eigenvalue_RationOfNA	JAR_hmohuckeleigenvalue	0	ChemAxonByJAR	2_0_43_8
458	JAR_hmohuckeleigenvalue_Eigenvalue_Mean	JAR_hmohuckeleigenvalue	8	ChemAxonByJAR	2_0_43_3
459	JAR_hmohuckeleigenvalue_Eigenvalue_Min	JAR_hmohuckeleigenvalue	8	ChemAxonByJAR	2_0_43_4
460	JAR_hmohuckeleigenvalue_Eigenvalue_Max	JAR_hmohuckeleigenvalue	8	ChemAxonByJAR	2_0_43_2
461	JAR_hmohuckeleigenvalue_Eigenvalue_Range	JAR_hmohuckeleigenvalue	8	ChemAxonByJAR	2_0_43_7
462	JAR_hmohuckeleigenvalue_Eigenvalue_Q1	JAR_hmohuckeleigenvalue	8	ChemAxonByJAR	2_0_43_5
463	JAR_hmohuckeleigenvalue_Eigenvalue_Q3	JAR_hmohuckeleigenvalue	8	ChemAxonByJAR	2_0_43_6
464	JAR_hmohuckeleigenvalue_Eigenvalue_IQR	JAR_hmohuckeleigenvalue	8	ChemAxonByJAR	2_0_43_1
465	JAR_hmohuckeleigenvalue_Eigenvalue_Std	JAR_hmohuckeleigenvalue	483	ChemAxonByJAR	2_0_43_9
466	JAR_electrondensity_Electron Density_RationOfNA	JAR_electrondensity	0	ChemAxonByJAR	2_0_28_8
467	JAR_electrondensity_Electron Density_Mean	JAR_electrondensity	58	ChemAxonByJAR	2_0_28_3
468	JAR_electrondensity_Electron Density_Min	JAR_electrondensity	58	ChemAxonByJAR	2_0_28_4
469	JAR_electrondensity_Electron Density_Max	JAR_electrondensity	58	ChemAxonByJAR	2_0_28_2
470	JAR_electrondensity_Electron Density_Range	JAR_electrondensity	58	ChemAxonByJAR	2_0_28_7
471	JAR_electrondensity_Electron Density_Q1	JAR_electrondensity	58	ChemAxonByJAR	2_0_28_5

No.	Feature Name	Chemcial Descriptors	#ofNA	Source	v5.1Code
472	JAR_electrondensity_Electron Density_Q3	JAR_electrondensity	58	ChemAxonByJAR	2_0_28_6
473	JAR_electrondensity_Electron Density_IQR	JAR_electrondensity	58	ChemAxonByJAR	2_0_28_1
474	JAR_electrondensity_Electron Density_Std	JAR_electrondensity	58	ChemAxonByJAR	2_0_28_9
475	JAR_hmonucleophiliclocalizationenergy_Localization energy L(-)_RationOfNA	JAR_hmonucleophiliclocalizationenergy	0	ChemAxonByJAR	2_0_45_8
476	JAR_hmonucleophiliclocalizationenergy_Localization energy L(-)_Mean	JAR_hmonucleophiliclocalizationenergy	17	ChemAxonByJAR	2_0_45_3
477	JAR_hmonucleophiliclocalizationenergy_Localization energy L(-)_Min	JAR_hmonucleophiliclocalizationenergy	17	ChemAxonByJAR	2_0_45_4
478	JAR_hmonucleophiliclocalizationenergy_Localization energy L(-)_Max	JAR_hmonucleophiliclocalizationenergy	17	ChemAxonByJAR	2_0_45_2
479	JAR_hmonucleophiliclocalizationenergy_Localization energy L(-)_Range	JAR_hmonucleophiliclocalizationenergy	17	ChemAxonByJAR	2_0_45_7
480	JAR_hmonucleophiliclocalizationenergy_Localization energy L(-)_Q1	JAR_hmonucleophiliclocalizationenergy	17	ChemAxonByJAR	2_0_45_5
481	JAR_hmonucleophiliclocalizationenergy_Localization energy L(-)_Q3	JAR_hmonucleophiliclocalizationenergy	17	ChemAxonByJAR	2_0_45_6
482	JAR_hmonucleophiliclocalizationenergy_Localization energy L(-)_IQR	JAR_hmonucleophiliclocalizationenergy	17	ChemAxonByJAR	2_0_45_1
483	JAR_hmonucleophiliclocalizationenergy_Localization energy L(-)_Std	JAR_hmonucleophiliclocalizationenergy	31	ChemAxonByJAR	2_0_45_9
484	JAR_hmopienergy_Pi energy	JAR_hmopienergy	17	ChemAxonByJAR	2_0_46_1
485	JAR_logd_(pH=0)	JAR_logd	8	ChemAxonByJAR	2_1_53_1
486	JAR_logd_(pH=1)	JAR_logd	8	ChemAxonByJAR	2_1_53_2
487	JAR_logd_(pH=2)	JAR_logd	8	ChemAxonByJAR	2_1_53_8
488	JAR_logd_(pH=3)	JAR_logd	8	ChemAxonByJAR	2_1_53_9
489	JAR_logd_(pH=4)	JAR_logd	8	ChemAxonByJAR	2_1_53_10
490	JAR_logd_(pH=5)	JAR_logd	8	ChemAxonByJAR	2_1_53_11
491	JAR_logd_(pH=6)	JAR_logd	8	ChemAxonByJAR	2_1_53_12
492	JAR_logd_(pH=7)	JAR_logd	8	ChemAxonByJAR	2_1_53_13
493	JAR_logd_(pH=8)	JAR_logd	8	ChemAxonByJAR	2_1_53_14
494	JAR_logd_(pH=9)	JAR_logd	8	ChemAxonByJAR	2_1_53_15
495	JAR_logd_(pH=10)	JAR_logd	8	ChemAxonByJAR	2_1_53_3
496	JAR_logd_(pH=11)	JAR_logd	8	ChemAxonByJAR	2_1_53_4
497	JAR_logd_(pH=12)	JAR_logd	8	ChemAxonByJAR	2_1_53_5
498	JAR_logd_(pH=13)	JAR_logd	8	ChemAxonByJAR	2_1_53_6
499	JAR_logd_(pH=14)	JAR_logd	8	ChemAxonByJAR	2_1_53_7
500	JAR_msa_Van der Waals surface area (3D)	JAR_msa	17	ChemAxonByJAR	2_0_56_1
501	JAR_msacc_(pH=0)	JAR_msacc	8	ChemAxonByJAR	2_0_57_1
502	JAR_msacc_(pH=1)	JAR_msacc	8	ChemAxonByJAR	2_0_57_2
503	JAR_msacc_(pH=2)	JAR_msacc	8	ChemAxonByJAR	2_0_57_8
504	JAR_msacc_(pH=3)	JAR_msacc	8	ChemAxonByJAR	2_0_57_9
505	JAR_msacc_(pH=4)	JAR_msacc	8	ChemAxonByJAR	2_0_57_10
506	JAR_msacc_(pH=5)	JAR_msacc	8	ChemAxonByJAR	2_0_57_11
507	JAR_msacc_(pH=6)	JAR_msacc	8	ChemAxonByJAR	2_0_57_12
508	JAR_msacc_(pH=7)	JAR_msacc	8	ChemAxonByJAR	2_0_57_13
509	JAR_msacc_(pH=8)	JAR_msacc	8	ChemAxonByJAR	2_0_57_14
510	JAR_msacc_(pH=9)	JAR_msacc	8	ChemAxonByJAR	2_0_57_15
511	JAR_msacc_(pH=10)	JAR_msacc	8	ChemAxonByJAR	2_0_57_3
512	JAR_msacc_(pH=11)	JAR_msacc	8	ChemAxonByJAR	2_0_57_4
513	JAR_msacc_(pH=12)	JAR_msacc	8	ChemAxonByJAR	2_0_57_5
514	JAR_msacc_(pH=13)	JAR_msacc	8	ChemAxonByJAR	2_0_57_6
515	JAR_msacc_(pH=14)	JAR_msacc	8	ChemAxonByJAR	2_0_57_7
516	JAR_msdon_(pH=0)	JAR_msdon	8	ChemAxonByJAR	2_0_58_1
517	JAR_msdon_(pH=1)	JAR_msdon	8	ChemAxonByJAR	2_0_58_2
518	JAR_msdon_(pH=2)	JAR_msdon	8	ChemAxonByJAR	2_0_58_8
519	JAR_msdon_(pH=3)	JAR_msdon	8	ChemAxonByJAR	2_0_58_9
520	JAR_msdon_(pH=4)	JAR_msdon	8	ChemAxonByJAR	2_0_58_10
521	JAR_msdon_(pH=5)	JAR_msdon	8	ChemAxonByJAR	2_0_58_11
522	JAR_msdon_(pH=6)	JAR_msdon	8	ChemAxonByJAR	2_0_58_12
523	JAR_msdon_(pH=7)	JAR_msdon	8	ChemAxonByJAR	2_0_58_13
524	JAR_msdon_(pH=8)	JAR_msdon	8	ChemAxonByJAR	2_0_58_14
525	JAR_msdon_(pH=9)	JAR_msdon	8	ChemAxonByJAR	2_0_58_15
526	JAR_msdon_(pH=10)	JAR_msdon	8	ChemAxonByJAR	2_0_58_3
527	JAR_msdon_(pH=11)	JAR_msdon	8	ChemAxonByJAR	2_0_58_4
528	JAR_msdon_(pH=12)	JAR_msdon	8	ChemAxonByJAR	2_0_58_5
529	JAR_msdon_(pH=13)	JAR_msdon	8	ChemAxonByJAR	2_0_58_6
530	JAR_msdon_(pH=14)	JAR_msdon	8	ChemAxonByJAR	2_0_58_7
531	JAR_nucleophiliclocalizationenergy_Localization energy L(-)_RationOfNA	JAR_nucleophiliclocalizationenergy	0	ChemAxonByJAR	2_0_59_8
532	JAR_nucleophiliclocalizationenergy_Localization energy L(-)_Mean	JAR_nucleophiliclocalizationenergy	14	ChemAxonByJAR	2_0_59_3
533	JAR_nucleophiliclocalizationenergy_Localization energy L(-)_Min	JAR_nucleophiliclocalizationenergy	14	ChemAxonByJAR	2_0_59_4
534	JAR_nucleophiliclocalizationenergy_Localization energy L(-)_Max	JAR_nucleophiliclocalizationenergy	14	ChemAxonByJAR	2_0_59_2
535	JAR_nucleophiliclocalizationenergy_Localization energy L(-)_Range	JAR_nucleophiliclocalizationenergy	14	ChemAxonByJAR	2_0_59_7
536	JAR_nucleophiliclocalizationenergy_Localization energy L(-)_Q1	JAR_nucleophiliclocalizationenergy	14	ChemAxonByJAR	2_0_59_5
537	JAR_nucleophiliclocalizationenergy_Localization energy L(-)_Q3	JAR_nucleophiliclocalizationenergy	14	ChemAxonByJAR	2_0_59_6
538	JAR_nucleophiliclocalizationenergy_Localization energy L(-)_IQR	JAR_nucleophiliclocalizationenergy	14	ChemAxonByJAR	2_0_59_1
539	JAR_nucleophiliclocalizationenergy_Localization energy L(-)_Std	JAR_nucleophiliclocalizationenergy	29	ChemAxonByJAR	2_0_59_9
540	JAR_pI	JAR_pi	476	ChemAxonByJAR	2_0_60_1
541	JAR_pichargedensity_Pi charge density_RationOfNA	JAR_pichargedensity	0	ChemAxonByJAR	2_0_61_8
542	JAR_pichargedensity_Pi charge density_Mean	JAR_pichargedensity	58	ChemAxonByJAR	2_0_61_3
543	JAR_pichargedensity_Pi charge density_Min	JAR_pichargedensity	58	ChemAxonByJAR	2_0_61_4
544	JAR_pichargedensity_Pi charge density_Max	JAR_pichargedensity	58	ChemAxonByJAR	2_0_61_2
545	JAR_pichargedensity_Pi charge density_Range	JAR_pichargedensity	58	ChemAxonByJAR	2_0_61_7
546	JAR_pichargedensity_Pi charge density_Q1	JAR_pichargedensity	58	ChemAxonByJAR	2_0_61_5
547	JAR_pichargedensity_Pi charge density_Q3	JAR_pichargedensity	58	ChemAxonByJAR	2_0_61_6
548	JAR_pichargedensity_Pi charge density_IQR	JAR_pichargedensity	58	ChemAxonByJAR	2_0_61_1
549	JAR_pichargedensity_Pi charge density_Std	JAR_pichargedensity	58	ChemAxonByJAR	2_0_61_9
550	JAR_pienergy_Pi energy	JAR_pienergy	14	ChemAxonByJAR	2_0_62_1

No.	Feature Name	Chemcial Descriptors	#ofNA	Source	v5.1Code
551	JAR_pka_apKa1	JAR_pka	310	ChemAxonByJAR	2_0_63_1
552	JAR_pka_apKa2	JAR_pka	735	ChemAxonByJAR	2_0_63_2
553	JAR_pka_bpKa1	JAR_pka	89	ChemAxonByJAR	2_0_63_12
554	JAR_pka_bpKa2	JAR_pka	293	ChemAxonByJAR	2_0_63_13
555	JAR_pka_atoms_RationOfNA	JAR_pka	0	ChemAxonByJAR	2_0_63_10
556	JAR_pka_atoms_Mean	JAR_pka	30	ChemAxonByJAR	2_0_63_5
557	JAR_pka_atoms_Min	JAR_pka	30	ChemAxonByJAR	2_0_63_6
558	JAR_pka_atoms_Max	JAR_pka	30	ChemAxonByJAR	2_0_63_4
559	JAR_pka_atoms_Range	JAR_pka	30	ChemAxonByJAR	2_0_63_9
560	JAR_pka_atoms_Q1	JAR_pka	30	ChemAxonByJAR	2_0_63_7
561	JAR_pka_atoms_Q3	JAR_pka	30	ChemAxonByJAR	2_0_63_8
562	JAR_pka_atoms_IQR	JAR_pka	30	ChemAxonByJAR	2_0_63_3
563	JAR_pka_atoms_Std	JAR_pka	129	ChemAxonByJAR	2_0_63_11
564	JAR_polarsurfacearea_Polar surface area	JAR_polarsurfacearea	0	ChemAxonByJAR	2_0_65_1
565	JAR_totalchargedensity_Total charge density_RationOfNA	JAR_totalchargedensity	0	ChemAxonByJAR	2_0_85_8
566	JAR_totalchargedensity_Total charge density_Mean	JAR_totalchargedensity	58	ChemAxonByJAR	2_0_85_3
567	JAR_totalchargedensity_Total charge density_Min	JAR_totalchargedensity	58	ChemAxonByJAR	2_0_85_4
568	JAR_totalchargedensity_Total charge density_Max	JAR_totalchargedensity	58	ChemAxonByJAR	2_0_85_2
569	JAR_totalchargedensity_Total charge density_Range	JAR_totalchargedensity	58	ChemAxonByJAR	2_0_85_7
570	JAR_totalchargedensity_Total charge density_Q1	JAR_totalchargedensity	58	ChemAxonByJAR	2_0_85_5
571	JAR_totalchargedensity_Total charge density_Q3	JAR_totalchargedensity	58	ChemAxonByJAR	2_0_85_6
572	JAR_totalchargedensity_Total charge density_IQR	JAR_totalchargedensity	58	ChemAxonByJAR	2_0_85_1
573	JAR_totalchargedensity_Total charge density_Std	JAR_totalchargedensity	58	ChemAxonByJAR	2_0_85_9
574	JAR_stericeffectindex_Steric effect index_RationOfNA	JAR_stericeffectindex	0	ChemAxonByJAR	2_0_80_8
575	JAR_stericeffectindex_Steric effect index_Mean	JAR_stericeffectindex	4	ChemAxonByJAR	2_0_80_3
576	JAR_stericeffectindex_Steric effect index_Min	JAR_stericeffectindex	4	ChemAxonByJAR	2_0_80_4
577	JAR_stericeffectindex_Steric effect index_Max	JAR_stericeffectindex	4	ChemAxonByJAR	2_0_80_2
578	JAR_stericeffectindex_Steric effect index_Range	JAR_stericeffectindex	4	ChemAxonByJAR	2_0_80_7
579	JAR_stericeffectindex_Steric effect index_Q1	JAR_stericeffectindex	4	ChemAxonByJAR	2_0_80_5
580	JAR_stericeffectindex_Steric effect index_Q3	JAR_stericeffectindex	4	ChemAxonByJAR	2_0_80_6
581	JAR_stericeffectindex_Steric effect index_IQR	JAR_stericeffectindex	4	ChemAxonByJAR	2_0_80_1
582	JAR_stericeffectindex_Steric effect index_Std	JAR_stericeffectindex	8	ChemAxonByJAR	2_0_80_9
583	JAR_refractivity_Refractivity	JAR_refractivity	0	ChemAxonByJAR	2_1_68_1
584	JAR_ringatom_Ring atom_NumberOfTRUE	JAR_ringatom	0	ChemAxonByJAR	2_0_69_3
585	JAR_ringatom_Ring atom_NumberOfFALSE	JAR_ringatom	0	ChemAxonByJAR	2_0_69_1
586	JAR_ringatom_Ring atom_NumberOfTotal	JAR_ringatom	0	ChemAxonByJAR	2_0_69_2
587	JAR_ringatom_Ring atom_RatioOfTRUE	JAR_ringatom	29	ChemAxonByJAR	2_0_69_5
588	JAR_ringatom_Ring atom_RatioOfFALSE	JAR_ringatom	29	ChemAxonByJAR	2_0_69_4
589	JAR_ringcountofatom_Ring count of atom	JAR_ringcountofatom	0	ChemAxonByJAR	2_0_73_1
590	JAR_ringsystemcount_Ring system count	JAR_ringsystemcount	0	ChemAxonByJAR	2_0_74_1
591	JAR_ringsystemcountofsize_Ring system count of size	JAR_ringsystemcountofsize	0	ChemAxonByJAR	2_0_75_1
592	JAR_smallestatomringsize_Smallest ring size of atom_RationOfNA	JAR_smallestatomringsize	121	ChemAxonByJAR	2_0_77_8
593	JAR_smallestatomringsize_Smallest ring size of atom_Mean	JAR_smallestatomringsize	4	ChemAxonByJAR	2_0_77_3
594	JAR_smallestatomringsize_Smallest ring size of atom_Min	JAR_smallestatomringsize	4	ChemAxonByJAR	2_0_77_4
595	JAR_smallestatomringsize_Smallest ring size of atom_Max	JAR_smallestatomringsize	4	ChemAxonByJAR	2_0_77_2
596	JAR_smallestatomringsize_Smallest ring size of atom_Range	JAR_smallestatomringsize	4	ChemAxonByJAR	2_0_77_7
597	JAR_smallestatomringsize_Smallest ring size of atom_Q1	JAR_smallestatomringsize	4	ChemAxonByJAR	2_0_77_5
598	JAR_smallestatomringsize_Smallest ring size of atom_Q3	JAR_smallestatomringsize	4	ChemAxonByJAR	2_0_77_6
599	JAR_smallestatomringsize_Smallest ring size of atom_IQR	JAR_smallestatomringsize	4	ChemAxonByJAR	2_0_77_1
600	JAR_smallestatomringsize_Smallest ring size of atom_Std	JAR_smallestatomringsize	8	ChemAxonByJAR	2_0_77_9
601	JAR_stereodoublebondcount_Stereo double bond count	JAR_stereodoublebondcount	0	ChemAxonByJAR	2_0_78_1
602	JAR_stereoisomercount_Stereoisomer count	JAR_stereoisomercount	0	ChemAxonByJAR	2_0_79_1
603	JAR_tetrahedralstereoisomercount_Stereoisomer count	JAR_tetrahedralstereoisomercount	0	ChemAxonByJAR	2_0_83_1
604	JAR_topanal_Atom count	JAR_topanal	0	ChemAxonByJAR	2_0_84_7
605	JAR_topanal_Aliphatic atom count	JAR_topanal	0	ChemAxonByJAR	2_0_84_1
606	JAR_topanal_Aromatic atom count	JAR_topanal	0	ChemAxonByJAR	2_0_84_4
607	JAR_topanal_Bond count	JAR_topanal	0	ChemAxonByJAR	2_0_84_8
608	JAR_topanal_Aliphatic bond count	JAR_topanal	0	ChemAxonByJAR	2_0_84_2
609	JAR_topanal_Aromatic bond count	JAR_topanal	0	ChemAxonByJAR	2_0_84_5
610	JAR_topanal_Rotatable bond count	JAR_topanal	0	ChemAxonByJAR	2_0_84_18
611	JAR_topanal_Ring count	JAR_topanal	0	ChemAxonByJAR	2_0_84_17
612	JAR_topanal_Aliphatic ring count	JAR_topanal	0	ChemAxonByJAR	2_0_84_3
613	JAR_topanal_Aromatic ring count	JAR_topanal	0	ChemAxonByJAR	2_0_84_6
614	JAR_topanal_Hetero ring count	JAR_topanal	0	ChemAxonByJAR	2_0_84_11
615	JAR_topanal_Heteroaliphatic ring count	JAR_topanal	0	ChemAxonByJAR	2_0_84_12
616	JAR_topanal_Heteroaromatic ring count	JAR_topanal	0	ChemAxonByJAR	2_0_84_13
617	JAR_topanal_Ring atom count	JAR_topanal	0	ChemAxonByJAR	2_0_84_15
618	JAR_topanal_Ring bond count	JAR_topanal	0	ChemAxonByJAR	2_0_84_16
619	JAR_topanal_Chain atom count	JAR_topanal	0	ChemAxonByJAR	2_0_84_9
620	JAR_topanal_Chain bond count	JAR_topanal	0	ChemAxonByJAR	2_0_84_10
621	JAR_topanal_Smallest ring size	JAR_topanal	0	ChemAxonByJAR	2_0_84_19
622	JAR_topanal_Largest ring size	JAR_topanal	0	ChemAxonByJAR	2_0_84_14
623	JAR_volume_van der Waals volume	JAR_volume	0	ChemAxonByJAR	2_0_87_1
624	JAR_wateraccessiblesurfacearea_ASA	JAR_wateraccessiblesurfacearea	12	ChemAxonByJAR	2_0_88_1
625	JAR_wateraccessiblesurfacearea_ASA+	JAR_wateraccessiblesurfacearea	12	ChemAxonByJAR	2_0_88_5
626	JAR_wateraccessiblesurfacearea_ASA-	JAR_wateraccessiblesurfacearea	12	ChemAxonByJAR	2_0_88_2
627	JAR_wateraccessiblesurfacearea_ASA_H	JAR_wateraccessiblesurfacearea	12	ChemAxonByJAR	2_0_88_3
628	JAR_wateraccessiblesurfacearea_ASA_P	JAR_wateraccessiblesurfacearea	12	ChemAxonByJAR	2_0_88_4
629	JAR_wienerindex_Wiener index	JAR_wienerindex	54	ChemAxonByJAR	2_0_89_1

No.	Feature Name	Chemcial Descriptors	#ofNA	Source	v5.1Code
630	JAR_wienerpolarity_Wiener polarity	JAR_wienerpolarity	54	ChemAxonByJAR	2_0_90_1
631	JAR_localizationenergy_L_minus_RationOfNA	JAR_localizationenergy	0	ChemAxonByJAR	2_0_52_9
632	JAR_localizationenergy_L_minus_Mean	JAR_localizationenergy	14	ChemAxonByJAR	2_0_52_4
633	JAR_localizationenergy_L_minus_Min	JAR_localizationenergy	14	ChemAxonByJAR	2_0_52_5
634	JAR_localizationenergy_L_minus_Max	JAR_localizationenergy	14	ChemAxonByJAR	2_0_52_3
635	JAR_localizationenergy_L_minus_Range	JAR_localizationenergy	14	ChemAxonByJAR	2_0_52_8
636	JAR_localizationenergy_L_minus_Q1	JAR_localizationenergy	14	ChemAxonByJAR	2_0_52_6
637	JAR_localizationenergy_L_minus_Q3	JAR_localizationenergy	14	ChemAxonByJAR	2_0_52_7
638	JAR_localizationenergy_L_minus_IQR	JAR_localizationenergy	14	ChemAxonByJAR	2_0_52_2
639	JAR_localizationenergy_L_minus_Std	JAR_localizationenergy	29	ChemAxonByJAR	2_0_52_10
640	JAR_localizationenergy_L_plus_RationOfNA	JAR_localizationenergy	0	ChemAxonByJAR	2_0_52_18
641	JAR_localizationenergy_L_plus_Mean	JAR_localizationenergy	14	ChemAxonByJAR	2_0_52_13
642	JAR_localizationenergy_L_plus_Min	JAR_localizationenergy	14	ChemAxonByJAR	2_0_52_14
643	JAR_localizationenergy_L_plus_Max	JAR_localizationenergy	14	ChemAxonByJAR	2_0_52_12
644	JAR_localizationenergy_L_plus_Range	JAR_localizationenergy	14	ChemAxonByJAR	2_0_52_17
645	JAR_localizationenergy_L_plus_Q1	JAR_localizationenergy	14	ChemAxonByJAR	2_0_52_15
646	JAR_localizationenergy_L_plus_Q3	JAR_localizationenergy	14	ChemAxonByJAR	2_0_52_16
647	JAR_localizationenergy_L_plus_IQR	JAR_localizationenergy	14	ChemAxonByJAR	2_0_52_11
648	JAR_localizationenergy_L_plus_Std	JAR_localizationenergy	29	ChemAxonByJAR	2_0_52_19
649	JAR_localizationenergy_intercept	JAR_localizationenergy	14	ChemAxonByJAR	2_0_52_1
650	JAR_localizationenergy_slope	JAR_localizationenergy	38	ChemAxonByJAR	2_0_52_20
651	JAR_hmolocalizationenergy_L_minus_RationOfNA	JAR_hmolocalizationenergy	0	ChemAxonByJAR	2_0_44_9
652	JAR_hmolocalizationenergy_L_minus_Mean	JAR_hmolocalizationenergy	17	ChemAxonByJAR	2_0_44_4
653	JAR_hmolocalizationenergy_L_minus_Min	JAR_hmolocalizationenergy	17	ChemAxonByJAR	2_0_44_5
654	JAR_hmolocalizationenergy_L_minus_Max	JAR_hmolocalizationenergy	17	ChemAxonByJAR	2_0_44_3
655	JAR_hmolocalizationenergy_L_minus_Range	JAR_hmolocalizationenergy	17	ChemAxonByJAR	2_0_44_8
656	JAR_hmolocalizationenergy_L_minus_Q1	JAR_hmolocalizationenergy	17	ChemAxonByJAR	2_0_44_6
657	JAR_hmolocalizationenergy_L_minus_Q3	JAR_hmolocalizationenergy	17	ChemAxonByJAR	2_0_44_7
658	JAR_hmolocalizationenergy_L_minus_Std	JAR_hmolocalizationenergy	17	ChemAxonByJAR	2_0_44_10
659	JAR_hmolocalizationenergy_L_minus_IQR	JAR_hmolocalizationenergy	31	ChemAxonByJAR	2_0_44_2
660	JAR_hmolocalizationenergy_L_plus_RationOfNA	JAR_hmolocalizationenergy	0	ChemAxonByJAR	2_0_44_18
661	JAR_hmolocalizationenergy_L_plus_Mean	JAR_hmolocalizationenergy	17	ChemAxonByJAR	2_0_44_13
662	JAR_hmolocalizationenergy_L_plus_Min	JAR_hmolocalizationenergy	17	ChemAxonByJAR	2_0_44_14
663	JAR_hmolocalizationenergy_L_plus_Max	JAR_hmolocalizationenergy	17	ChemAxonByJAR	2_0_44_12
664	JAR_hmolocalizationenergy_L_plus_Range	JAR_hmolocalizationenergy	17	ChemAxonByJAR	2_0_44_17
665	JAR_hmolocalizationenergy_L_plus_Q1	JAR_hmolocalizationenergy	17	ChemAxonByJAR	2_0_44_15
666	JAR_hmolocalizationenergy_L_plus_Q3	JAR_hmolocalizationenergy	17	ChemAxonByJAR	2_0_44_16
667	JAR_hmolocalizationenergy_L_plus_IQR	JAR_hmolocalizationenergy	17	ChemAxonByJAR	2_0_44_11
668	JAR_hmolocalizationenergy_L_plus_Std	JAR_hmolocalizationenergy	31	ChemAxonByJAR	2_0_44_19
669	JAR_hmolocalizationenergy_intercept	JAR_hmolocalizationenergy	17	ChemAxonByJAR	2_0_44_1
670	JAR_hmolocalizationenergy_slope	JAR_hmolocalizationenergy	42	ChemAxonByJAR	2_0_44_20
671	JAR_hmohuckel_Bcolumn_E_plus_RationOfNA	JAR_hmohuckel	0	ChemAxonByJAR	2_0_42_6
672	JAR_hmohuckel_Bcolumn_E_plus_Mean	JAR_hmohuckel	17	ChemAxonByJAR	2_0_42_3
673	JAR_hmohuckel_Bcolumn_E_plus_Max	JAR_hmohuckel	17	ChemAxonByJAR	2_0_42_2
674	JAR_hmohuckel_Bcolumn_E_plus_Q1	JAR_hmohuckel	17	ChemAxonByJAR	2_0_42_4
675	JAR_hmohuckel_Bcolumn_E_plus_Q3	JAR_hmohuckel	17	ChemAxonByJAR	2_0_42_5
676	JAR_hmohuckel_Bcolumn_E_plus_IQR	JAR_hmohuckel	17	ChemAxonByJAR	2_0_42_1
677	JAR_hmohuckel_Bcolumn_E_plus_Std	JAR_hmohuckel	31	ChemAxonByJAR	2_0_42_7
678	JAR_hmohuckel_Bcolumn_intercept	JAR_hmohuckel	18	ChemAxonByJAR	2_0_42_8
679	JAR_hmohuckel_Bcolumn_slope	JAR_hmohuckel	32	ChemAxonByJAR	2_0_42_9
680	JAR_huckeltable_Bcolumn_intercept	JAR_huckeltable	15	ChemAxonByJAR	2_0_48_8
681	JAR_huckeltable_Bcolumn_slope	JAR_huckeltable	30	ChemAxonByJAR	2_0_48_9
682	JAR_huckeltable_Bcolumn_E_plus_RationOfNA	JAR_huckeltable	0	ChemAxonByJAR	2_0_48_6
683	JAR_huckeltable_Bcolumn_E_plus_Mean	JAR_huckeltable	14	ChemAxonByJAR	2_0_48_2
684	JAR_huckeltable_Bcolumn_E_plus_Range	JAR_huckeltable	14	ChemAxonByJAR	2_0_48_5
685	JAR_huckeltable_Bcolumn_E_plus_Q1	JAR_huckeltable	14	ChemAxonByJAR	2_0_48_3
686	JAR_huckeltable_Bcolumn_E_plus_Q3	JAR_huckeltable	14	ChemAxonByJAR	2_0_48_4
687	JAR_huckeltable_Bcolumn_E_plus_IQR	JAR_huckeltable	14	ChemAxonByJAR	2_0_48_1
688	JAR_huckeltable_Bcolumn_E_plus_Std	JAR_huckeltable	29	ChemAxonByJAR	2_0_48_7
689	SDF_JCHEM_ACCEPTOR_COUNT	SDF_JCHEM_ACCEPTOR_COUNT	2	SDF	3_1_4_1
690	SDF_JCHEM_DONOR_COUNT	SDF_JCHEM_DONOR_COUNT	2	SDF	3_1_6_1
691	SDF_JCHEM_ACIDIC_PKA	SDF_JCHEM_ACIDIC_PKA	733	SDF	3_1_5_1
692	SDF_ALOGPS_LOGP	SDF_ALOGPS_LOGP	46	SDF	3_0_1_1
693	SDF_JCHEM_LOGP	SDF_JCHEM_LOGP	2	SDF	3_1_7_1
694	SDF_ALOGPS_LOGS	SDF_ALOGPS_LOGS	46	SDF	3_0_2_1
695	SDF_JCHEM_POLARIZABILITY	SDF_JCHEM_POLARIZABILITY	6	SDF	3_1_9_1
696	SDF_JCHEM_POLAR_SURFACE_AREA	SDF_JCHEM_POLAR_SURFACE_AREA	6	SDF	3_1_8_1
697	SDF_JCHEM_REFRACTIVITY	SDF_JCHEM_REFRACTIVITY	0	SDF	3_1_10_1
698	SDF_JCHEM_ROTATABLE_BOND_COUNT	SDF_JCHEM_ROTATABLE_BOND_COU	6	SDF	3_1_11_1
699	SDF_ALOGPS_SOLUBILITY	SDF_ALOGPS_SOLUBILITY	46	SDF	3_0_3_1
700	RCDK_apol	RCDK_APolDescriptor	3	RCDK	4_0_4_1
701	RCDK_bpol	RCDK_BPolDescriptor	3	RCDK	4_0_14_1
702	RCDK_PPSA.1	RCDK_CPSADescriptor	8	RCDK	4_1_20_13
703	RCDK_PPSA.2	RCDK_CPSADescriptor	8	RCDK	4_1_20_14
704	RCDK_PPSA.3	RCDK_CPSADescriptor	8	RCDK	4_1_20_15
705	RCDK_PNSA.1	RCDK_CPSADescriptor	8	RCDK	4_1_20_10
706	RCDK_PNSA.2	RCDK_CPSADescriptor	11	RCDK	4_1_20_11
707	RCDK_PNSA.3	RCDK_CPSADescriptor	11	RCDK	4_1_20_12
708	RCDK_DPSA.1	RCDK_CPSADescriptor	8	RCDK	4_1_20_1

No.	Feature Name	Chemcial Descriptors	#ofNA	Source	v5.1Code
709	RCDK_DPSA.2	RCDK_CPSADescriptor	11	RCDK	4_1_20_2
710	RCDK_DPSA.3	RCDK_CPSADescriptor	11	RCDK	4_1_20_3
711	RCDK_FPSA.1	RCDK_CPSADescriptor	8	RCDK	4_1_20_7
712	RCDK_FPSA.2	RCDK_CPSADescriptor	8	RCDK	4_1_20_8
713	RCDK_FPSA.3	RCDK_CPSADescriptor	8	RCDK	4_1_20_9
714	RCDK_FNSA.1	RCDK_CPSADescriptor	8	RCDK	4_1_20_4
715	RCDK_FNSA.2	RCDK_CPSADescriptor	11	RCDK	4_1_20_5
716	RCDK_FNSA.3	RCDK_CPSADescriptor	11	RCDK	4_1_20_6
717	RCDK_WPSA.1	RCDK_CPSADescriptor	8	RCDK	4_1_20_27
718	RCDK_WPSA.2	RCDK_CPSADescriptor	8	RCDK	4_1_20_28
719	RCDK_WPSA.3	RCDK_CPSADescriptor	8	RCDK	4_1_20_29
720	RCDK_WNSA.1	RCDK_CPSADescriptor	8	RCDK	4_1_20_24
721	RCDK_WNSA.2	RCDK_CPSADescriptor	11	RCDK	4_1_20_25
722	RCDK_WNSA.3	RCDK_CPSADescriptor	11	RCDK	4_1_20_26
723	RCDK_RPCG	RCDK_CPSADescriptor	53	RCDK	4_1_20_19
724	RCDK_RNCG	RCDK_CPSADescriptor	55	RCDK	4_1_20_17
725	RCDK_RPCS	RCDK_CPSADescriptor	53	RCDK	4_1_20_20
726	RCDK_RNCS	RCDK_CPSADescriptor	55	RCDK	4_1_20_18
727	RCDK_THSA	RCDK_CPSADescriptor	8	RCDK	4_0_20_22
728	RCDK_TPSA	RCDK_CPSADescriptor	8	RCDK	4_0_20_23
729	RCDK_RHSA	RCDK_CPSADescriptor	8	RCDK	4_0_20_16
730	RCDK_RPSA	RCDK_CPSADescriptor	8	RCDK	4_0_20_21
731	RCDK_nHBAcc	RCDK_HBondAcceptorCountDescriptor	0	RCDK	4_0_25_1
732	RCDK_nHBDon	RCDK_HBondDonorCountDescriptor	0	RCDK	4_0_26_1
733	RCDK_TopoPSA	RCDK_TPSADescriptor	2	RCDK	4_0_41_1
734	RCDK_nA	RCDK_AminoAcidCountDescriptor	0	RCDK	4_0_3_1
735	RCDK_nR	RCDK_AminoAcidCountDescriptor	0	RCDK	4_0_3_15
736	RCDK_nN	RCDK_AminoAcidCountDescriptor	0	RCDK	4_0_3_12
737	RCDK_nD	RCDK_AminoAcidCountDescriptor	0	RCDK	4_0_3_3
738	RCDK_nC	RCDK_AminoAcidCountDescriptor	0	RCDK	4_0_3_2
739	RCDK_nF	RCDK_AminoAcidCountDescriptor	0	RCDK	4_0_3_5
740	RCDK_nQ	RCDK_AminoAcidCountDescriptor	0	RCDK	4_0_3_14
741	RCDK_nE	RCDK_AminoAcidCountDescriptor	0	RCDK	4_0_3_4
742	RCDK_nG	RCDK_AminoAcidCountDescriptor	0	RCDK	4_0_3_6
743	RCDK_nH	RCDK_AminoAcidCountDescriptor	0	RCDK	4_0_3_7
744	RCDK_nI	RCDK_AminoAcidCountDescriptor	0	RCDK	4_0_3_8
745	RCDK_nP	RCDK_AminoAcidCountDescriptor	0	RCDK	4_0_3_13
746	RCDK_nL	RCDK_AminoAcidCountDescriptor	0	RCDK	4_0_3_10
747	RCDK_nK	RCDK_AminoAcidCountDescriptor	0	RCDK	4_0_3_9
748	RCDK_nM	RCDK_AminoAcidCountDescriptor	0	RCDK	4_0_3_11
749	RCDK_nS	RCDK_AminoAcidCountDescriptor	0	RCDK	4_0_3_16
750	RCDK_nT	RCDK_AminoAcidCountDescriptor	0	RCDK	4_0_3_17
751	RCDK_nY	RCDK_AminoAcidCountDescriptor	0	RCDK	4_0_3_20
752	RCDK_nV	RCDK_AminoAcidCountDescriptor	0	RCDK	4_0_3_18
753	RCDK_nW	RCDK_AminoAcidCountDescriptor	0	RCDK	4_0_3_19
754	RCDK_ATSc1	RCDK_AutocorrelationDescriptorCharge	3	RCDK	4_0_8_1
755	RCDK_ATSc2	RCDK_AutocorrelationDescriptorCharge	3	RCDK	4_0_8_2
756	RCDK_ATSc3	RCDK_AutocorrelationDescriptorCharge	3	RCDK	4_0_8_3
757	RCDK_ATSc4	RCDK_AutocorrelationDescriptorCharge	2	RCDK	4_0_8_4
758	RCDK_ATSc5	RCDK_AutocorrelationDescriptorCharge	2	RCDK	4_0_8_5
759	RCDK_ATSm1	RCDK_AutocorrelationDescriptorMass	0	RCDK	4_0_9_1
760	RCDK_ATSm2	RCDK_AutocorrelationDescriptorMass	0	RCDK	4_0_9_2
761	RCDK_ATSm3	RCDK_AutocorrelationDescriptorMass	0	RCDK	4_0_9_3
762	RCDK_ATSm4	RCDK_AutocorrelationDescriptorMass	0	RCDK	4_0_9_4
763	RCDK_ATSm5	RCDK_AutocorrelationDescriptorMass	0	RCDK	4_0_9_5
764	RCDK_ATSp1	RCDK_AutocorrelationDescriptorPolarizab	26	RCDK	4_0_10_1
765	RCDK_ATSp2	RCDK_AutocorrelationDescriptorPolarizab	26	RCDK	4_0_10_2
766	RCDK_ATSp3	RCDK_AutocorrelationDescriptorPolarizab	26	RCDK	4_0_10_3
767	RCDK_ATSp4	RCDK_AutocorrelationDescriptorPolarizab	26	RCDK	4_0_10_4
768	RCDK_ATSp5	RCDK_AutocorrelationDescriptorPolarizab	26	RCDK	4_0_10_5
769	RCDK_C1SP1	RCDK_CarbonTypesDescriptor	0	RCDK	4_0_15_1
770	RCDK_C2SP1	RCDK_CarbonTypesDescriptor	0	RCDK	4_0_15_4
771	RCDK_C1SP2	RCDK_CarbonTypesDescriptor	0	RCDK	4_0_15_2
772	RCDK_C2SP2	RCDK_CarbonTypesDescriptor	0	RCDK	4_0_15_5
773	RCDK_C3SP2	RCDK_CarbonTypesDescriptor	0	RCDK	4_0_15_7
774	RCDK_C1SP3	RCDK_CarbonTypesDescriptor	0	RCDK	4_0_15_3
775	RCDK_C2SP3	RCDK_CarbonTypesDescriptor	0	RCDK	4_0_15_6
776	RCDK_C3SP3	RCDK_CarbonTypesDescriptor	0	RCDK	4_0_15_8
777	RCDK_C4SP3	RCDK_CarbonTypesDescriptor	0	RCDK	4_0_15_9
778	RCDK_ECCEN	RCDK_EccentricConnectivityIndexDescript	0	RCDK	4_0_21_1
779	RCDK_fragC	RCDK_FragmentComplexityDescriptor	0	RCDK	4_0_23_1
780	RCDK_HybRatio	RCDK_HybridizationRatioDescriptor	16	RCDK	4_0_27_1
781	RCDK_Kier1	RCDK_KappaShapeIndicesDescriptor	0	RCDK	4_1_28_1
782	RCDK_Kier2	RCDK_KappaShapeIndicesDescriptor	44	RCDK	4_1_28_2
783	RCDK_Kier3	RCDK_KappaShapeIndicesDescriptor	51	RCDK	4_1_28_3
784	RCDK_khs.sLi	RCDK_KierHallSmartsDescriptor	2	RCDK	4_0_29_32
785	RCDK_khs.ssBe	RCDK_KierHallSmartsDescriptor	2	RCDK	4_0_29_39
786	RCDK_khs.ssssBe	RCDK_KierHallSmartsDescriptor	2	RCDK	4_0_29_66
787	RCDK_khs.ssBH	RCDK_KierHallSmartsDescriptor	2	RCDK	4_0_29_40

No.	Feature Name	Chemcial Descriptors	#ofNA	Source	v5.1Code
788	RCDK_khs.sssB	RCDK_KierHallSmartsDescriptor	2	RCDK	4_0_29_54
789	RCDK_khs.ssssB	RCDK_KierHallSmartsDescriptor	2	RCDK	4_0_29_65
790	RCDK_khs.sCH3	RCDK_KierHallSmartsDescriptor	2	RCDK	4_0_29_27
791	RCDK_khs.dCH2	RCDK_KierHallSmartsDescriptor	2	RCDK	4_0_29_10
792	RCDK_khs.ssCH2	RCDK_KierHallSmartsDescriptor	2	RCDK	4_0_29_41
793	RCDK_khs.tCH	RCDK_KierHallSmartsDescriptor	2	RCDK	4_0_29_77
794	RCDK_khs.dsCH	RCDK_KierHallSmartsDescriptor	2	RCDK	4_0_29_18
795	RCDK_khs.aaCH	RCDK_KierHallSmartsDescriptor	2	RCDK	4_0_29_2
796	RCDK_khs.sssCH	RCDK_KierHallSmartsDescriptor	2	RCDK	4_0_29_55
797	RCDK_khs.ddC	RCDK_KierHallSmartsDescriptor	2	RCDK	4_0_29_11
798	RCDK_khs.tsC	RCDK_KierHallSmartsDescriptor	2	RCDK	4_0_29_79
799	RCDK_khs.dssC	RCDK_KierHallSmartsDescriptor	2	RCDK	4_0_29_21
800	RCDK_khs.aasC	RCDK_KierHallSmartsDescriptor	2	RCDK	4_0_29_7
801	RCDK_khs.aaaC	RCDK_KierHallSmartsDescriptor	2	RCDK	4_0_29_1
802	RCDK_khs.ssssC	RCDK_KierHallSmartsDescriptor	2	RCDK	4_0_29_67
803	RCDK_khs.sNH3	RCDK_KierHallSmartsDescriptor	2	RCDK	4_0_29_34
804	RCDK_khs.sNH2	RCDK_KierHallSmartsDescriptor	2	RCDK	4_0_29_33
805	RCDK_khs.ssNH2	RCDK_KierHallSmartsDescriptor	2	RCDK	4_0_29_47
806	RCDK_khs.dNH	RCDK_KierHallSmartsDescriptor	2	RCDK	4_0_29_15
807	RCDK_khs.ssNH	RCDK_KierHallSmartsDescriptor	2	RCDK	4_0_29_46
808	RCDK_khs.aaNH	RCDK_KierHallSmartsDescriptor	2	RCDK	4_0_29_4
809	RCDK_khs.tN	RCDK_KierHallSmartsDescriptor	2	RCDK	4_0_29_78
810	RCDK_khs.sssNH	RCDK_KierHallSmartsDescriptor	2	RCDK	4_0_29_61
811	RCDK_khs.dsN	RCDK_KierHallSmartsDescriptor	2	RCDK	4_0_29_20
812	RCDK_khs.aaN	RCDK_KierHallSmartsDescriptor	2	RCDK	4_0_29_3
813	RCDK_khs.sssN	RCDK_KierHallSmartsDescriptor	2	RCDK	4_0_29_60
814	RCDK_khs.ddsN	RCDK_KierHallSmartsDescriptor	2	RCDK	4_0_29_12
815	RCDK_khs.aasN	RCDK_KierHallSmartsDescriptor	2	RCDK	4_0_29_9
816	RCDK_khs.ssssN	RCDK_KierHallSmartsDescriptor	2	RCDK	4_0_29_70
817	RCDK_khs.sOH	RCDK_KierHallSmartsDescriptor	2	RCDK	4_0_29_35
818	RCDK_khs.dO	RCDK_KierHallSmartsDescriptor	2	RCDK	4_0_29_16
819	RCDK_khs.ssO	RCDK_KierHallSmartsDescriptor	2	RCDK	4_0_29_49
820	RCDK_khs.aaO	RCDK_KierHallSmartsDescriptor	2	RCDK	4_0_29_5
821	RCDK_khs.sF	RCDK_KierHallSmartsDescriptor	2	RCDK	4_0_29_29
822	RCDK_khs.sSiH3	RCDK_KierHallSmartsDescriptor	2	RCDK	4_0_29_45
823	RCDK_khs.ssSiH2	RCDK_KierHallSmartsDescriptor	2	RCDK	4_0_29_59
824	RCDK_khs.sssSiH	RCDK_KierHallSmartsDescriptor	2	RCDK	4_0_29_69
825	RCDK_khs.ssssSi	RCDK_KierHallSmartsDescriptor	2	RCDK	4_0_29_74
826	RCDK_khs.sPH2	RCDK_KierHallSmartsDescriptor	2	RCDK	4_0_29_37
827	RCDK_khs.ssPH	RCDK_KierHallSmartsDescriptor	2	RCDK	4_0_29_51
828	RCDK_khs.sssP	RCDK_KierHallSmartsDescriptor	2	RCDK	4_0_29_63
829	RCDK_khs.dsssP	RCDK_KierHallSmartsDescriptor	2	RCDK	4_0_29_24
830	RCDK_khs.ssssssP	RCDK_KierHallSmartsDescriptor	2	RCDK	4_0_29_76
831	RCDK_khs.sSH	RCDK_KierHallSmartsDescriptor	2	RCDK	4_0_29_44
832	RCDK_khs.dS	RCDK_KierHallSmartsDescriptor	2	RCDK	4_0_29_17
833	RCDK_khs.ssS	RCDK_KierHallSmartsDescriptor	2	RCDK	4_0_29_52
834	RCDK_khs.aaS	RCDK_KierHallSmartsDescriptor	2	RCDK	4_0_29_6
835	RCDK_khs.dssS	RCDK_KierHallSmartsDescriptor	2	RCDK	4_0_29_22
836	RCDK_khs.ddssS	RCDK_KierHallSmartsDescriptor	2	RCDK	4_0_29_13
837	RCDK_khs.sCl	RCDK_KierHallSmartsDescriptor	2	RCDK	4_0_29_28
838	RCDK_khs.sGeH3	RCDK_KierHallSmartsDescriptor	2	RCDK	4_0_29_30
839	RCDK_khs.ssGeH2	RCDK_KierHallSmartsDescriptor	2	RCDK	4_0_29_43
840	RCDK_khs.sssGeH	RCDK_KierHallSmartsDescriptor	2	RCDK	4_0_29_58
841	RCDK_khs.ssssGe	RCDK_KierHallSmartsDescriptor	2	RCDK	4_0_29_68
842	RCDK_khs.sAsH2	RCDK_KierHallSmartsDescriptor	2	RCDK	4_0_29_25
843	RCDK_khs.ssAsH	RCDK_KierHallSmartsDescriptor	2	RCDK	4_0_29_38
844	RCDK_khs.sssAs	RCDK_KierHallSmartsDescriptor	2	RCDK	4_0_29_53
845	RCDK_khs.ssssAs	RCDK_KierHallSmartsDescriptor	2	RCDK	4_0_29_56
846	RCDK_khs.ssssssAs	RCDK_KierHallSmartsDescriptor	2	RCDK	4_0_29_73
847	RCDK_khs.sSeH	RCDK_KierHallSmartsDescriptor	2	RCDK	4_0_29_42
848	RCDK_khs.dSe	RCDK_KierHallSmartsDescriptor	2	RCDK	4_0_29_19
849	RCDK_khs.ssSe	RCDK_KierHallSmartsDescriptor	2	RCDK	4_0_29_57
850	RCDK_khs.aaSe	RCDK_KierHallSmartsDescriptor	2	RCDK	4_0_29_8
851	RCDK_khs.dssSe	RCDK_KierHallSmartsDescriptor	2	RCDK	4_0_29_23
852	RCDK_khs.ddssSe	RCDK_KierHallSmartsDescriptor	2	RCDK	4_0_29_14
853	RCDK_khs.sBr	RCDK_KierHallSmartsDescriptor	2	RCDK	4_0_29_26
854	RCDK_khs.sSnH3	RCDK_KierHallSmartsDescriptor	2	RCDK	4_0_29_48
855	RCDK_khs.ssSnH2	RCDK_KierHallSmartsDescriptor	2	RCDK	4_0_29_62
856	RCDK_khs.sssSnH	RCDK_KierHallSmartsDescriptor	2	RCDK	4_0_29_71
857	RCDK_khs.ssssSn	RCDK_KierHallSmartsDescriptor	2	RCDK	4_0_29_75
858	RCDK_khs.sI	RCDK_KierHallSmartsDescriptor	2	RCDK	4_0_29_31
859	RCDK_khs.sPbH3	RCDK_KierHallSmartsDescriptor	2	RCDK	4_0_29_36
860	RCDK_khs.ssPbH2	RCDK_KierHallSmartsDescriptor	2	RCDK	4_0_29_50
861	RCDK_khs.sssPbH	RCDK_KierHallSmartsDescriptor	2	RCDK	4_0_29_64
862	RCDK_khs.ssssPb	RCDK_KierHallSmartsDescriptor	2	RCDK	4_0_29_72
863	RCDK_MDEC.11	RCDK_MDEDescriptor	0	RCDK	4_0_35_1
864	RCDK_MDEC.12	RCDK_MDEDescriptor	0	RCDK	4_0_35_2
865	RCDK_MDEC.13	RCDK_MDEDescriptor	0	RCDK	4_0_35_3
866	RCDK_MDEC.14	RCDK_MDEDescriptor	0	RCDK	4_0_35_4

No.	Feature Name	Chemcial Descriptors	#ofNA	Source	v5.1Code
867	RCDK_MDEC.22	RCDK_MDEDescriptor	0	RCDK	4_0_35_5
868	RCDK_MDEC.23	RCDK_MDEDescriptor	0	RCDK	4_0_35_6
869	RCDK_MDEC.24	RCDK_MDEDescriptor	0	RCDK	4_0_35_7
870	RCDK_MDEC.33	RCDK_MDEDescriptor	0	RCDK	4_0_35_8
871	RCDK_MDEC.34	RCDK_MDEDescriptor	0	RCDK	4_0_35_9
872	RCDK_MDEC.44	RCDK_MDEDescriptor	0	RCDK	4_0_35_10
873	RCDK_MDEO.11	RCDK_MDEDescriptor	0	RCDK	4_0_35_17
874	RCDK_MDEO.12	RCDK_MDEDescriptor	0	RCDK	4_0_35_18
875	RCDK_MDEO.22	RCDK_MDEDescriptor	0	RCDK	4_0_35_19
876	RCDK_MDEN.11	RCDK_MDEDescriptor	0	RCDK	4_0_35_11
877	RCDK_MDEN.12	RCDK_MDEDescriptor	0	RCDK	4_0_35_12
878	RCDK_MDEN.13	RCDK_MDEDescriptor	0	RCDK	4_0_35_13
879	RCDK_MDEN.22	RCDK_MDEDescriptor	0	RCDK	4_0_35_14
880	RCDK_MDEN.23	RCDK_MDEDescriptor	0	RCDK	4_0_35_15
881	RCDK_MDEN.33	RCDK_MDEDescriptor	0	RCDK	4_0_35_16
882	RCDK_PetitjeanNumber	RCDK_PetitjeanNumberDescriptor	0	RCDK	4_1_37_1
883	RCDK_topoShape	RCDK_PetitjeanShapeIndexDescriptor	4	RCDK	4_1_38_2
884	RCDK_geomShape	RCDK_PetitjeanShapeIndexDescriptor	10	RCDK	4_1_38_1
885	RCDK_VABC	RCDK_VABCDescriptor	48	RCDK	4_0_42_1
886	RCDK_VAdjMat	RCDK_VAdjMaDescriptor	0	RCDK	4_0_43_1
887	RCDK_WPATH	RCDK_WienerNumbersDescriptor	0	RCDK	4_1_47_1
888	RCDK_WPOL	RCDK_WienerNumbersDescriptor	0	RCDK	4_1_47_2
889	RCDK_Zagreb	RCDK_ZagrebIndexDescriptor	0	RCDK	4_1_49_1
890	RCDK_MOMI.X	RCDK_MomentOfInertiaDescriptor	9	RCDK	4_1_36_2
891	RCDK_MOMI.Y	RCDK_MomentOfInertiaDescriptor	9	RCDK	4_1_36_5
892	RCDK_MOMI.Z	RCDK_MomentOfInertiaDescriptor	9	RCDK	4_1_36_7
893	RCDK_MOMI.XY	RCDK_MomentOfInertiaDescriptor	9	RCDK	4_1_36_3
894	RCDK_MOMI.XZ	RCDK_MomentOfInertiaDescriptor	9	RCDK	4_1_36_4
895	RCDK_MOMI.YZ	RCDK_MomentOfInertiaDescriptor	9	RCDK	4_1_36_6
896	RCDK_MOMI.R	RCDK_MomentOfInertiaDescriptor	9	RCDK	4_1_36_1
897	RCDK_ALogP	RCDK_ALOGPDescriptor	92	RCDK	4_0_2_1
898	RCDK_ALogp2	RCDK_ALOGPDescriptor	92	RCDK	4_0_2_2
899	RCDK_AMR	RCDK_ALOGPDescriptor	92	RCDK	4_0_2_3
900	RCDK_nAcid	RCDK_AcidicGroupCountDescriptor	2	RCDK	4_0_1_1
901	RCDK_naAromAtom	RCDK_AromaticAtomsCountDescriptor	0	RCDK	4_0_5_1
902	RCDK_nAromBond	RCDK_AromaticBondsCountDescriptor	0	RCDK	4_0_6_1
903	RCDK_nAtom	RCDK_AtomCountDescriptor	0	RCDK	4_0_7_1
904	RCDK_nBase	RCDK_BasicGroupCountDescriptor	2	RCDK	4_0_11_1
905	RCDK_nB	RCDK_BondCountDescriptor	0	RCDK	4_0_13_1
906	RCDK_nAtomLC	RCDK_LargestChainDescriptor	0	RCDK	4_0_30_1
907	RCDK_nAtomP	RCDK_LargestPiSystemDescriptor	0	RCDK	4_0_31_1
908	RCDK_nAtomLAC	RCDK_LongestAliphaticChainDescriptor	0	RCDK	4_0_33_1
909	RCDK_MLogP	RCDK_MannholdLogPDescriptor	0	RCDK	4_0_34_1
910	RCDK_nRotB	RCDK_RotatableBondsCountDescriptor	0	RCDK	4_0_39_1
911	RCDK_MW	RCDK_WeightDescriptor	3	RCDK	4_0_44_1
912	RCDK_Wlambda1.unity	RCDK_WHIMDescriptor	6	RCDK	4_0_46_11
913	RCDK_Wlambda2.unity	RCDK_WHIMDescriptor	6	RCDK	4_0_46_12
914	RCDK_Wlambda3.unity	RCDK_WHIMDescriptor	6	RCDK	4_0_46_13
915	RCDK_Wnu1.unity	RCDK_WHIMDescriptor	10	RCDK	4_0_46_14
916	RCDK_Wnu2.unity	RCDK_WHIMDescriptor	10	RCDK	4_0_46_15
917	RCDK_Wgamma1.unity	RCDK_WHIMDescriptor	12	RCDK	4_0_46_7
918	RCDK_Wgamma2.unity	RCDK_WHIMDescriptor	1402	RCDK	4_0_46_8
919	RCDK_Wgamma3.unity	RCDK_WHIMDescriptor	1402	RCDK	4_0_46_9
920	RCDK_Weta1.unity	RCDK_WHIMDescriptor	1409	RCDK	4_0_46_3
921	RCDK_Weta2.unity	RCDK_WHIMDescriptor	15	RCDK	4_0_46_4
922	RCDK_Weta3.unity	RCDK_WHIMDescriptor	10	RCDK	4_0_46_5
923	RCDK_WT.unity	RCDK_WHIMDescriptor	6	RCDK	4_0_46_16
924	RCDK_WA.unity	RCDK_WHIMDescriptor	6	RCDK	4_0_46_1
925	RCDK_WV.unity	RCDK_WHIMDescriptor	6	RCDK	4_0_46_17
926	RCDK_WK.unity	RCDK_WHIMDescriptor	10	RCDK	4_0_46_10
927	RCDK_WG.unity	RCDK_WHIMDescriptor	1405	RCDK	4_0_46_6
928	RCDK_WD.unity	RCDK_WHIMDescriptor	1409	RCDK	4_0_46_2
929	RCDK_GRAV.1	RCDK_GravitationalIndexDescriptor	9	RCDK	4_1_24_1
930	RCDK_GRAV.2	RCDK_GravitationalIndexDescriptor	9	RCDK	4_1_24_2
931	RCDK_GRAV.3	RCDK_GravitationalIndexDescriptor	9	RCDK	4_1_24_3
932	RCDK_GRAVH.1	RCDK_GravitationalIndexDescriptor	9	RCDK	4_1_24_7
933	RCDK_GRAVH.2	RCDK_GravitationalIndexDescriptor	9	RCDK	4_1_24_8
934	RCDK_GRAVH.3	RCDK_GravitationalIndexDescriptor	9	RCDK	4_1_24_9
935	RCDK_GRAV.4	RCDK_GravitationalIndexDescriptor	9	RCDK	4_1_24_4
936	RCDK_GRAV.5	RCDK_GravitationalIndexDescriptor	9	RCDK	4_1_24_5
937	RCDK_GRAV.6	RCDK_GravitationalIndexDescriptor	9	RCDK	4_1_24_6
938	RCDK_XLogP	RCDK_XLogPDescriptor	40	RCDK	4_1_48_1
939	RCDK_SCH.3	RCDK_ChiChainDescriptor	28	RCDK	4_0_16_1
940	RCDK_SCH.4	RCDK_ChiChainDescriptor	28	RCDK	4_0_16_2
941	RCDK_SCH.5	RCDK_ChiChainDescriptor	28	RCDK	4_0_16_3
942	RCDK_SCH.6	RCDK_ChiChainDescriptor	28	RCDK	4_0_16_4
943	RCDK_SCH.7	RCDK_ChiChainDescriptor	28	RCDK	4_0_16_5
944	RCDK_VCH.3	RCDK_ChiChainDescriptor	28	RCDK	4_0_16_6
945	RCDK_VCH.4	RCDK_ChiChainDescriptor	28	RCDK	4_0_16_7

No.	Feature Name	Chemcial Descriptors	#ofNA	Source	v5.1Code
946	RCDK_VCH.5	RCDK_ChiChainDescriptor	28	RCDK	4_0_16_8
947	RCDK_VCH.6	RCDK_ChiChainDescriptor	28	RCDK	4_0_16_9
948	RCDK_VCH.7	RCDK_ChiChainDescriptor	28	RCDK	4_0_16_10
949	RCDK_SC.3	RCDK_ChiClusterDescriptor	28	RCDK	4_0_17_1
950	RCDK_SC.4	RCDK_ChiClusterDescriptor	28	RCDK	4_0_17_2
951	RCDK_SC.5	RCDK_ChiClusterDescriptor	28	RCDK	4_0_17_3
952	RCDK_SC.6	RCDK_ChiClusterDescriptor	28	RCDK	4_0_17_4
953	RCDK_VC.3	RCDK_ChiClusterDescriptor	28	RCDK	4_0_17_5
954	RCDK_VC.4	RCDK_ChiClusterDescriptor	28	RCDK	4_0_17_6
955	RCDK_VC.5	RCDK_ChiClusterDescriptor	28	RCDK	4_0_17_7
956	RCDK_VC.6	RCDK_ChiClusterDescriptor	28	RCDK	4_0_17_8
957	RCDK_SPC.4	RCDK_ChiPathClusterDescriptor	28	RCDK	4_0_18_1
958	RCDK_SPC.5	RCDK_ChiPathClusterDescriptor	28	RCDK	4_0_18_2
959	RCDK_SPC.6	RCDK_ChiPathClusterDescriptor	28	RCDK	4_0_18_3
960	RCDK_VPC.4	RCDK_ChiPathClusterDescriptor	28	RCDK	4_0_18_4
961	RCDK_VPC.5	RCDK_ChiPathClusterDescriptor	28	RCDK	4_0_18_5
962	RCDK_VPC.6	RCDK_ChiPathClusterDescriptor	28	RCDK	4_0_18_6
963	RCDK_SP.0	RCDK_ChiPathDescriptor	28	RCDK	4_0_19_1
964	RCDK_SP.1	RCDK_ChiPathDescriptor	28	RCDK	4_0_19_2
965	RCDK_SP.2	RCDK_ChiPathDescriptor	28	RCDK	4_0_19_3
966	RCDK_SP.3	RCDK_ChiPathDescriptor	28	RCDK	4_0_19_4
967	RCDK_SP.4	RCDK_ChiPathDescriptor	28	RCDK	4_0_19_5
968	RCDK_SP.5	RCDK_ChiPathDescriptor	28	RCDK	4_0_19_6
969	RCDK_SP.6	RCDK_ChiPathDescriptor	28	RCDK	4_0_19_7
970	RCDK_SP.7	RCDK_ChiPathDescriptor	28	RCDK	4_0_19_8
971	RCDK_VP.0	RCDK_ChiPathDescriptor	28	RCDK	4_0_19_9
972	RCDK_VP.1	RCDK_ChiPathDescriptor	28	RCDK	4_0_19_10
973	RCDK_VP.2	RCDK_ChiPathDescriptor	28	RCDK	4_0_19_11
974	RCDK_VP.3	RCDK_ChiPathDescriptor	28	RCDK	4_0_19_12
975	RCDK_VP.4	RCDK_ChiPathDescriptor	28	RCDK	4_0_19_13
976	RCDK_VP.5	RCDK_ChiPathDescriptor	28	RCDK	4_0_19_14
977	RCDK_VP.6	RCDK_ChiPathDescriptor	28	RCDK	4_0_19_15
978	RCDK_VP.7	RCDK_ChiPathDescriptor	28	RCDK	4_0_19_16
979	RCDK_FMF	RCDK_FMFDescriptor	4	RCDK	4_0_22_1
980	RCDK_WTPT.1	RCDK_WeightedPathDescriptor	0	RCDK	4_0_45_1
981	RCDK_WTPT.2	RCDK_WeightedPathDescriptor	0	RCDK	4_0_45_2
982	RCDK_WTPT.3	RCDK_WeightedPathDescriptor	0	RCDK	4_0_45_3
983	RCDK_WTPT.4	RCDK_WeightedPathDescriptor	0	RCDK	4_0_45_4
984	RCDK_WTPT.5	RCDK_WeightedPathDescriptor	0	RCDK	4_0_45_5
985	RCDK_LOBMAX	RCDK_LengthOverBreadthDescriptor	16	RCDK	4_0_32_1
986	RCDK_LOBMIN	RCDK_LengthOverBreadthDescriptor	16	RCDK	4_0_32_2
987	RCDK_LipinskiFailures	RCDK_RuleOfFiveDescriptor	14	RCDK	4_0_40_1
988	RCDK_BCUTw.1l	RCDK_BCUTDescriptor	29	RCDK	4_1_12_6
989	RCDK_BCUTw.1h	RCDK_BCUTDescriptor	29	RCDK	4_1_12_5
990	RCDK_BCUTc.1l	RCDK_BCUTDescriptor	29	RCDK	4_1_12_2
991	RCDK_BCUTc.1h	RCDK_BCUTDescriptor	29	RCDK	4_1_12_1
992	RCDK_BCUTp.1l	RCDK_BCUTDescriptor	29	RCDK	4_1_12_4
993	RCDK_BCUTp.1h	RCDK_BCUTDescriptor	29	RCDK	4_1_12_3

Appendix C

ADE_i	FileName	HIGH	LOW	N	G.R.	Accuracy	Acc/G.R.	FeatureSelected
11427	Combine_outY_PT_all_PT11427_iPR0_3_2_3.csv	216	288	504	0.571	0.921	1.611	X1_1_87_1$X2_0_28_6$X2_0_41_4$X2_1_35_1$X4_0_19_3$X4_1_12_5
11464	Combine_outY_PT_all_PT11464_iPR0_6_2.csv	420	288	708	0.593	0.953	1.607	X4_0_19_6$X4_0_21_1$X4_0_9_5
11832	Combine_outY_PT_all_PT11832_iPR0_3_2.csv	371	351	722	0.514	0.921	1.792	X4_0_14_1$X4_0_35_6$X4_0_35_8$X4_1_24_4$X4_1_36_1
12025	Combine_outY_PT_all_PT12025_iPR0_1.csv	404	471	875	0.538	0.744	1.382	X1_0_117_3$X1_0_18_2$X2_1_68_1$X4_0_27_1$X4_0_29_2$X4_0_42_1$X4_1_36_7
1209	Combine_outY_PT_all_PT1209_iPR0_3.csv	466	420	886	0.526	0.703	1.337	X1_0_21_4$X2_0_27_1$X4_0_25_1$X4_0_8_5$X4_1_12_2$X4_1_12_5$X4_1_20_14$ X4_1_36_2$X4_1_38_1
12146	Combine_outY_PT_all_PT12146_iPR0_1_6.csv	365	352	717	0.509	0.929	1.825	X1_0_119_1$X1_0_72_1$X4_0_10_5$X4_0_19_12$X4_0_21_1
127	Combine_outY_PT_all_PT127_iPR0_2_3.csv	223	500	723	0.692	0.885	1.280	X2_0_19_6$X2_0_39_5$X2_0_39_9$X2_0_41_3$X2_0_41_6$X2_0_58_9$X2_1_53_15 $X4_0_42_1$X4_0_46_4
13423	Combine_outY_PT_all_PT13423_iPR0_6.csv	455	421	876	0.519	0.770	1.483	X2_0_41_3$X2_0_44_7$X2_0_57_14$X2_0_57_3$X2_0_80_1$X2_0_80_6$X2_0_88_1 $X4_0_20_16$X4_0_46_15
13961	Combine_outY_PT_all_PT13961_iPR0_2_2.csv	404	414	818	0.506	0.704	1.391	X1_1_20_2$X2_0_19_5$X2_0_41_2$X2_1_53_7$X4_0_17_3$X4_1_20_5
14115	Combine_outY_PT_all_PT14115_iPR0_2_3.csv	217	480	697	0.689	0.905	1.314	X4_0_10_3$X4_0_16_10$X4_0_42_1$X4_1_20_5
15621	Combine_outY_PT_all_PT15621_iPR0_1_3.csv	372	342	714	0.521	0.920	1.766	X4_0_19_4$X4_1_20_2
15877	Combine_outY_PT_all_PT15877_iPR0_3_2.csv	508	231	739	0.687	0.910	1.323	X2_0_21_29$X2_0_39_9$X2_0_44_1$X2_0_44_7$X2_0_52_6$X2_0_57_1$X2_1_8_1 $X4_0_29_7$X4_1_20_6
15894	Combine_outY_PT_all_PT15894_iPR0_6_1_6.csv	247	257	504	0.510	0.946	1.856	X4_0_19_9
15965	Combine_outY_PT_all_PT15965_iPR0_2_3.csv	397	326	723	0.549	0.892	1.625	X1_0_76_1$X2_0_22_3$X2_0_41_1$X2_1_55_1$X4_0_14_1$X4_0_19_4
17426	Combine_outY_PT_all_PT17426_iPR0_3_2.csv	349	302	651	0.536	0.966	1.802	X1_0_46_1$X2_0_89_1$X4_0_9_2
2730	Combine_outY_PT_all_PT2730_iPR0_6_1.csv	468	241	709	0.660	0.939	1.423	X1_0_56_1$X4_0_10_1$X4_0_17_1$X4_1_24_1
2820	Combine_outY_PT_all_PT2820_iPR0_6_1_6.csv	248	274	522	0.525	0.939	1.788	X4_0_10_3$X4_1_20_13
285	Combine_outY_PT_all_PT285_iPR0.csv	303	367	670	0.548	0.915	1.670	X1_1_99_1$X2_1_82_1$X4_1_12_4
3427	Combine_outY_PT_all_PT3427_iPR0_1_6.csv	364	320	684	0.532	0.927	1.742	X4_0_21_1$X4_0_9_3$X4_1_24_4$X4_1_28_2
4682	Combine_outY_PT_all_PT4682_iPR0_6_1_6.csv	282	243	525	0.537	0.928	1.727	X2_0_90_1$X4_1_20_6$X4_1_24_4$X4_1_36_5$X4_1_47_1
5658	Combine_outY_PT_all_PT5658_iPR0_3.csv	475	433	908	0.523	0.708	1.354	X1_1_87_1$X2_0_39_3$X2_0_52_8$X2_0_57_3$X2_0_80_3$X2_0_9_9$X4_0_18_1 $X4_0_18_2$X4_0_19_2$X4_0_8_2$X4_0_8_4$X4_1_20_24
5768	Combine_outY_PT_all_PT5768_iPR0_6_1.csv	489	244	733	0.667	0.871	1.305	X1_0_113_2$X1_0_75_1$X1_0_77_1$X2_0_41_1$X2_0_81_1$X2_0_90_1$X3_0_2_1
6036	Combine_outY_PT_all_PT6036_iPR0_1.csv	414	479	893	0.536	0.700	1.305	X3_0_1_1$X3_0_2_1$X4_0_45_2
6071	Combine_outY_PT_all_PT6071_iPR0_2_3.csv	353	352	705	0.501	0.912	1.822	X1_1_98_1$X2_0_39_9$X2_0_88_3$X2_0_88_4$X4_0_19_5
6142	Combine_outY_PT_all_PT6142_iPR0_3_2_3.csv	221	290	511	0.568	0.963	1.697	X4_0_19_11$X4_0_35_5
6161	Combine_outY_PT_all_PT6161_iPR0_1_6.csv	388	330	718	0.540	0.936	1.732	X1_0_78_1$X4_0_10_1$X4_0_15_5$X4_0_35_5$X4_0_4_1
6806	Combine_outY_PT_all_PT6806_iPR0_2.csv	416	495	911	0.543	0.709	1.305	X1_0_73_1$X1_0_76_1$X2_0_52_4$X2_1_68_1$X4_0_19_4$X4_0_35_14$X4_0_35_19 $X4_0_8_5$X4_0_9_5
7246	Combine_outY_PT_all_PT7246_iPR0_3_3.csv	284	363	647	0.561	0.778	1.386	X1_0_73_1$X2_0_41_3$X2_0_42_9$X2_0_57_3$X2_0_80_6$X4_0_35_5$X4_1_12_2 $X4_1_20_13$X4_1_20_14$X4_1_20_28$X4_1_36_5$X4_1_48_1
7405	Combine_outY_PT_all_PT7405_iPR0_2_6.csv	379	328	707	0.536	0.951	1.773	X2_1_35_1$X4_0_8_2$X4_0_9_3
8110	Combine_outY_PT_all_PT8110_iPR0_1.csv	410	450	860	0.523	0.700	1.338	X2_0_21_29$X2_0_29_5$X2_0_29_9$X2_0_39_9$X2_0_44_4$X2_1_53_9$X4_0_19_2 $X4_0_35_5
8306	Combine_outY_PT_all_PT8306_iPR0_2_3.csv	393	327	720	0.546	0.864	1.583	X1_0_46_1$X1_0_71_1$X2_0_44_3$X2_0_88_5$X4_0_35_5$X4_0_35_6$X4_0_46_17
8433	Combine_outY_PT_all_PT8433_iPR0_1.csv	432	471	903	0.522	0.659	1.263	X1_0_36_1$X2_0_21_25$X2_0_21_29$X2_0_29_5$X2_0_41_6$X2_0_85_3$X2_0_88_4 $X3_0_1_1$X4_0_20_22$X4_0_46_10
9163	Combine_outY_PT_all_PT9163_iPR0_3_2.csv	356	316	672	0.530	0.931	1.758	X2_1_55_1$X4_0_19_7$X4_0_2_3$X4_0_8_4$X4_1_36_2
9260	Combine_outY_PT_all_PT9260_iPR0_6_6_2.csv	263	243	506	0.520	0.718	1.381	X1_0_38_1$X2_0_39_9$X2_0_88_4$X4_0_34_1$X4_0_35_6$X4_0_45_2$X4_1_12_3 $X4_1_12_4$X4_1_20_1
9566	Combine_outY_PT_all_PT9566_iPR0_2_3.csv	244	423	667	0.634	0.928	1.463	X2_1_53_5$X4_1_12_5$X4_1_20_2$X4_1_20_8

Appendix B

ADE_i	iPR	CutValue	high	low	n	I	RG	Accuracy(H2010)	Accuracy(New)	Accuracy(H2010+New)
1	9	0.011373162	503	496	999	1.014	0.504	0.546	0.525	0.519
31	4	0.002279678	621	634	1255	1.021	0.505	0.505	0.503	0.484
41	4	0.002395959	620	636	1256	1.026	0.506	0.490	0.502	0.506
42	8	0.007406189	527	533	1060	1.011	0.503	0.521	0.477	0.479
45	0	0	431	980	1411	2.274	0.695	0.690	0.661	0.662
56	12	0.02973952	404	401	805	1.007	0.502	0.455	0.489	0.513
57	0	0	653	758	1411	1.161	0.537	0.494	0.524	0.514
58	10	0.013145551	473	465	938	1.017	0.504	0.467	0.502	0.499
66	0	0	529	882	1411	1.667	0.625	0.612	0.583	0.601
84	5	0.002316553	604	606	1210	1.003	0.501	0.514	0.505	0.520
87	0	0	561	850	1411	1.515	0.602	0.584	0.556	0.554
88	0	0	448	963	1411	2.150	0.682	0.649	0.650	0.601
94	0	0	418	993	1411	2.376	0.704	0.702	0.678	0.682
108	0	0	454	957	1411	2.108	0.678	0.648	0.630	0.649
118	0	0	609	802	1411	1.317	0.568	0.556	0.515	0.515
125	0	0	667	744	1411	1.115	0.527	0.488	0.503	0.481
127	0	0	406	1005	1411	2.475	0.712	0.700	0.690	0.698
166	0	0	487	924	1411	1.897	0.655	0.621	0.635	0.629
171	0	0	577	834	1411	1.445	0.591	0.561	0.556	0.529
173	0	0	688	723	1411	1.051	0.512	0.486	0.503	0.505
193	0	0	683	728	1411	1.066	0.516	0.533	0.505	0.499
198	0	0	542	869	1411	1.603	0.616	0.558	0.576	0.585
279	0	0	679	732	1411	1.078	0.519	0.510	0.466	0.481
285	1	0.000753998	688	686	1374	1.003	0.501	0.507	0.506	0.524
291	0	0	578	833	1411	1.441	0.590	0.559	0.561	0.562
296	0	0	454	957	1411	2.108	0.678	0.678	0.653	0.645
304	0	0	540	871	1411	1.613	0.617	0.573	0.551	0.558
318	0	0	529	882	1411	1.667	0.625	0.588	0.583	0.551
322	4	0.002486878	636	616	1252	1.032	0.508	0.504	0.469	0.471
327	0	0	489	922	1411	1.885	0.653	0.622	0.596	0.606
332	0	0	593	818	1411	1.379	0.580	0.549	0.549	0.527
334	3	0.001488877	652	643	1295	1.014	0.503	0.513	0.471	0.486
335	0	0	698	713	1411	1.021	0.505	0.500	0.491	0.512
337	0	0	418	993	1411	2.376	0.704	0.685	0.677	0.675
422	0	0	541	870	1411	1.608	0.617	0.595	0.553	0.575
448	0	0	622	789	1411	1.268	0.559	0.521	0.520	0.520
449	0	0	655	756	1411	1.154	0.536	0.488	0.487	0.498
456	0	0	482	929	1411	1.927	0.658	0.626	0.618	0.635
457	0	0	467	944	1411	2.021	0.669	0.643	0.619	0.626
464	0	0	520	891	1411	1.713	0.631	0.593	0.585	0.562
465	4	0.001811763	619	637	1256	1.029	0.507	0.510	0.505	0.500
467	9	0.008717112	493	515	1008	1.045	0.511	0.485	0.488	0.480
475	0	0	665	746	1411	1.122	0.529	0.492	0.501	0.511
493	0	0	404	1007	1411	2.493	0.714	0.695	0.686	0.680
498	12	0.021285002	397	419	816	1.055	0.513	0.499	0.511	0.494
525	0	0	556	855	1411	1.538	0.606	0.585	0.555	0.571
591	5	0.003677606	611	596	1207	1.025	0.506	0.517	0.497	0.499
651	0	0	672	739	1411	1.100	0.524	0.504	0.502	0.485
680	0	0	432	979	1411	2.266	0.694	0.692	0.655	0.666
696	0	0	514	897	1411	1.745	0.636	0.624	0.600	0.590
699	6	0.004158428	577	586	1163	1.016	0.504	0.494	0.518	0.498
746	13	0.042241635	362	378	740	1.044	0.511	0.504	0.492	0.509
750	0	0	414	997	1411	2.408	0.707	0.685	0.651	0.662
792	0	0	406	1005	1411	2.475	0.712	0.706	0.671	0.667
834	3	0.001279685	653	642	1295	1.017	0.504	0.518	0.496	0.498

ADE_i	iPR	CutValue	high	low	n	I	RG	Accuracy(H2010)	Accuracy(New)	Accuracy(H2010+New)
835	0	0	702	709	1411	1.010	0.502	0.486	0.494	0.515
837	0	0	465	946	1411	2.034	0.670	0.654	0.624	0.627
874	0	0	415	996	1411	2.400	0.706	0.689	0.694	0.675
881	0	0	629	782	1411	1.243	0.554	0.522	0.527	0.519
884	4	0.002341379	627	627	1254	1.000	0.500	0.486	0.490	0.494
885	0	0	598	813	1411	1.360	0.576	0.544	0.541	0.514
895	0	0	658	753	1411	1.144	0.534	0.508	0.535	0.520
926	0	0	624	787	1411	1.261	0.558	0.521	0.532	0.494
927	0	0	569	842	1411	1.480	0.597	0.543	0.546	0.539
951	0	0	611	800	1411	1.309	0.567	0.557	0.542	0.524
974	0	0	458	953	1411	2.081	0.675	0.646	0.629	0.621
1007	9	0.010363249	505	492	997	1.026	0.507	0.510	0.516	0.513
1011	0	0	450	961	1411	2.136	0.681	0.664	0.635	0.647
1017	0	0	441	970	1411	2.200	0.687	0.657	0.651	0.635
1161	0	0	524	887	1411	1.693	0.629	0.609	0.603	0.583
1208	0	0	706	705	1411	1.001	0.500	0.541	0.486	0.490
1209	12	0.037650602	396	420	816	1.061	0.515	0.520	0.541	0.535
1210	0	0	417	994	1411	2.384	0.704	0.671	0.658	0.660
1218	0	0	496	915	1411	1.845	0.648	0.635	0.614	0.578
1222	0	0	493	918	1411	1.862	0.651	0.615	0.632	0.622
1239	0	0	481	930	1411	1.933	0.659	0.634	0.633	0.627
1246	0	0	636	775	1411	1.219	0.549	0.524	0.515	0.518
1250	0	0	411	1000	1411	2.433	0.709	0.697	0.671	0.661
1267	0	0	581	830	1411	1.429	0.588	0.544	0.519	0.514
1273	0	0	451	960	1411	2.129	0.680	0.646	0.629	0.638
1276	2	0.001180086	667	669	1336	1.003	0.501	0.510	0.490	0.493
1278	0	0	420	991	1411	2.360	0.702	0.674	0.676	0.671
1281	0	0	509	902	1411	1.772	0.639	0.622	0.568	0.584
1287	0	0	427	984	1411	2.304	0.697	0.685	0.674	0.646
1288	0	0	501	910	1411	1.816	0.645	0.606	0.621	0.593
1289	0	0	627	784	1411	1.250	0.556	0.520	0.493	0.494
1325	0	0	478	933	1411	1.952	0.661	0.636	0.621	0.592
1348	0	0	417	994	1411	2.384	0.704	0.673	0.671	0.665
1399	0	0	517	894	1411	1.729	0.634	0.580	0.595	0.605
1417	8	0.006070226	523	540	1063	1.033	0.508	0.517	0.462	0.484
1432	0	0	406	1005	1411	2.475	0.712	0.701	0.667	0.670
1439	0	0	519	892	1411	1.719	0.632	0.607	0.590	0.606
1466	0	0	670	741	1411	1.106	0.525	0.527	0.504	0.527
1467	0	0	604	807	1411	1.336	0.572	0.535	0.532	0.538
1472	0	0	408	1003	1411	2.458	0.711	0.697	0.675	0.670
1498	11	0.025454545	442	430	872	1.028	0.507	0.558	0.503	0.491
1500	2	0.001156404	676	660	1336	1.024	0.506	0.494	0.486	0.494
1519	0	0	676	735	1411	1.087	0.521	0.483	0.500	0.492
1520	0	0	420	991	1411	2.360	0.702	0.673	0.677	0.657
1545	5	0.00314877	600	611	1211	1.018	0.505	0.492	0.501	0.514
1553	11	0.018904427	444	425	869	1.045	0.511	0.486	0.534	0.511
1558	0	0	477	934	1411	1.958	0.662	0.617	0.602	0.612
1564	0	0	422	989	1411	2.344	0.701	0.687	0.666	0.663
1566	0	0	649	762	1411	1.174	0.540	0.505	0.501	0.512
1596	13	0.045927543	369	356	725	1.037	0.509	0.523	0.518	0.505
1599	5	0.003466205	613	594	1207	1.032	0.508	0.511	0.511	0.507
1616	0	0	608	803	1411	1.321	0.569	0.534	0.532	0.528
1618	2	0.001388311	669	667	1336	1.003	0.501	0.491	0.475	0.502
1621	0	0	417	994	1411	2.384	0.704	0.686	0.670	0.666
1634	9	0.013570495	502	498	1000	1.008	0.502	0.501	0.526	0.508
1635	0	0	606	805	1411	1.328	0.571	0.528	0.544	0.534
1645	0	0	449	962	1411	2.143	0.682	0.662	0.649	0.639
1651	0	0	603	808	1411	1.340	0.573	0.565	0.527	0.546

ADE_i	iPR	CutValue	high	low	n	I	RG	Accuracy(H2010)	Accuracy(New)	Accuracy(H2010+New)
1652	0	0	582	829	1411	1.424	0.588	0.541	0.529	0.528
1653	0	0	590	821	1411	1.392	0.582	0.553	0.545	0.544
1654	0	0	470	941	1411	2.002	0.667	0.642	0.639	0.627
1665	0	0	421	990	1411	2.352	0.702	0.687	0.668	0.666
1700	0	0	474	937	1411	1.977	0.664	0.653	0.623	0.606
1701	0	0	436	975	1411	2.236	0.691	0.681	0.671	0.664
1740	0	0	550	861	1411	1.565	0.610	0.591	0.563	0.551
1750	0	0	432	979	1411	2.266	0.694	0.665	0.639	0.639
1751	0	0	442	969	1411	2.192	0.687	0.667	0.635	0.641
1752	11	0.023025691	438	438	876	1.000	0.500	0.491	0.507	0.497
1753	0	0	609	802	1411	1.317	0.568	0.536	0.534	0.515
1776	2	0.001106328	671	665	1336	1.009	0.502	0.527	0.498	0.491
1783	0	0	432	979	1411	2.266	0.694	0.678	0.665	0.662
1797	5	0.003570367	609	599	1208	1.017	0.504	0.544	0.538	0.502
1848	0	0	498	913	1411	1.833	0.647	0.621	0.624	0.619
1905	0	0	572	839	1411	1.467	0.595	0.553	0.549	0.544
1980	0	0	518	893	1411	1.724	0.633	0.578	0.586	0.590
2075	0	0	425	986	1411	2.320	0.699	0.686	0.668	0.668
2087	0	0	411	1000	1411	2.433	0.709	0.707	0.665	0.680
2098	0	0	518	893	1411	1.724	0.633	0.617	0.606	0.603
2325	0	0	508	903	1411	1.778	0.640	0.609	0.588	0.593
2349	0	0	431	980	1411	2.274	0.695	0.653	0.668	0.663
2369	0	0	508	903	1411	1.778	0.640	0.612	0.597	0.589
2459	0	0	691	720	1411	1.042	0.510	0.478	0.502	0.476
2464	0	0	497	914	1411	1.839	0.648	0.627	0.577	0.609
2466	0	0	572	839	1411	1.467	0.595	0.544	0.512	0.532
2467	5	0.002389915	598	614	1212	1.027	0.507	0.524	0.509	0.501
2484	3	0.001438613	647	649	1296	1.003	0.501	0.499	0.500	0.495
2500	9	0.009454552	502	498	1000	1.008	0.502	0.506	0.498	0.488
2513	0	0	640	771	1411	1.205	0.546	0.532	0.516	0.519
2541	0	0	522	889	1411	1.703	0.630	0.602	0.602	0.596
2547	7	0.005198109	559	551	1110	1.015	0.504	0.508	0.450	0.487
2574	0	0	713	698	1411	1.021	0.505	0.537	0.519	0.500
2575	0	0	504	907	1411	1.800	0.643	0.622	0.607	0.593
2593	0	0	621	790	1411	1.272	0.560	0.524	0.532	0.534
2594	0	0	528	883	1411	1.672	0.626	0.583	0.569	0.561
2599	4	0.003134796	633	620	1253	1.021	0.505	0.513	0.500	0.490
2643	0	0	589	822	1411	1.396	0.583	0.552	0.524	0.531
2650	8	0.00642992	525	536	1061	1.021	0.505	0.478	0.486	0.508
2654	0	0	512	899	1411	1.756	0.637	0.607	0.564	0.571
2662	0	0	496	915	1411	1.845	0.648	0.629	0.619	0.601
2663	10	0.013779528	467	478	945	1.024	0.506	0.509	0.501	0.485
2667	0	0	634	777	1411	1.226	0.551	0.529	0.525	0.522
2673	0	0	518	893	1411	1.724	0.633	0.619	0.571	0.579
2696	0	0	432	979	1411	2.266	0.694	0.687	0.651	0.657
2726	0	0	463	948	1411	2.048	0.672	0.651	0.638	0.637
2727	1	0.000703157	691	683	1374	1.012	0.503	0.504	0.509	0.496
2729	0	0	468	943	1411	2.015	0.668	0.645	0.623	0.622
2730	10	0.013018997	469	473	942	1.009	0.502	0.503	0.512	0.534
2804	0	0	445	966	1411	2.171	0.685	0.658	0.619	0.629
2820	6	0.003759587	586	573	1159	1.023	0.506	0.497	0.523	0.525
2825	0	0	473	938	1411	1.983	0.665	0.652	0.635	0.637
2840	0	0	538	873	1411	1.623	0.619	0.576	0.577	0.577
2870	0	0	560	851	1411	1.520	0.603	0.568	0.584	0.585
2871	0	0	415	996	1411	2.400	0.706	0.702	0.651	0.638
2875	0	0	457	954	1411	2.088	0.676	0.664	0.629	0.631
2876	0	0	450	961	1411	2.136	0.681	0.665	0.629	0.627
2880	5	0.003349796	610	597	1207	1.022	0.505	0.524	0.505	0.493

ADE_i	iPR	CutValue	high	low	n	I	RG	Accuracy(H2010)	Accuracy(New)	Accuracy(H2010+New)
2881	2	0.001204094	676	660	1336	1.024	0.506	0.497	0.514	0.501
2885	0	0	539	872	1411	1.618	0.618	0.587	0.585	0.558
2891	9	0.008921368	507	489	996	1.037	0.509	0.513	0.491	0.510
2894	0	0	638	773	1411	1.212	0.548	0.524	0.551	0.538
2895	0	0	438	973	1411	2.221	0.690	0.660	0.656	0.649
2898	0	0	573	838	1411	1.462	0.594	0.561	0.543	0.526
2899	0	0	487	924	1411	1.897	0.655	0.634	0.627	0.634
2900	0	0	471	940	1411	1.996	0.666	0.655	0.619	0.622
2901	10	0.013259598	475	461	936	1.030	0.507	0.483	0.484	0.474
2911	0	0	590	821	1411	1.392	0.582	0.550	0.524	0.522
2912	2	0.000829992	660	677	1337	1.026	0.506	0.512	0.506	0.507
2943	5	0.002949173	597	615	1212	1.030	0.507	0.515	0.474	0.496
2944	0	0	512	899	1411	1.756	0.637	0.609	0.594	0.575
2950	0	0	452	959	1411	2.122	0.680	0.673	0.648	0.627
2974	0	0	448	963	1411	2.150	0.682	0.681	0.654	0.652
2975	0	0	487	924	1411	1.897	0.655	0.630	0.613	0.619
2980	1	0.000646377	691	683	1374	1.012	0.503	0.503	0.511	0.512
2986	0	0	489	922	1411	1.885	0.653	0.642	0.612	0.594
2987	7	0.005893632	559	551	1110	1.015	0.504	0.488	0.487	0.514
2995	0	0	554	857	1411	1.547	0.607	0.552	0.549	0.549
2999	0	0	626	785	1411	1.254	0.556	0.534	0.522	0.522
3022	0	0	408	1003	1411	2.458	0.711	0.702	0.680	0.672
3030	0	0	635	776	1411	1.222	0.550	0.508	0.514	0.522
3032	4	0.001739847	633	619	1252	1.023	0.506	0.499	0.501	0.502
3043	0	0	427	984	1411	2.304	0.697	0.670	0.673	0.636
3048	0	0	503	908	1411	1.805	0.644	0.614	0.622	0.612
3051	0	0	699	712	1411	1.019	0.505	0.539	0.505	0.500
3071	0	0	461	950	1411	2.061	0.673	0.636	0.635	0.645
3077	0	0	523	888	1411	1.698	0.629	0.609	0.566	0.575
3078	0	0	407	1004	1411	2.467	0.712	0.706	0.678	0.651
3081	0	0	668	743	1411	1.112	0.527	0.515	0.542	0.527
3106	3	0.001837815	641	657	1298	1.025	0.506	0.491	0.478	0.502
3172	9	0.008417485	499	503	1002	1.008	0.502	0.479	0.488	0.458
3176	0	0	405	1006	1411	2.484	0.713	0.680	0.681	0.672
3183	0	0	475	936	1411	1.971	0.663	0.650	0.612	0.611
3184	0	0	468	943	1411	2.015	0.668	0.659	0.624	0.621
3194	0	0	526	885	1411	1.683	0.627	0.590	0.590	0.586
3196	0	0	438	973	1411	2.221	0.690	0.686	0.639	0.627
3199	0	0	697	714	1411	1.024	0.506	0.486	0.531	0.515
3201	0	0	404	1007	1411	2.493	0.714	0.711	0.690	0.663
3227	0	0	625	786	1411	1.258	0.557	0.517	0.503	0.498
3228	0	0	517	894	1411	1.729	0.634	0.594	0.595	0.578
3231	0	0	405	1006	1411	2.484	0.713	0.707	0.674	0.679
3267	0	0	491	920	1411	1.874	0.652	0.627	0.610	0.615
3275	0	0	457	954	1411	2.088	0.676	0.651	0.647	0.646
3292	0	0	486	925	1411	1.903	0.656	0.642	0.607	0.626
3334	0	0	431	980	1411	2.274	0.695	0.673	0.664	0.658
3337	6	0.004762829	574	591	1165	1.030	0.507	0.504	0.508	0.502
3338	0	0	417	994	1411	2.384	0.704	0.673	0.662	0.668
3359	0	0	638	773	1411	1.212	0.548	0.541	0.548	0.537
3361	0	0	453	958	1411	2.115	0.679	0.670	0.648	0.636
3368	0	0	672	739	1411	1.100	0.524	0.498	0.478	0.473
3384	0	0	420	991	1411	2.360	0.702	0.695	0.669	0.668
3399	0	0	599	812	1411	1.356	0.575	0.515	0.536	0.517
3400	0	0	634	777	1411	1.226	0.551	0.522	0.532	0.498
3427	4	0.002098691	627	627	1254	1.000	0.500	0.487	0.508	0.522
3439	0	0	530	881	1411	1.662	0.624	0.590	0.576	0.551
3452	0	0	556	855	1411	1.538	0.606	0.557	0.542	0.557

ADE_i	iPR	CutValue	high	low	n	I	RG	Accuracy(H2010)	Accuracy(New)	Accuracy(H2010+New)
3458	0	0	608	803	1411	1.321	0.569	0.540	0.510	0.520
3467	0	0	463	948	1411	2.048	0.672	0.653	0.641	0.633
3515	2	0.001102565	665	672	1337	1.011	0.503	0.506	0.506	0.493
3565	0	0	408	1003	1411	2.458	0.711	0.706	0.702	0.689
3605	10	0.013513514	468	476	944	1.017	0.504	0.512	0.479	0.506
3614	6	0.004301331	588	571	1159	1.030	0.507	0.518	0.516	0.512
3619	0	0	436	975	1411	2.236	0.691	0.658	0.641	0.647
3621	9	0.00941883	497	507	1004	1.020	0.505	0.487	0.479	0.483
3622	0	0	514	897	1411	1.745	0.636	0.617	0.585	0.602
3624	7	0.008886411	562	546	1108	1.029	0.507	0.475	0.476	0.523
3628	0	0	422	989	1411	2.344	0.701	0.688	0.687	0.678
3651	0	0	685	726	1411	1.060	0.515	0.496	0.506	0.507
3664	0	0	430	981	1411	2.281	0.695	0.684	0.649	0.647
3683	0	0	455	956	1411	2.101	0.678	0.666	0.634	0.629
3689	0	0	506	905	1411	1.789	0.641	0.600	0.573	0.575
3712	0	0	414	997	1411	2.408	0.707	0.689	0.677	0.668
3714	0	0	612	799	1411	1.306	0.566	0.548	0.481	0.522
3718	6	0.004358662	578	585	1163	1.012	0.503	0.511	0.500	0.502
3719	1	0.000888297	689	685	1374	1.006	0.501	0.504	0.509	0.495
3725	0	0	511	900	1411	1.761	0.638	0.622	0.590	0.583
3727	7	0.005945424	559	550	1109	1.016	0.504	0.500	0.502	0.509
3738	0	0	692	719	1411	1.039	0.510	0.476	0.476	0.485
3770	0	0	428	983	1411	2.297	0.697	0.688	0.644	0.641
3771	0	0	567	844	1411	1.489	0.598	0.536	0.571	0.544
3789	0	0	521	890	1411	1.708	0.631	0.616	0.605	0.618
3805	0	0	712	699	1411	1.019	0.505	0.504	0.514	0.506
3810	0	0	494	917	1411	1.856	0.650	0.627	0.595	0.590
3825	0	0	508	903	1411	1.778	0.640	0.608	0.591	0.588
3826	0	0	561	850	1411	1.515	0.602	0.579	0.545	0.567
3877	6	0.005573381	581	581	1162	1.000	0.500	0.500	0.495	0.508
3902	0	0	408	1003	1411	2.458	0.711	0.700	0.691	0.681
3914	0	0	416	995	1411	2.392	0.705	0.697	0.667	0.648
3955	0	0	647	764	1411	1.181	0.541	0.520	0.518	0.508
3963	0	0	482	929	1411	1.927	0.658	0.636	0.644	0.629
3969	3	0.001620374	645	652	1297	1.011	0.503	0.514	0.520	0.496
3977	4	0.002358441	623	632	1255	1.014	0.504	0.516	0.514	0.499
3979	0	0	666	745	1411	1.119	0.528	0.520	0.494	0.519
4011	9	0.012345679	505	494	999	1.022	0.506	0.522	0.522	0.499
4014	0	0	542	869	1411	1.603	0.616	0.599	0.561	0.573
4095	0	0	502	909	1411	1.811	0.644	0.609	0.594	0.597
4130	8	0.006843456	529	530	1059	1.002	0.500	0.507	0.511	0.490
4133	12	0.030277649	404	402	806	1.005	0.501	0.504	0.534	0.484
4142	0	0	629	782	1411	1.243	0.554	0.524	0.551	0.522
4159	10	0.011911211	471	469	940	1.004	0.501	0.517	0.476	0.484
4181	0	0	546	865	1411	1.584	0.613	0.603	0.571	0.582
4191	0	0	489	922	1411	1.885	0.653	0.624	0.612	0.608
4196	0	0	512	899	1411	1.756	0.637	0.597	0.590	0.575
4197	0	0	653	758	1411	1.161	0.537	0.524	0.489	0.512
4198	0	0	492	919	1411	1.868	0.651	0.626	0.593	0.591
4216	5	0.003791585	603	607	1210	1.007	0.502	0.493	0.474	0.517
4221	0	0	713	698	1411	1.021	0.505	0.516	0.512	0.508
4285	0	0	695	716	1411	1.030	0.507	0.510	0.508	0.494
4329	2	0.001436782	667	670	1337	1.004	0.501	0.501	0.504	0.505
4335	0	0	468	943	1411	2.015	0.668	0.653	0.641	0.636
4357	2	0.001162111	665	672	1337	1.011	0.503	0.473	0.502	0.476
4398	0	0	573	838	1411	1.462	0.594	0.560	0.552	0.546
4400	0	0	504	907	1411	1.800	0.643	0.627	0.601	0.586
4401	0	0	576	835	1411	1.450	0.592	0.537	0.527	0.536

ADE_i	iPR	CutValue	high	low	n	I	RG	Accuracy(H2010)	Accuracy(New)	Accuracy(H2010+New)
4478	2	0.001148232	664	673	1337	1.014	0.503	0.491	0.501	0.508
4493	0	0	696	715	1411	1.027	0.507	0.513	0.493	0.496
4503	0	0	660	751	1411	1.138	0.532	0.515	0.508	0.506
4509	0	0	687	724	1411	1.054	0.513	0.515	0.518	0.507
4513	0	0	543	868	1411	1.599	0.615	0.562	0.560	0.563
4517	0	0	537	874	1411	1.628	0.619	0.594	0.575	0.552
4523	0	0	456	955	1411	2.094	0.677	0.639	0.649	0.648
4528	0	0	503	908	1411	1.805	0.644	0.636	0.597	0.609
4550	0	0	550	861	1411	1.565	0.610	0.598	0.572	0.577
4585	8	0.006048544	532	524	1056	1.015	0.504	0.494	0.499	0.508
4600	0	0	488	923	1411	1.891	0.654	0.641	0.607	0.607
4623	0	0	638	773	1411	1.212	0.548	0.501	0.507	0.502
4643	0	0	464	947	1411	2.041	0.671	0.661	0.638	0.641
4656	0	0	597	814	1411	1.363	0.577	0.588	0.528	0.533
4670	13	0.028988351	370	353	723	1.048	0.512	0.499	0.493	0.525
4673	0	0	425	986	1411	2.320	0.699	0.674	0.652	0.666
4682	11	0.023043021	436	442	878	1.014	0.503	0.498	0.527	0.531
4693	0	0	442	969	1411	2.192	0.687	0.668	0.655	0.629
4908	0	0	560	851	1411	1.520	0.603	0.576	0.571	0.573
4923	0	0	417	994	1411	2.384	0.704	0.706	0.670	0.671
4938	0	0	667	744	1411	1.115	0.527	0.488	0.504	0.510
4952	11	0.019858797	431	454	885	1.053	0.513	0.470	0.505	0.481
4977	5	0.003875969	613	594	1207	1.032	0.508	0.548	0.482	0.498
4981	11	0.021922277	443	426	869	1.040	0.510	0.500	0.500	0.486
4998	0	0	692	719	1411	1.039	0.510	0.505	0.490	0.487
5065	0	0	413	998	1411	2.416	0.707	0.675	0.686	0.667
5068	4	0.002714136	632	621	1253	1.018	0.504	0.514	0.510	0.508
5072	0	0	639	772	1411	1.208	0.547	0.529	0.539	0.526
5076	0	0	630	781	1411	1.240	0.554	0.537	0.534	0.519
5109	11	0.018688914	440	434	874	1.014	0.503	0.533	0.500	0.518
5154	6	0.003761787	582	579	1161	1.005	0.501	0.506	0.494	0.494
5164	0	0	517	894	1411	1.729	0.634	0.608	0.580	0.590
5173	0	0	526	885	1411	1.683	0.627	0.607	0.587	0.614
5199	0	0	684	727	1411	1.063	0.515	0.483	0.489	0.479
5352	0	0	524	887	1411	1.693	0.629	0.625	0.612	0.595
5376	4	0.001678825	634	618	1252	1.026	0.506	0.486	0.507	0.506
5396	0	0	581	830	1411	1.429	0.588	0.554	0.560	0.564
5422	0	0	653	758	1411	1.161	0.537	0.519	0.496	0.493
5468	0	0	597	814	1411	1.363	0.577	0.524	0.514	0.510
5483	0	0	583	828	1411	1.420	0.587	0.575	0.521	0.525
5522	0	0	680	731	1411	1.075	0.518	0.524	0.487	0.484
5525	0	0	467	944	1411	2.021	0.669	0.664	0.614	0.595
5530	0	0	430	981	1411	2.281	0.695	0.685	0.673	0.664
5531	11	0.019031142	433	450	883	1.039	0.510	0.493	0.493	0.492
5541	0	0	438	973	1411	2.221	0.690	0.659	0.658	0.653
5546	0	0	562	849	1411	1.511	0.602	0.554	0.551	0.548
5547	9	0.013114756	505	493	998	1.024	0.506	0.506	0.512	0.517
5552	0	0	496	915	1411	1.845	0.648	0.617	0.605	0.580
5556	0	0	609	802	1411	1.317	0.568	0.528	0.535	0.543
5558	6	0.005926229	587	572	1159	1.026	0.506	0.492	0.493	0.470
5564	0	0	490	921	1411	1.880	0.653	0.610	0.616	0.595
5569	11	0.023617399	440	433	873	1.016	0.504	0.512	0.490	0.521
5585	3	0.001815716	651	645	1296	1.009	0.502	0.501	0.478	0.488
5592	0	0	626	785	1411	1.254	0.556	0.529	0.515	0.510
5606	0	0	658	753	1411	1.144	0.534	0.498	0.510	0.495
5614	0	0	450	961	1411	2.136	0.681	0.653	0.615	0.632
5620	0	0	584	827	1411	1.416	0.586	0.544	0.521	0.525
5648	0	0	413	998	1411	2.416	0.707	0.693	0.660	0.651

ADE_i	iPR	CutValue	high	low	n	I	RG	Accuracy(H2010)	Accuracy(New)	Accuracy(H2010+New)
5656	9	0.008984299	504	495	999	1.018	0.505	0.468	0.495	0.474
5657	0	0	656	755	1411	1.151	0.535	0.499	0.500	0.515
5658	11	0.028686212	440	433	873	1.016	0.504	0.535	0.512	0.538
5669	0	0	640	771	1411	1.205	0.546	0.537	0.532	0.529
5671	0	0	537	874	1411	1.628	0.619	0.590	0.563	0.566
5674	0	0	551	860	1411	1.561	0.609	0.556	0.571	0.561
5675	0	0	503	908	1411	1.805	0.644	0.617	0.583	0.594
5677	0	0	639	772	1411	1.208	0.547	0.530	0.537	0.537
5731	0	0	487	924	1411	1.897	0.655	0.622	0.616	0.615
5754	0	0	527	884	1411	1.677	0.627	0.609	0.593	0.584
5768	8	0.008531602	524	538	1062	1.027	0.507	0.530	0.520	0.527
5769	0	0	673	738	1411	1.097	0.523	0.536	0.544	0.526
5773	0	0	504	907	1411	1.800	0.643	0.617	0.594	0.592
5804	0	0	543	868	1411	1.599	0.615	0.574	0.590	0.559
5810	0	0	430	981	1411	2.281	0.695	0.665	0.665	0.643
5812	0	0	508	903	1411	1.778	0.640	0.615	0.588	0.600
5816	0	0	422	989	1411	2.344	0.701	0.685	0.673	0.667
5822	4	0.001824818	625	630	1255	1.008	0.502	0.476	0.499	0.489
5842	14	0.053504197	320	345	665	1.078	0.519	0.489	0.490	0.503
5843	0	0	528	883	1411	1.672	0.626	0.578	0.622	0.600
5848	0	0	499	912	1411	1.828	0.646	0.639	0.597	0.596
5861	0	0	692	719	1411	1.039	0.510	0.490	0.517	0.493
5880	0	0	549	862	1411	1.570	0.611	0.586	0.551	0.551
5884	0	0	607	804	1411	1.325	0.570	0.537	0.516	0.526
5893	0	0	713	698	1411	1.021	0.505	0.510	0.514	0.502
5899	0	0	497	914	1411	1.839	0.648	0.624	0.597	0.600
5906	0	0	682	729	1411	1.069	0.517	0.516	0.526	0.522
5910	7	0.004645038	550	565	1115	1.027	0.507	0.504	0.498	0.503
5911	4	0.001801802	633	620	1253	1.021	0.505	0.503	0.531	0.518
5920	7	0.005462492	557	554	1111	1.005	0.501	0.494	0.503	0.500
5924	3	0.001441071	653	642	1295	1.017	0.504	0.483	0.482	0.502
5939	3	0.001669136	644	653	1297	1.014	0.503	0.478	0.492	0.497
5951	0	0	642	769	1411	1.198	0.545	0.519	0.484	0.471
5955	0	0	607	804	1411	1.325	0.570	0.532	0.517	0.520
5958	0	0	529	882	1411	1.667	0.625	0.612	0.583	0.601
5964	13	0.051464999	372	349	721	1.066	0.516	0.498	0.491	0.470
5966	0	0	511	900	1411	1.761	0.638	0.606	0.588	0.585
5992	0	0	420	991	1411	2.360	0.702	0.683	0.670	0.661
5995	0	0	509	902	1411	1.772	0.639	0.618	0.602	0.600
5996	0	0	527	884	1411	1.677	0.627	0.591	0.576	0.563
6001	0	0	684	727	1411	1.063	0.515	0.484	0.485	0.462
6008	0	0	639	772	1411	1.208	0.547	0.505	0.498	0.515
6012	0	0	564	847	1411	1.502	0.600	0.594	0.549	0.538
6014	0	0	603	808	1411	1.340	0.573	0.542	0.536	0.537
6015	4	0.00186742	636	616	1252	1.032	0.508	0.529	0.470	0.487
6019	0	0	710	701	1411	1.013	0.503	0.493	0.518	0.503
6021	8	0.008389145	521	542	1063	1.040	0.510	0.503	0.497	0.510
6025	8	0.005055794	523	539	1062	1.031	0.508	0.504	0.459	0.475
6028	14	0.047378595	323	335	658	1.037	0.509	0.461	0.503	0.501
6030	12	0.027162088	409	388	797	1.054	0.513	0.484	0.521	0.505
6033	0	0	664	747	1411	1.125	0.529	0.508	0.483	0.492
6036	0	0	414	997	1411	2.408	0.707	0.697	0.681	0.692
6037	0	0	424	987	1411	2.328	0.700	0.681	0.668	0.660
6039	0	0	512	899	1411	1.756	0.637	0.599	0.607	0.602
6041	0	0	701	710	1411	1.013	0.503	0.505	0.496	0.481
6045	0	0	490	921	1411	1.880	0.653	0.627	0.595	0.581
6046	0	0	499	912	1411	1.828	0.646	0.620	0.632	0.589
6048	0	0	518	893	1411	1.724	0.633	0.606	0.580	0.573

ADE_i	iPR	CutValue	high	low	n	I	RG	Accuracy(H2010)	Accuracy(New)	Accuracy(H2010+New)
6052	0	0	496	915	1411	1.845	0.648	0.641	0.611	0.617
6061	9	0.008336228	504	495	999	1.018	0.505	0.476	0.502	0.505
6067	0	0	703	708	1411	1.007	0.502	0.495	0.500	0.483
6069	0	0	563	848	1411	1.506	0.601	0.549	0.558	0.546
6071	3	0.001956183	647	649	1296	1.003	0.501	0.523	0.515	0.529
6072	0	0	682	729	1411	1.069	0.517	0.524	0.502	0.490
6096	0	0	566	845	1411	1.493	0.599	0.587	0.554	0.542
6097	0	0	416	995	1411	2.392	0.705	0.690	0.659	0.661
6104	0	0	485	926	1411	1.909	0.656	0.639	0.587	0.614
6118	0	0	441	970	1411	2.200	0.687	0.675	0.639	0.639
6120	5	0.003407218	607	601	1208	1.010	0.502	0.497	0.512	0.511
6125	3	0.001821328	641	657	1298	1.025	0.506	0.503	0.492	0.496
6129	4	0.001867793	631	622	1253	1.014	0.504	0.517	0.477	0.488
6134	0	0	483	928	1411	1.921	0.658	0.628	0.622	0.625
6142	5	0.003852056	598	613	1211	1.025	0.506	0.518	0.524	0.528
6143	9	0.010813198	501	500	1001	1.002	0.500	0.499	0.494	0.481
6144	0	0	434	977	1411	2.251	0.692	0.678	0.632	0.637
6146	1	0.000767244	695	679	1374	1.024	0.506	0.504	0.514	0.499
6152	14	0.06504065	330	310	640	1.065	0.516	0.489	0.488	0.475
6155	3	0.00180795	641	656	1297	1.023	0.506	0.516	0.495	0.494
6161	0	0	700	711	1411	1.016	0.504	0.494	0.536	0.531
6163	0	0	558	853	1411	1.529	0.605	0.561	0.565	0.551
6166	5	0.002975781	600	611	1211	1.018	0.505	0.495	0.505	0.508
6179	0	0	422	989	1411	2.344	0.701	0.683	0.678	0.678
6182	0	0	513	898	1411	1.750	0.636	0.610	0.596	0.598
6195	0	0	614	797	1411	1.298	0.565	0.535	0.538	0.528
6213	0	0	666	745	1411	1.119	0.528	0.508	0.515	0.503
6222	0	0	621	790	1411	1.272	0.560	0.528	0.502	0.507
6230	0	0	431	980	1411	2.274	0.695	0.667	0.662	0.656
6244	0	0	611	800	1411	1.309	0.567	0.526	0.511	0.501
6267	0	0	669	742	1411	1.109	0.526	0.551	0.542	0.529
6292	2	0.000908166	663	674	1337	1.017	0.504	0.502	0.496	0.491
6305	0	0	641	770	1411	1.201	0.546	0.526	0.491	0.498
6330	0	0	451	960	1411	2.129	0.680	0.674	0.647	0.657
6333	0	0	477	934	1411	1.958	0.662	0.641	0.632	0.619
6338	3	0.001489655	650	646	1296	1.006	0.502	0.496	0.488	0.516
6344	0	0	433	978	1411	2.259	0.693	0.662	0.669	0.645
6345	0	0	524	887	1411	1.693	0.629	0.592	0.580	0.581
6346	0	0	532	879	1411	1.652	0.623	0.593	0.589	0.601
6348	0	0	465	946	1411	2.034	0.670	0.656	0.627	0.622
6352	0	0	483	928	1411	1.921	0.658	0.630	0.606	0.614
6356	0	0	546	865	1411	1.584	0.613	0.575	0.561	0.542
6373	0	0	594	817	1411	1.375	0.579	0.554	0.554	0.561
6378	0	0	646	765	1411	1.184	0.542	0.510	0.497	0.515
6381	0	0	540	871	1411	1.613	0.617	0.603	0.551	0.566
6428	0	0	546	865	1411	1.584	0.613	0.565	0.569	0.576
6437	0	0	596	815	1411	1.367	0.578	0.555	0.525	0.512
6439	1	0.000765717	691	683	1374	1.012	0.503	0.480	0.485	0.498
6443	0	0	632	779	1411	1.233	0.552	0.539	0.539	0.510
6457	0	0	509	902	1411	1.772	0.639	0.633	0.605	0.600
6490	4	0.002411963	621	635	1256	1.023	0.506	0.481	0.531	0.520
6509	0	0	507	904	1411	1.783	0.641	0.611	0.570	0.543
6540	0	0	421	990	1411	2.352	0.702	0.665	0.664	0.660
6604	0	0	420	991	1411	2.360	0.702	0.695	0.655	0.663
6623	0	0	446	965	1411	2.164	0.684	0.673	0.649	0.658
6638	0	0	583	828	1411	1.420	0.587	0.539	0.557	0.548
6641	0	0	455	956	1411	2.101	0.678	0.663	0.634	0.635
6675	0	0	604	807	1411	1.336	0.572	0.535	0.519	0.517

ADE_i	iPR	CutValue	high	low	n	I	RG	Accuracy(H2010)	Accuracy(New)	Accuracy(H2010+New)
6684	0	0	698	713	1411	1.021	0.505	0.502	0.511	0.513
6744	0	0	410	1001	1411	2.441	0.709	0.685	0.673	0.670
6755	0	0	700	711	1411	1.016	0.504	0.512	0.502	0.504
6778	6	0.004330944	575	590	1165	1.026	0.506	0.479	0.509	0.496
6791	0	0	407	1004	1411	2.467	0.712	0.689	0.660	0.658
6800	0	0	611	800	1411	1.309	0.567	0.527	0.534	0.521
6806	0	0	416	995	1411	2.392	0.705	0.691	0.672	0.689
6808	0	0	501	910	1411	1.816	0.645	0.617	0.597	0.610
6814	11	0.013849757	438	438	876	1.000	0.500	0.522	0.519	0.496
6823	0	0	629	782	1411	1.243	0.554	0.534	0.524	0.517
6860	0	0	621	790	1411	1.272	0.560	0.517	0.525	0.505
6861	0	0	427	984	1411	2.304	0.697	0.688	0.651	0.663
6863	0	0	493	918	1411	1.862	0.651	0.634	0.597	0.607
6876	0	0	433	978	1411	2.259	0.693	0.685	0.649	0.652
6910	0	0	585	826	1411	1.412	0.585	0.543	0.558	0.536
6922	0	0	410	1001	1411	2.441	0.709	0.680	0.668	0.660
6933	0	0	507	904	1411	1.783	0.641	0.595	0.618	0.613
7012	0	0	536	875	1411	1.632	0.620	0.591	0.583	0.588
7022	0	0	580	831	1411	1.433	0.589	0.560	0.574	0.542
7041	0	0	694	717	1411	1.033	0.508	0.512	0.455	0.478
7045	0	0	510	901	1411	1.767	0.639	0.624	0.582	0.605
7046	0	0	416	995	1411	2.392	0.705	0.680	0.667	0.676
7060	0	0	568	843	1411	1.484	0.597	0.581	0.549	0.561
7065	0	0	467	944	1411	2.021	0.669	0.648	0.636	0.634
7075	0	0	694	717	1411	1.033	0.508	0.533	0.505	0.496
7081	0	0	498	913	1411	1.833	0.647	0.607	0.608	0.604
7083	0	0	422	989	1411	2.344	0.701	0.687	0.665	0.652
7084	0	0	649	762	1411	1.174	0.540	0.488	0.520	0.500
7104	0	0	641	770	1411	1.201	0.546	0.525	0.514	0.546
7107	0	0	535	876	1411	1.637	0.621	0.597	0.585	0.595
7122	0	0	422	989	1411	2.344	0.701	0.695	0.662	0.653
7124	2	0.001056245	676	660	1336	1.024	0.506	0.512	0.519	0.515
7138	0	0	518	893	1411	1.724	0.633	0.619	0.596	0.588
7139	0	0	652	759	1411	1.164	0.538	0.487	0.498	0.500
7166	0	0	636	775	1411	1.219	0.549	0.505	0.522	0.506
7173	0	0	485	926	1411	1.909	0.656	0.634	0.608	0.607
7176	0	0	638	773	1411	1.212	0.548	0.524	0.530	0.505
7188	0	0	485	926	1411	1.909	0.656	0.655	0.608	0.587
7189	12	0.036363636	405	402	807	1.007	0.502	0.507	0.458	0.475
7246	13	0.049653092	367	363	730	1.011	0.503	0.567	0.518	0.560
7250	0	0	639	772	1411	1.208	0.547	0.527	0.529	0.523
7265	1	0.000814427	694	680	1374	1.021	0.505	0.497	0.480	0.461
7274	10	0.013350726	466	479	945	1.028	0.507	0.474	0.505	0.511
7275	0	0	690	721	1411	1.045	0.511	0.507	0.505	0.485
7276	0	0	416	995	1411	2.392	0.705	0.685	0.661	0.664
7278	2	0.001152038	671	665	1336	1.009	0.502	0.507	0.483	0.469
7280	0	0	506	905	1411	1.789	0.641	0.617	0.591	0.604
7315	0	0	449	962	1411	2.143	0.682	0.673	0.651	0.661
7326	0	0	575	836	1411	1.454	0.592	0.563	0.566	0.568
7336	0	0	534	877	1411	1.642	0.622	0.576	0.562	0.558
7358	0	0	522	889	1411	1.703	0.630	0.606	0.590	0.593
7366	0	0	523	888	1411	1.698	0.629	0.612	0.601	0.587
7389	0	0	523	888	1411	1.698	0.629	0.608	0.598	0.590
7398	0	0	597	814	1411	1.363	0.577	0.545	0.555	0.554
7405	2	0.001299656	673	663	1336	1.015	0.504	0.534	0.494	0.526
7422	0	0	487	924	1411	1.897	0.655	0.638	0.597	0.593
7424	0	0	628	783	1411	1.247	0.555	0.524	0.504	0.500
7426	0	0	698	713	1411	1.021	0.505	0.515	0.507	0.483

ADE_i	iPR	CutValue	high	low	n	I	RG	Accuracy(H2010)	Accuracy(New)	Accuracy(H2010+New)
7431	5	0.003141745	613	593	1206	1.034	0.508	0.482	0.483	0.491
7497	0	0	420	991	1411	2.360	0.702	0.666	0.655	0.658
7510	0	0	406	1005	1411	2.475	0.712	0.691	0.673	0.672
7511	0	0	528	883	1411	1.672	0.626	0.591	0.589	0.585
7530	0	0	452	959	1411	2.122	0.680	0.675	0.656	0.639
7535	0	0	526	885	1411	1.683	0.627	0.583	0.568	0.529
7572	0	0	457	954	1411	2.088	0.676	0.665	0.632	0.632
7613	0	0	705	706	1411	1.001	0.500	0.501	0.497	0.481
7639	0	0	411	1000	1411	2.433	0.709	0.692	0.656	0.673
7645	9	0.012071836	505	492	997	1.026	0.507	0.526	0.534	0.513
7675	0	0	636	775	1411	1.219	0.549	0.515	0.521	0.503
7719	7	0.005519162	563	545	1108	1.033	0.508	0.527	0.505	0.490
7725	0	0	494	917	1411	1.856	0.650	0.634	0.617	0.577
7742	0	0	446	965	1411	2.164	0.684	0.639	0.651	0.641
7752	0	0	636	775	1411	1.219	0.549	0.510	0.499	0.520
7759	0	0	546	865	1411	1.584	0.613	0.588	0.570	0.573
7788	0	0	714	697	1411	1.024	0.506	0.499	0.508	0.502
7789	0	0	548	863	1411	1.575	0.612	0.578	0.583	0.578
7803	4	0.002899686	633	619	1252	1.023	0.506	0.496	0.487	0.502
7808	0	0	548	863	1411	1.575	0.612	0.576	0.583	0.577
7822	1	0.000839916	691	683	1374	1.012	0.503	0.496	0.486	0.488
7850	0	0	527	884	1411	1.677	0.627	0.595	0.546	0.557
7864	5	0.002773941	610	597	1207	1.022	0.505	0.480	0.501	0.504
7878	7	0.006937381	563	545	1108	1.033	0.508	0.510	0.462	0.475
7881	0	0	458	953	1411	2.081	0.675	0.667	0.626	0.639
7886	0	0	414	997	1411	2.408	0.707	0.670	0.663	0.659
7892	0	0	446	965	1411	2.164	0.684	0.678	0.649	0.663
7896	0	0	455	956	1411	2.101	0.678	0.651	0.656	0.635
7924	4	0.003377252	630	623	1253	1.011	0.503	0.518	0.489	0.517
7951	0	0	522	889	1411	1.703	0.630	0.602	0.582	0.566
7953	11	0.017037156	438	438	876	1.000	0.500	0.501	0.504	0.508
7956	0	0	577	834	1411	1.445	0.591	0.575	0.583	0.569
7958	0	0	710	701	1411	1.013	0.503	0.460	0.493	0.451
8032	0	0	597	814	1411	1.363	0.577	0.577	0.563	0.553
8037	0	0	430	981	1411	2.281	0.695	0.666	0.653	0.639
8049	0	0	473	938	1411	1.983	0.665	0.643	0.617	0.623
8053	0	0	453	958	1411	2.115	0.679	0.658	0.655	0.650
8056	0	0	532	879	1411	1.652	0.623	0.584	0.581	0.593
8063	0	0	585	826	1411	1.412	0.585	0.574	0.546	0.544
8091	0	0	451	960	1411	2.129	0.680	0.680	0.637	0.634
8110	0	0	410	1001	1411	2.441	0.709	0.709	0.706	0.702
8111	0	0	546	865	1411	1.584	0.613	0.575	0.563	0.572
8125	0	0	499	912	1411	1.828	0.646	0.625	0.617	0.610
8133	0	0	406	1005	1411	2.475	0.712	0.702	0.675	0.670
8170	0	0	592	819	1411	1.383	0.580	0.539	0.524	0.527
8174	0	0	504	907	1411	1.800	0.643	0.614	0.603	0.588
8185	0	0	548	863	1411	1.575	0.612	0.590	0.570	0.588
8198	0	0	409	1002	1411	2.450	0.710	0.700	0.656	0.656
8206	4	0.001782531	625	630	1255	1.008	0.502	0.502	0.504	0.502
8215	0	0	519	892	1411	1.719	0.632	0.610	0.582	0.574
8218	0	0	473	938	1411	1.983	0.665	0.616	0.626	0.629
8234	0	0	511	900	1411	1.761	0.638	0.601	0.600	0.601
8246	0	0	432	979	1411	2.266	0.694	0.679	0.666	0.648
8258	0	0	498	913	1411	1.833	0.647	0.617	0.596	0.594
8262	0	0	439	972	1411	2.214	0.689	0.676	0.656	0.643
8274	4	0.002434358	624	631	1255	1.011	0.503	0.523	0.488	0.488
8277	2	0.001397317	669	667	1336	1.003	0.501	0.516	0.494	0.517
8283	8	0.006864007	529	530	1059	1.002	0.500	0.514	0.509	0.492

ADE_i	iPR	CutValue	high	low	n	I	RG	Accuracy(H2010)	Accuracy(New)	Accuracy(H2010+New)
8290	2	0.001091371	668	668	1336	1.000	0.500	0.480	0.497	0.487
8301	5	0.003280695	612	595	1207	1.029	0.507	0.498	0.489	0.497
8306	4	0.001946913	631	622	1253	1.014	0.504	0.470	0.497	0.528
8311	0	0	597	814	1411	1.363	0.577	0.522	0.540	0.524
8329	11	0.019913325	446	421	867	1.059	0.514	0.501	0.518	0.508
8341	0	0	457	954	1411	2.088	0.676	0.644	0.654	0.634
8353	0	0	559	852	1411	1.524	0.604	0.562	0.563	0.586
8355	0	0	610	801	1411	1.313	0.568	0.543	0.537	0.544
8375	2	0.001260071	663	674	1337	1.017	0.504	0.491	0.485	0.485
8376	8	0.006357864	522	541	1063	1.036	0.509	0.501	0.505	0.478
8380	0	0	564	847	1411	1.502	0.600	0.573	0.543	0.571
8383	0	0	436	975	1411	2.236	0.691	0.673	0.653	0.653
8391	0	0	464	947	1411	2.041	0.671	0.672	0.624	0.624
8399	0	0	454	957	1411	2.108	0.678	0.656	0.648	0.647
8406	0	0	695	716	1411	1.030	0.507	0.483	0.479	0.507
8410	0	0	443	968	1411	2.185	0.686	0.665	0.635	0.620
8426	6	0.004840276	586	574	1160	1.021	0.505	0.502	0.491	0.500
8427	0	0	620	791	1411	1.276	0.561	0.524	0.483	0.507
8432	0	0	695	716	1411	1.030	0.507	0.488	0.512	0.488
8433	0	0	432	979	1411	2.266	0.694	0.680	0.663	0.680
8474	0	0	710	701	1411	1.013	0.503	0.499	0.504	0.483
8479	13	0.046992481	371	350	721	1.060	0.515	0.496	0.491	0.506
8483	0	0	532	879	1411	1.652	0.623	0.598	0.573	0.595
8491	2	0.001096073	667	669	1336	1.003	0.501	0.474	0.478	0.503
8492	10	0.010305099	466	479	945	1.028	0.507	0.509	0.474	0.490
8493	0	0	680	731	1411	1.075	0.518	0.505	0.483	0.474
8522	0	0	435	976	1411	2.244	0.692	0.665	0.651	0.638
8540	0	0	711	700	1411	1.016	0.504	0.490	0.481	0.509
8542	0	0	608	803	1411	1.321	0.569	0.520	0.515	0.507
8557	0	0	461	950	1411	2.061	0.673	0.651	0.633	0.628
8579	0	0	634	777	1411	1.226	0.551	0.542	0.532	0.526
8580	0	0	494	917	1411	1.856	0.650	0.627	0.612	0.629
8581	0	0	512	899	1411	1.756	0.637	0.609	0.614	0.597
8588	0	0	600	811	1411	1.352	0.575	0.549	0.543	0.528
8591	0	0	413	998	1411	2.416	0.707	0.686	0.671	0.674
8593	7	0.004505329	550	564	1114	1.025	0.506	0.518	0.494	0.493
8594	6	0.004200158	576	588	1164	1.021	0.505	0.508	0.490	0.481
8595	0	0	495	916	1411	1.851	0.649	0.629	0.583	0.587
8596	6	0.003600896	573	592	1165	1.033	0.508	0.497	0.477	0.511
8608	0	0	477	934	1411	1.958	0.662	0.644	0.638	0.631
8610	0	0	600	811	1411	1.352	0.575	0.532	0.548	0.545
8612	0	0	514	897	1411	1.745	0.636	0.619	0.605	0.603
8620	4	0.002220251	623	632	1255	1.014	0.504	0.492	0.510	0.514
8628	5	0.002877011	613	593	1206	1.034	0.508	0.498	0.508	0.503
8641	0	0	619	792	1411	1.279	0.561	0.515	0.540	0.535
8643	0	0	439	972	1411	2.214	0.689	0.678	0.646	0.653
8670	0	0	545	866	1411	1.589	0.614	0.585	0.587	0.563
8685	0	0	554	857	1411	1.547	0.607	0.590	0.562	0.566
8712	0	0	478	933	1411	1.952	0.661	0.647	0.631	0.641
8725	0	0	486	925	1411	1.903	0.656	0.653	0.610	0.620
8738	0	0	616	795	1411	1.291	0.563	0.539	0.504	0.502
8741	0	0	432	979	1411	2.266	0.694	0.692	0.676	0.646
8745	1	0.000795779	695	679	1374	1.024	0.506	0.508	0.499	0.500
8751	0	0	496	915	1411	1.845	0.648	0.639	0.610	0.615
8753	0	0	677	734	1411	1.084	0.520	0.519	0.514	0.529
8779	0	0	462	949	1411	2.054	0.673	0.650	0.630	0.622
8796	0	0	584	827	1411	1.416	0.586	0.568	0.559	0.540
8806	0	0	481	930	1411	1.933	0.659	0.630	0.645	0.621

ADE_i	iPR	CutValue	high	low	n	I	RG	Accuracy(H2010)	Accuracy(New)	Accuracy(H2010+New)
8807	2	0.00118461	661	676	1337	1.023	0.506	0.494	0.505	0.523
8824	0	0	663	748	1411	1.128	0.530	0.500	0.549	0.515
8826	0	0	476	935	1411	1.964	0.663	0.631	0.627	0.635
8831	0	0	418	993	1411	2.376	0.704	0.683	0.677	0.678
8850	0	0	471	940	1411	1.996	0.666	0.629	0.615	0.620
8854	0	0	588	823	1411	1.400	0.583	0.565	0.552	0.527
9009	0	0	553	858	1411	1.552	0.608	0.567	0.555	0.569
9011	0	0	702	709	1411	1.010	0.502	0.528	0.493	0.481
9052	0	0	459	952	1411	2.074	0.675	0.666	0.635	0.629
9054	0	0	409	1002	1411	2.450	0.710	0.692	0.669	0.677
9075	0	0	503	908	1411	1.805	0.644	0.609	0.582	0.588
9081	0	0	598	813	1411	1.360	0.576	0.554	0.530	0.536
9112	0	0	496	915	1411	1.845	0.648	0.629	0.612	0.614
9116	0	0	411	1000	1411	2.433	0.709	0.678	0.697	0.682
9121	0	0	612	799	1411	1.306	0.566	0.549	0.531	0.525
9123	0	0	614	797	1411	1.298	0.565	0.544	0.529	0.527
9128	0	0	510	901	1411	1.767	0.639	0.617	0.596	0.605
9136	0	0	631	780	1411	1.236	0.553	0.549	0.542	0.519
9141	0	0	422	989	1411	2.344	0.701	0.696	0.664	0.666
9156	5	0.004444444	608	601	1209	1.012	0.503	0.525	0.516	0.500
9159	10	0.014267185	465	482	947	1.037	0.509	0.482	0.456	0.486
9163	5	0.00363307	603	607	1210	1.007	0.502	0.503	0.487	0.521
9165	0	0	494	917	1411	1.856	0.650	0.619	0.604	0.615
9173	1	0.000780898	692	682	1374	1.015	0.504	0.495	0.495	0.482
9180	0	0	505	906	1411	1.794	0.642	0.627	0.597	0.596
9191	0	0	417	994	1411	2.384	0.704	0.688	0.666	0.663
9202	0	0	470	941	1411	2.002	0.667	0.641	0.631	0.632
9203	10	0.010124921	473	465	938	1.017	0.504	0.480	0.506	0.501
9205	0	0	618	793	1411	1.283	0.562	0.543	0.520	0.498
9213	12	0.02962022	406	397	803	1.023	0.506	0.538	0.508	0.512
9218	0	0	536	875	1411	1.632	0.620	0.607	0.567	0.582
9221	0	0	436	975	1411	2.236	0.691	0.675	0.668	0.655
9225	0	0	604	807	1411	1.336	0.572	0.545	0.537	0.537
9228	0	0	542	869	1411	1.603	0.616	0.571	0.588	0.573
9229	0	0	491	920	1411	1.874	0.652	0.627	0.620	0.603
9234	0	0	519	892	1411	1.719	0.632	0.606	0.585	0.589
9243	0	0	440	971	1411	2.207	0.688	0.675	0.654	0.652
9245	0	0	585	826	1411	1.412	0.585	0.569	0.551	0.534
9259	0	0	574	837	1411	1.458	0.593	0.576	0.557	0.573
9260	10	0.014925373	467	478	945	1.024	0.506	0.492	0.533	0.529
9262	0	0	453	958	1411	2.115	0.679	0.651	0.648	0.639
9264	0	0	597	814	1411	1.363	0.577	0.526	0.534	0.551
9266	0	0	635	776	1411	1.222	0.550	0.520	0.507	0.498
9268	0	0	648	763	1411	1.177	0.541	0.512	0.524	0.527
9287	6	0.004793782	586	573	1159	1.023	0.506	0.499	0.508	0.508
9300	7	0.00785494	561	548	1109	1.024	0.506	0.508	0.508	0.492
9302	0	0	606	805	1411	1.328	0.571	0.517	0.522	0.508
9305	0	0	585	826	1411	1.412	0.585	0.551	0.538	0.558
9309	7	0.00800674	563	544	1107	1.035	0.509	0.476	0.468	0.494
9315	0	0	669	742	1411	1.109	0.526	0.499	0.528	0.512
9326	0	0	491	920	1411	1.874	0.652	0.622	0.611	0.609
9338	0	0	436	975	1411	2.236	0.691	0.684	0.636	0.652
9341	0	0	482	929	1411	1.927	0.658	0.641	0.592	0.603
9349	13	0.034921181	360	384	744	1.067	0.516	0.503	0.535	0.532
9355	0	0	601	810	1411	1.348	0.574	0.544	0.528	0.514
9358	1	0.000770132	696	678	1374	1.027	0.507	0.501	0.498	0.506
9360	0	0	615	796	1411	1.294	0.564	0.521	0.514	0.524
9368	0	0	542	869	1411	1.603	0.616	0.582	0.569	0.567

ADE_i	iPR	CutValue	high	low	n	I	RG	Accuracy(H2010)	Accuracy(New)	Accuracy(H2010+New)
9371	0	0	643	768	1411	1.194	0.544	0.527	0.483	0.511
9372	0	0	437	974	1411	2.229	0.690	0.675	0.651	0.641
9373	7	0.005010496	554	559	1113	1.009	0.502	0.497	0.501	0.484
9374	0	0	437	974	1411	2.229	0.690	0.690	0.654	0.631
9378	0	0	437	974	1411	2.229	0.690	0.677	0.629	0.629
9391	0	0	479	932	1411	1.946	0.661	0.658	0.601	0.608
9407	0	0	524	887	1411	1.693	0.629	0.610	0.576	0.568
9433	0	0	704	707	1411	1.004	0.501	0.499	0.485	0.476
9434	0	0	601	810	1411	1.348	0.574	0.536	0.551	0.539
9446	1	0.00070016	689	685	1374	1.006	0.501	0.523	0.507	0.512
9455	0	0	449	962	1411	2.143	0.682	0.675	0.645	0.628
9464	0	0	538	873	1411	1.623	0.619	0.584	0.588	0.583
9489	0	0	490	921	1411	1.880	0.653	0.629	0.609	0.615
9492	0	0	515	896	1411	1.740	0.635	0.611	0.611	0.581
9494	0	0	474	937	1411	1.977	0.664	0.634	0.612	0.612
9495	0	0	703	708	1411	1.007	0.502	0.463	0.483	0.477
9499	0	0	599	812	1411	1.356	0.575	0.550	0.534	0.541
9566	0	0	464	947	1411	2.041	0.671	0.656	0.629	0.660
9572	0	0	577	834	1411	1.445	0.591	0.551	0.558	0.558
9577	0	0	586	825	1411	1.408	0.585	0.561	0.550	0.547
9602	0	0	579	832	1411	1.437	0.590	0.541	0.530	0.540
9604	0	0	606	805	1411	1.328	0.571	0.555	0.522	0.524
9606	4	0.001699356	625	630	1255	1.008	0.502	0.506	0.475	0.466
9608	0	0	425	986	1411	2.320	0.699	0.683	0.671	0.654
9612	0	0	492	919	1411	1.868	0.651	0.635	0.600	0.600
9615	0	0	489	922	1411	1.885	0.653	0.612	0.615	0.616
9619	0	0	446	965	1411	2.164	0.684	0.661	0.649	0.631
9620	0	0	469	942	1411	2.009	0.668	0.656	0.617	0.633
9646	0	0	472	939	1411	1.989	0.665	0.650	0.637	0.628
9658	9	0.009980925	499	504	1003	1.010	0.502	0.496	0.511	0.498
9694	6	0.003619152	589	569	1158	1.035	0.509	0.486	0.510	0.477
9708	1	0.000775781	679	696	1375	1.025	0.506	0.508	0.483	0.492
9715	2	0.001196172	667	670	1337	1.004	0.501	0.511	0.474	0.504
9724	0	0	693	718	1411	1.036	0.509	0.512	0.488	0.486
9774	0	0	444	967	1411	2.178	0.685	0.660	0.638	0.634
9785	0	0	434	977	1411	2.251	0.692	0.674	0.654	0.649
9809	0	0	623	788	1411	1.265	0.558	0.527	0.518	0.515
9813	0	0	445	966	1411	2.171	0.685	0.669	0.656	0.635
9814	0	0	554	857	1411	1.547	0.607	0.578	0.568	0.583
9821	0	0	442	969	1411	2.192	0.687	0.661	0.654	0.649
9839	0	0	659	752	1411	1.141	0.533	0.516	0.495	0.503
9846	0	0	451	960	1411	2.129	0.680	0.656	0.637	0.644
9848	0	0	406	1005	1411	2.475	0.712	0.682	0.691	0.668
9849	0	0	593	818	1411	1.379	0.580	0.561	0.515	0.529
9856	0	0	502	909	1411	1.811	0.644	0.631	0.619	0.604
9863	5	0.004066543	610	598	1208	1.020	0.505	0.533	0.516	0.501
9873	11	0.023046792	438	437	875	1.002	0.501	0.482	0.509	0.503
9920	0	0	586	825	1411	1.408	0.585	0.557	0.547	0.521
9922	0	0	415	996	1411	2.400	0.706	0.695	0.676	0.676
9923	0	0	602	809	1411	1.344	0.573	0.550	0.510	0.519
9924	0	0	447	964	1411	2.157	0.683	0.655	0.653	0.647
9949	0	0	413	998	1411	2.416	0.707	0.692	0.675	0.676
9958	0	0	562	849	1411	1.511	0.602	0.572	0.563	0.556
9960	6	0.004232601	575	589	1164	1.024	0.506	0.499	0.501	0.482
9965	4	0.00280264	635	617	1252	1.029	0.507	0.506	0.505	0.486
9971	0	0	562	849	1411	1.511	0.602	0.578	0.549	0.555
9972	0	0	470	941	1411	2.002	0.667	0.628	0.638	0.634
9976	0	0	677	734	1411	1.084	0.520	0.510	0.511	0.493

ADE_i	iPR	CutValue	high	low	n	I	RG	Accuracy(H2010)	Accuracy(New)	Accuracy(H2010+New)
10001	0	0	561	850	1411	1.515	0.602	0.561	0.550	0.556
10006	0	0	707	704	1411	1.004	0.501	0.502	0.497	0.518
10008	0	0	525	886	1411	1.688	0.628	0.588	0.573	0.559
10044	0	0	483	928	1411	1.921	0.658	0.643	0.629	0.604
10054	0	0	473	938	1411	1.983	0.665	0.632	0.624	0.619
10076	0	0	465	946	1411	2.034	0.670	0.655	0.612	0.595
10163	0	0	604	807	1411	1.336	0.572	0.546	0.509	0.520
10167	3	0.001507513	641	656	1297	1.023	0.506	0.505	0.499	0.507
10169	0	0	535	876	1411	1.637	0.621	0.570	0.583	0.557
10170	0	0	610	801	1411	1.313	0.568	0.556	0.507	0.515
10171	0	0	473	938	1411	1.983	0.665	0.653	0.626	0.615
10181	0	0	565	846	1411	1.497	0.600	0.573	0.540	0.551
10204	7	0.004536162	553	560	1113	1.013	0.503	0.497	0.495	0.503
10206	0	0	515	896	1411	1.740	0.635	0.607	0.586	0.591
10211	0	0	508	903	1411	1.778	0.640	0.609	0.602	0.604
10243	0	0	529	882	1411	1.667	0.625	0.605	0.566	0.581
10247	0	0	490	921	1411	1.880	0.653	0.633	0.610	0.602
10251	0	0	551	860	1411	1.561	0.609	0.580	0.566	0.556
10259	0	0	493	918	1411	1.862	0.651	0.622	0.614	0.607
10262	0	0	488	923	1411	1.891	0.654	0.639	0.612	0.616
10264	0	0	553	858	1411	1.552	0.608	0.563	0.571	0.571
10266	4	0.002390214	621	634	1255	1.021	0.505	0.521	0.494	0.520
10340	0	0	486	925	1411	1.903	0.656	0.628	0.606	0.617
10352	0	0	539	872	1411	1.618	0.618	0.573	0.563	0.558
10362	0	0	472	939	1411	1.989	0.665	0.636	0.605	0.606
10397	0	0	680	731	1411	1.075	0.518	0.473	0.522	0.522
10407	0	0	547	864	1411	1.580	0.612	0.580	0.563	0.554
10425	0	0	584	827	1411	1.416	0.586	0.563	0.543	0.535
10439	0	0	608	803	1411	1.321	0.569	0.516	0.542	0.534
10446	0	0	499	912	1411	1.828	0.646	0.622	0.602	0.600
10475	0	0	408	1003	1411	2.458	0.711	0.695	0.663	0.658
10481	0	0	494	917	1411	1.856	0.650	0.629	0.599	0.601
10514	0	0	542	869	1411	1.603	0.616	0.581	0.562	0.551
10529	0	0	434	977	1411	2.251	0.692	0.659	0.646	0.642
10588	0	0	448	963	1411	2.150	0.682	0.664	0.654	0.637
10591	0	0	536	875	1411	1.632	0.620	0.600	0.574	0.572
10595	0	0	510	901	1411	1.767	0.639	0.605	0.592	0.578
10597	0	0	576	835	1411	1.450	0.592	0.551	0.551	0.545
10599	0	0	442	969	1411	2.192	0.687	0.663	0.641	0.637
10644	6	0.005091552	584	576	1160	1.014	0.503	0.489	0.534	0.508
10649	0	0	431	980	1411	2.274	0.695	0.681	0.671	0.643
10675	0	0	506	905	1411	1.789	0.641	0.627	0.600	0.604
10676	3	0.001747266	647	649	1296	1.003	0.501	0.505	0.485	0.500
10681	0	0	420	991	1411	2.360	0.702	0.690	0.663	0.670
10684	6	0.004567253	582	580	1162	1.003	0.501	0.498	0.505	0.506
10697	0	0	476	935	1411	1.964	0.663	0.629	0.630	0.641
10735	0	0	494	917	1411	1.856	0.650	0.617	0.607	0.602
10738	0	0	562	849	1411	1.511	0.602	0.593	0.559	0.547
10779	0	0	621	790	1411	1.272	0.560	0.546	0.524	0.523
10785	0	0	611	800	1411	1.309	0.567	0.517	0.533	0.527
10829	0	0	405	1006	1411	2.484	0.713	0.687	0.646	0.654
10832	0	0	410	1001	1411	2.441	0.709	0.675	0.673	0.672
10837	8	0.005438281	527	532	1059	1.009	0.502	0.523	0.509	0.486
10839	7	0.005276301	556	556	1112	1.000	0.500	0.490	0.475	0.494
10843	0	0	540	871	1411	1.613	0.617	0.594	0.572	0.576
10857	0	0	591	820	1411	1.387	0.581	0.543	0.549	0.532
10860	0	0	596	815	1411	1.367	0.578	0.547	0.547	0.548
10862	0	0	543	868	1411	1.599	0.615	0.584	0.582	0.568

ADE_i	iPR	CutValue	high	low	n	I	RG	Accuracy(H2010)	Accuracy(New)	Accuracy(H2010+New)
10864	0	0	461	950	1411	2.061	0.673	0.651	0.616	0.631
10881	0	0	419	992	1411	2.368	0.703	0.682	0.641	0.651
10886	12	0.022269063	408	392	800	1.041	0.510	0.475	0.489	0.480
10900	0	0	536	875	1411	1.632	0.620	0.595	0.563	0.551
10907	0	0	428	983	1411	2.297	0.697	0.665	0.658	0.664
10909	0	0	451	960	1411	2.129	0.680	0.661	0.631	0.644
10911	0	0	569	842	1411	1.480	0.597	0.569	0.543	0.535
10925	0	0	463	948	1411	2.048	0.672	0.656	0.637	0.624
10949	0	0	524	887	1411	1.693	0.629	0.610	0.565	0.571
10954	6	0.003911163	580	582	1162	1.003	0.501	0.490	0.474	0.477
10958	0	0	635	776	1411	1.222	0.550	0.511	0.520	0.527
10960	1	0.000865747	695	679	1374	1.024	0.506	0.493	0.500	0.518
10964	0	0	652	759	1411	1.164	0.538	0.505	0.494	0.495
10965	0	0	632	779	1411	1.233	0.552	0.513	0.517	0.512
11012	6	0.003546099	575	591	1166	1.028	0.507	0.499	0.509	0.517
11013	0	0	440	971	1411	2.207	0.688	0.665	0.643	0.634
11044	0	0	636	775	1411	1.219	0.549	0.533	0.512	0.514
11045	0	0	428	983	1411	2.297	0.697	0.674	0.651	0.647
11052	0	0	491	920	1411	1.874	0.652	0.612	0.629	0.624
11068	0	0	483	928	1411	1.921	0.658	0.643	0.615	0.612
11075	0	0	611	800	1411	1.309	0.567	0.555	0.510	0.515
11081	0	0	537	874	1411	1.628	0.619	0.602	0.587	0.568
11119	0	0	445	966	1411	2.171	0.685	0.678	0.636	0.640
11140	0	0	548	863	1411	1.575	0.612	0.569	0.563	0.568
11145	12	0.026724449	408	390	798	1.046	0.511	0.516	0.502	0.475
11190	0	0	429	982	1411	2.289	0.696	0.682	0.669	0.668
11228	4	0.002184361	626	628	1254	1.003	0.501	0.502	0.518	0.506
11250	0	0	703	708	1411	1.007	0.502	0.512	0.490	0.488
11269	0	0	580	831	1411	1.433	0.589	0.551	0.527	0.544
11294	0	0	489	922	1411	1.885	0.653	0.639	0.593	0.605
11299	0	0	620	791	1411	1.276	0.561	0.522	0.525	0.524
11304	0	0	418	993	1411	2.376	0.704	0.700	0.662	0.668
11326	0	0	575	836	1411	1.454	0.592	0.563	0.537	0.525
11380	0	0	439	972	1411	2.214	0.689	0.679	0.655	0.654
11413	0	0	560	851	1411	1.520	0.603	0.563	0.557	0.562
11427	7	0.00487013	559	550	1109	1.016	0.504	0.527	0.491	0.531
11450	2	0.001124607	674	662	1336	1.018	0.504	0.510	0.479	0.502
11464	6	0.004029315	579	583	1162	1.007	0.502	0.517	0.510	0.524
11478	0	0	502	909	1411	1.811	0.644	0.627	0.612	0.600
11530	0	0	407	1004	1411	2.467	0.712	0.692	0.675	0.676
11541	0	0	481	930	1411	1.933	0.659	0.611	0.630	0.605
11549	3	0.00149285	650	646	1296	1.006	0.502	0.506	0.502	0.478
11551	0	0	647	764	1411	1.181	0.541	0.513	0.522	0.519
11554	3	0.002329572	649	647	1296	1.003	0.501	0.495	0.507	0.490
11582	5	0.0028602	597	615	1212	1.030	0.507	0.489	0.541	0.516
11585	0	0	549	862	1411	1.570	0.611	0.585	0.560	0.571
11586	0	0	452	959	1411	2.122	0.680	0.654	0.630	0.625
11617	0	0	594	817	1411	1.375	0.579	0.572	0.549	0.554
11620	0	0	508	903	1411	1.778	0.640	0.595	0.580	0.585
11632	0	0	607	804	1411	1.325	0.570	0.551	0.539	0.535
11633	0	0	536	875	1411	1.632	0.620	0.593	0.578	0.558
11634	0	0	520	891	1411	1.713	0.631	0.599	0.568	0.568
11673	0	0	483	928	1411	1.921	0.658	0.629	0.610	0.607
11681	0	0	465	946	1411	2.034	0.670	0.660	0.597	0.605
11705	0	0	490	921	1411	1.880	0.653	0.627	0.615	0.585
11746	0	0	514	897	1411	1.745	0.636	0.614	0.622	0.610
11757	0	0	525	886	1411	1.688	0.628	0.596	0.603	0.598
11760	0	0	710	701	1411	1.013	0.503	0.499	0.490	0.483

ADE_i	iPR	CutValue	high	low	n	I	RG	Accuracy(H2010)	Accuracy(New)	Accuracy(H2010+New)
11784	0	0	478	933	1411	1.952	0.661	0.630	0.606	0.609
11809	0	0	443	968	1411	2.185	0.686	0.674	0.646	0.656
11812	5	0.002793325	598	613	1211	1.025	0.506	0.487	0.504	0.503
11832	0	0	708	703	1411	1.007	0.502	0.497	0.510	0.522
11857	0	0	461	950	1411	2.061	0.673	0.646	0.629	0.634
11879	0	0	463	948	1411	2.048	0.672	0.648	0.647	0.641
11883	0	0	621	790	1411	1.272	0.560	0.534	0.527	0.520
11885	0	0	571	840	1411	1.471	0.595	0.557	0.546	0.537
11900	0	0	573	838	1411	1.462	0.594	0.523	0.526	0.541
11908	0	0	547	864	1411	1.580	0.612	0.597	0.584	0.590
11911	0	0	661	750	1411	1.135	0.532	0.513	0.529	0.497
11912	2	0.000772157	665	672	1337	1.011	0.503	0.537	0.513	0.500
11947	0	0	659	752	1411	1.141	0.533	0.522	0.498	0.501
11953	0	0	465	946	1411	2.034	0.670	0.648	0.635	0.622
11962	0	0	427	984	1411	2.304	0.697	0.694	0.651	0.661
11963	7	0.005705755	558	552	1110	1.011	0.503	0.522	0.518	0.498
11971	0	0	514	897	1411	1.745	0.636	0.619	0.593	0.597
11973	0	0	433	978	1411	2.259	0.693	0.669	0.664	0.651
11985	0	0	548	863	1411	1.575	0.612	0.549	0.537	0.536
11987	0	0	584	827	1411	1.416	0.586	0.551	0.529	0.546
11990	0	0	534	877	1411	1.642	0.622	0.585	0.588	0.578
11991	0	0	414	997	1411	2.408	0.707	0.691	0.675	0.665
12007	0	0	576	835	1411	1.450	0.592	0.549	0.505	0.532
12009	0	0	446	965	1411	2.164	0.684	0.661	0.656	0.635
12011	0	0	510	901	1411	1.767	0.639	0.630	0.593	0.585
12012	0	0	571	840	1411	1.471	0.595	0.556	0.538	0.554
12021	0	0	416	995	1411	2.392	0.705	0.689	0.677	0.682
12025	0	0	404	1007	1411	2.493	0.714	0.685	0.697	0.699
12038	0	0	592	819	1411	1.383	0.580	0.564	0.524	0.546
12040	8	0.009417112	527	533	1060	1.011	0.503	0.498	0.506	0.487
12041	0	0	409	1002	1411	2.450	0.710	0.693	0.687	0.682
12042	0	0	453	958	1411	2.115	0.679	0.659	0.664	0.644
12045	0	0	515	896	1411	1.740	0.635	0.634	0.608	0.605
12046	0	0	680	731	1411	1.075	0.518	0.514	0.510	0.517
12049	8	0.009017413	535	520	1055	1.029	0.507	0.447	0.475	0.479
12051	0	0	583	828	1411	1.420	0.587	0.554	0.532	0.534
12053	0	0	545	866	1411	1.589	0.614	0.600	0.571	0.575
12054	0	0	464	947	1411	2.041	0.671	0.640	0.641	0.633
12055	2	0.001341244	663	674	1337	1.017	0.504	0.522	0.496	0.506
12056	4	0.002476488	623	632	1255	1.014	0.504	0.511	0.512	0.491
12059	10	0.014840471	465	481	946	1.034	0.508	0.483	0.486	0.505
12107	0	0	653	758	1411	1.161	0.537	0.523	0.519	0.495
12126	0	0	575	836	1411	1.454	0.592	0.570	0.538	0.548
12145	11	0.020041023	436	443	879	1.016	0.504	0.515	0.491	0.520
12146	2	0.001090528	661	676	1337	1.023	0.506	0.507	0.492	0.528
12151	0	0	491	920	1411	1.874	0.652	0.628	0.624	0.624
12165	0	0	645	766	1411	1.188	0.543	0.527	0.522	0.520
12173	0	0	460	951	1411	2.067	0.674	0.658	0.642	0.652
12184	0	0	584	827	1411	1.416	0.586	0.535	0.552	0.544
12194	0	0	568	843	1411	1.484	0.597	0.566	0.551	0.546
12228	0	0	412	999	1411	2.425	0.708	0.698	0.663	0.666
12258	0	0	660	751	1411	1.138	0.532	0.498	0.503	0.513
12308	4	0.002163625	624	631	1255	1.011	0.503	0.511	0.485	0.508
12320	14	0.07652219	332	305	637	1.089	0.521	0.517	0.499	0.523
12327	3	0.00202273	656	639	1295	1.027	0.507	0.495	0.538	0.492
12333	0	0	648	763	1411	1.177	0.541	0.494	0.508	0.531
12378	0	0	434	977	1411	2.251	0.692	0.685	0.660	0.659
12408	0	0	489	922	1411	1.885	0.653	0.609	0.597	0.614

ADE_i	iPR	CutValue	high	low	n	I	RG	Accuracy(H2010)	Accuracy(New)	Accuracy(H2010+New)
12410	0	0	605	806	1411	1.332	0.571	0.527	0.544	0.545
12415	0	0	430	981	1411	2.281	0.695	0.690	0.683	0.678
12429	0	0	560	851	1411	1.520	0.603	0.583	0.566	0.559
12438	0	0	710	701	1411	1.013	0.503	0.497	0.469	0.478
12440	0	0	471	940	1411	1.996	0.666	0.646	0.630	0.634
12441	0	0	515	896	1411	1.740	0.635	0.632	0.601	0.593
12450	0	0	520	891	1411	1.713	0.631	0.618	0.604	0.607
12453	0	0	418	993	1411	2.376	0.704	0.701	0.667	0.665
12459	0	0	494	917	1411	1.856	0.650	0.606	0.605	0.600
12470	4	0.001918731	620	636	1256	1.026	0.506	0.509	0.470	0.479
12475	2	0.000935021	662	675	1337	1.020	0.505	0.527	0.500	0.506
12478	0	0	628	783	1411	1.247	0.555	0.521	0.518	0.491
12505	0	0	427	984	1411	2.304	0.697	0.687	0.658	0.667
12510	0	0	507	904	1411	1.783	0.641	0.618	0.598	0.598
12520	0	0	558	853	1411	1.529	0.605	0.574	0.558	0.557
12541	0	0	572	839	1411	1.467	0.595	0.551	0.545	0.534
12542	5	0.004670718	612	595	1207	1.029	0.507	0.503	0.519	0.514
12557	0	0	474	937	1411	1.977	0.664	0.639	0.627	0.618
12563	8	0.00780097	532	525	1057	1.013	0.503	0.487	0.500	0.490
12567	0	0	429	982	1411	2.289	0.696	0.691	0.667	0.660
12573	0	0	714	697	1411	1.024	0.506	0.489	0.501	0.518
12574	0	0	628	783	1411	1.247	0.555	0.553	0.520	0.544
12588	0	0	504	907	1411	1.800	0.643	0.627	0.590	0.605
12605	0	0	650	761	1411	1.171	0.539	0.557	0.502	0.514
12606	0	0	622	789	1411	1.268	0.559	0.524	0.509	0.527
12633	0	0	536	875	1411	1.632	0.620	0.590	0.596	0.577
12636	3	0.001087401	651	645	1296	1.009	0.502	0.501	0.512	0.497
12641	0	0	532	879	1411	1.652	0.623	0.575	0.579	0.571
12654	0	0	418	993	1411	2.376	0.704	0.698	0.670	0.669
12659	0	0	516	895	1411	1.734	0.634	0.603	0.590	0.586
12661	0	0	461	950	1411	2.061	0.673	0.652	0.637	0.632
12724	0	0	542	869	1411	1.603	0.616	0.589	0.568	0.565
12745	0	0	482	929	1411	1.927	0.658	0.634	0.648	0.640
12747	0	0	512	899	1411	1.756	0.637	0.607	0.589	0.591
12766	0	0	497	914	1411	1.839	0.648	0.630	0.619	0.616
12767	0	0	613	798	1411	1.302	0.566	0.531	0.526	0.517
12773	0	0	489	922	1411	1.885	0.653	0.633	0.598	0.607
12782	0	0	582	829	1411	1.424	0.588	0.553	0.543	0.541
12790	0	0	481	930	1411	1.933	0.659	0.622	0.624	0.622
12812	0	0	617	794	1411	1.287	0.563	0.532	0.504	0.516
12814	0	0	483	928	1411	1.921	0.658	0.627	0.605	0.602
12845	0	0	494	917	1411	1.856	0.650	0.609	0.620	0.606
12846	9	0.007655451	496	509	1005	1.026	0.506	0.513	0.526	0.504
12851	0	0	511	900	1411	1.761	0.638	0.610	0.594	0.579
12854	12	0.031381248	406	396	802	1.025	0.506	0.526	0.488	0.478
12868	0	0	514	897	1411	1.745	0.636	0.610	0.580	0.571
12875	0	0	430	981	1411	2.281	0.695	0.675	0.669	0.668
12918	0	0	478	933	1411	1.952	0.661	0.652	0.622	0.637
12925	0	0	665	746	1411	1.122	0.529	0.512	0.514	0.514
12968	2	0.000868573	674	662	1336	1.018	0.504	0.508	0.502	0.491
12982	0	0	650	761	1411	1.171	0.539	0.537	0.518	0.507
13005	0	0	441	970	1411	2.200	0.687	0.678	0.632	0.636
13018	0	0	459	952	1411	2.074	0.675	0.670	0.651	0.653
13064	0	0	456	955	1411	2.094	0.677	0.651	0.615	0.627
13077	0	0	635	776	1411	1.222	0.550	0.512	0.528	0.514
13083	0	0	465	946	1411	2.034	0.670	0.666	0.609	0.646
13084	0	0	507	904	1411	1.783	0.641	0.597	0.590	0.591
13090	0	0	459	952	1411	2.074	0.675	0.659	0.637	0.640

ADE_i	iPR	CutValue	high	low	n	I	RG	Accuracy(H2010)	Accuracy(New)	Accuracy(H2010+New)
13091	0	0	406	1005	1411	2.475	0.712	0.685	0.695	0.666
13092	0	0	690	721	1411	1.045	0.511	0.527	0.508	0.486
13107	0	0	614	797	1411	1.298	0.565	0.534	0.500	0.503
13137	0	0	425	986	1411	2.320	0.699	0.682	0.653	0.668
13161	0	0	697	714	1411	1.024	0.506	0.503	0.499	0.470
13179	0	0	542	869	1411	1.603	0.616	0.622	0.538	0.576
13185	0	0	702	709	1411	1.010	0.502	0.488	0.488	0.495
13203	0	0	442	969	1411	2.192	0.687	0.654	0.649	0.649
13206	2	0.001261337	661	676	1337	1.023	0.506	0.499	0.497	0.498
13221	0	0	701	710	1411	1.013	0.503	0.499	0.502	0.495
13230	3	0.002686259	653	642	1295	1.017	0.504	0.515	0.492	0.489
13231	0	0	610	801	1411	1.313	0.568	0.546	0.529	0.539
13233	0	0	603	808	1411	1.340	0.573	0.536	0.551	0.528
13236	0	0	674	737	1411	1.093	0.522	0.527	0.519	0.501
13266	0	0	489	922	1411	1.885	0.653	0.622	0.593	0.608
13302	0	0	507	904	1411	1.783	0.641	0.600	0.569	0.576
13373	9	0.008739244	503	497	1000	1.012	0.503	0.499	0.473	0.521
13392	7	0.00407896	554	558	1112	1.007	0.502	0.500	0.469	0.512
13420	13	0.047068951	367	363	730	1.011	0.503	0.503	0.522	0.504
13423	11	0.022797417	446	421	867	1.059	0.514	0.508	0.543	0.538
13424	0	0	670	741	1411	1.106	0.525	0.515	0.492	0.492
13427	0	0	487	924	1411	1.897	0.655	0.621	0.592	0.598
13447	5	0.002460036	597	615	1212	1.030	0.507	0.479	0.498	0.498
13450	0	0	500	911	1411	1.822	0.646	0.601	0.585	0.595
13454	9	0.010479538	499	503	1002	1.008	0.502	0.487	0.496	0.482
13468	0	0	436	975	1411	2.236	0.691	0.673	0.656	0.653
13479	0	0	459	952	1411	2.074	0.675	0.639	0.628	0.632
13517	5	0.004074797	603	607	1210	1.007	0.502	0.481	0.512	0.505
13518	2	0.001402852	665	672	1337	1.011	0.503	0.506	0.488	0.472
13533	7	0.007407407	559	550	1109	1.016	0.504	0.481	0.508	0.485
13537	0	0	675	736	1411	1.090	0.522	0.513	0.517	0.512
13541	0	0	425	986	1411	2.320	0.699	0.676	0.666	0.658
13559	0	0	450	961	1411	2.136	0.681	0.663	0.664	0.648
13582	10	0.01279082	465	481	946	1.034	0.508	0.536	0.517	0.521
13588	0	0	540	871	1411	1.613	0.617	0.594	0.584	0.580
13596	0	0	642	769	1411	1.198	0.545	0.511	0.500	0.507
13628	0	0	609	802	1411	1.317	0.568	0.541	0.539	0.544
13687	0	0	427	984	1411	2.304	0.697	0.667	0.645	0.648
13698	0	0	480	931	1411	1.940	0.660	0.632	0.626	0.595
13703	0	0	451	960	1411	2.129	0.680	0.679	0.653	0.651
13725	0	0	426	985	1411	2.312	0.698	0.689	0.651	0.646
13745	0	0	471	940	1411	1.996	0.666	0.651	0.622	0.613
13746	0	0	452	959	1411	2.122	0.680	0.668	0.646	0.644
13754	0	0	545	866	1411	1.589	0.614	0.593	0.563	0.566
13755	0	0	452	959	1411	2.122	0.680	0.670	0.640	0.638
13784	0	0	422	989	1411	2.344	0.701	0.675	0.658	0.655
13799	0	0	492	919	1411	1.868	0.651	0.625	0.607	0.607
13861	0	0	491	920	1411	1.874	0.652	0.627	0.624	0.627
13880	0	0	479	932	1411	1.946	0.661	0.635	0.604	0.614
13896	2	0.001280473	671	665	1336	1.009	0.502	0.505	0.482	0.489
13909	0	0	553	858	1411	1.552	0.608	0.568	0.578	0.598
13961	0	0	404	1007	1411	2.493	0.714	0.709	0.706	0.706
13969	0	0	443	968	1411	2.185	0.686	0.658	0.649	0.634
13981	0	0	644	767	1411	1.191	0.544	0.508	0.498	0.506
13983	0	0	490	921	1411	1.880	0.653	0.642	0.604	0.599
14009	0	0	431	980	1411	2.274	0.695	0.671	0.645	0.644
14017	0	0	578	833	1411	1.441	0.590	0.552	0.549	0.543
14076	0	0	659	752	1411	1.141	0.533	0.510	0.513	0.494

ADE_i	iPR	CutValue	high	low	n	I	RG	Accuracy(H2010)	Accuracy(New)	Accuracy(H2010+New)
14094	0	0	446	965	1411	2.164	0.684	0.684	0.657	0.643
14104	0	0	501	910	1411	1.816	0.645	0.608	0.602	0.603
14114	0	0	654	757	1411	1.157	0.536	0.513	0.522	0.528
14115	0	0	409	1002	1411	2.450	0.710	0.707	0.695	0.692
14152	4	0.002117037	632	621	1253	1.018	0.504	0.474	0.522	0.495
14187	0	0	659	752	1411	1.141	0.533	0.518	0.508	0.520
14195	0	0	630	781	1411	1.240	0.554	0.518	0.499	0.518
14203	2	0.001025277	661	676	1337	1.023	0.506	0.493	0.509	0.512
14216	0	0	497	914	1411	1.839	0.648	0.632	0.615	0.598
14263	0	0	638	773	1411	1.212	0.548	0.543	0.501	0.514
14264	0	0	461	950	1411	2.061	0.673	0.652	0.651	0.638
14268	0	0	598	813	1411	1.360	0.576	0.562	0.538	0.544
14301	0	0	462	949	1411	2.054	0.673	0.652	0.624	0.621
14321	0	0	512	899	1411	1.756	0.637	0.610	0.610	0.617
14410	9	0.011784502	506	491	997	1.031	0.508	0.464	0.545	0.514
14411	1	0.000533524	687	687	1374	1.000	0.500	0.488	0.521	0.501
14452	9	0.014718337	503	496	999	1.014	0.504	0.485	0.479	0.506
14453	0	0	448	963	1411	2.150	0.682	0.661	0.633	0.638
14469	0	0	558	853	1411	1.529	0.605	0.561	0.580	0.580
14471	0	0	494	917	1411	1.856	0.650	0.612	0.598	0.600
14498	0	0	502	909	1411	1.811	0.644	0.624	0.593	0.590
14502	12	0.035714286	404	400	804	1.010	0.502	0.457	0.501	0.503
14506	3	0.001639648	645	652	1297	1.011	0.503	0.490	0.511	0.509
14507	0	0	524	887	1411	1.693	0.629	0.609	0.573	0.564
14528	0	0	410	1001	1411	2.441	0.709	0.691	0.664	0.665
14531	0	0	476	935	1411	1.964	0.663	0.639	0.612	0.612
14537	0	0	653	758	1411	1.161	0.537	0.496	0.513	0.514
14544	0	0	666	745	1411	1.119	0.528	0.517	0.481	0.504
14550	0	0	554	857	1411	1.547	0.607	0.593	0.535	0.568
14562	0	0	470	941	1411	2.002	0.667	0.651	0.619	0.605
14573	0	0	710	701	1411	1.013	0.503	0.493	0.495	0.510
14585	0	0	501	910	1411	1.816	0.645	0.634	0.598	0.626
14602	0	0	598	813	1411	1.360	0.576	0.532	0.530	0.510
14612	0	0	461	950	1411	2.061	0.673	0.658	0.624	0.623
14620	0	0	590	821	1411	1.392	0.582	0.551	0.524	0.532
14623	0	0	434	977	1411	2.251	0.692	0.683	0.652	0.636
14626	0	0	491	920	1411	1.874	0.652	0.619	0.617	0.590
14658	0	0	413	998	1411	2.416	0.707	0.681	0.658	0.655
14697	7	0.003266703	553	560	1113	1.013	0.503	0.474	0.479	0.502
14707	0	0	614	797	1411	1.298	0.565	0.514	0.498	0.512
14764	0	0	421	990	1411	2.352	0.702	0.700	0.671	0.647
14771	0	0	435	976	1411	2.244	0.692	0.680	0.645	0.649
14844	0	0	653	758	1411	1.161	0.537	0.522	0.514	0.509
14867	0	0	565	846	1411	1.497	0.600	0.556	0.525	0.515
14872	0	0	464	947	1411	2.041	0.671	0.641	0.638	0.620
14891	0	0	450	961	1411	2.136	0.681	0.670	0.639	0.639
14897	0	0	609	802	1411	1.317	0.568	0.511	0.537	0.520
14922	0	0	406	1005	1411	2.475	0.712	0.698	0.665	0.661
14934	0	0	704	707	1411	1.004	0.501	0.514	0.459	0.489
14940	0	0	506	905	1411	1.789	0.641	0.612	0.602	0.610
14946	0	0	490	921	1411	1.880	0.653	0.642	0.627	0.605
15010	0	0	649	762	1411	1.174	0.540	0.507	0.497	0.517
15016	0	0	409	1002	1411	2.450	0.710	0.697	0.666	0.680
15020	1	0.000874876	686	688	1374	1.003	0.501	0.532	0.500	0.495
15084	0	0	545	866	1411	1.589	0.614	0.596	0.552	0.566
15124	0	0	427	984	1411	2.304	0.697	0.668	0.666	0.648
15163	0	0	621	790	1411	1.272	0.560	0.519	0.512	0.533
15164	0	0	453	958	1411	2.115	0.679	0.662	0.644	0.639

ADE_i	iPR	CutValue	high	low	n	I	RG	Accuracy(H2010)	Accuracy(New)	Accuracy(H2010+New)
15168	0	0	553	858	1411	1.552	0.608	0.575	0.573	0.549
15170	0	0	666	745	1411	1.119	0.528	0.510	0.500	0.498
15183	3	0.001478385	641	657	1298	1.025	0.506	0.487	0.502	0.497
15188	0	0	463	948	1411	2.048	0.672	0.644	0.650	0.632
15192	11	0.018837145	446	421	867	1.059	0.514	0.473	0.492	0.486
15195	0	0	690	721	1411	1.045	0.511	0.495	0.502	0.484
15223	0	0	442	969	1411	2.192	0.687	0.682	0.640	0.627
15228	0	0	647	764	1411	1.181	0.541	0.524	0.507	0.507
15252	0	0	602	809	1411	1.344	0.573	0.542	0.504	0.522
15260	0	0	448	963	1411	2.150	0.682	0.668	0.650	0.635
15267	0	0	564	847	1411	1.502	0.600	0.576	0.539	0.561
15278	0	0	708	703	1411	1.007	0.502	0.512	0.493	0.483
15297	0	0	444	967	1411	2.178	0.685	0.678	0.641	0.633
15327	2	0.001051543	665	672	1337	1.011	0.503	0.512	0.523	0.518
15330	8	0.00919231	530	527	1057	1.006	0.501	0.479	0.501	0.487
15332	0	0	661	750	1411	1.135	0.532	0.519	0.514	0.514
15344	0	0	596	815	1411	1.367	0.578	0.541	0.510	0.527
15348	3	0.001973907	645	652	1297	1.011	0.503	0.486	0.494	0.480
15351	0	0	415	996	1411	2.400	0.706	0.687	0.661	0.663
15354	0	0	466	945	1411	2.028	0.670	0.648	0.659	0.653
15359	8	0.007727432	535	520	1055	1.029	0.507	0.481	0.480	0.478
15374	0	0	412	999	1411	2.425	0.708	0.701	0.663	0.658
15381	0	0	411	1000	1411	2.433	0.709	0.700	0.680	0.677
15397	0	0	635	776	1411	1.222	0.550	0.521	0.513	0.503
15419	0	0	476	935	1411	1.964	0.663	0.636	0.621	0.611
15425	0	0	448	963	1411	2.150	0.682	0.662	0.649	0.637
15432	0	0	668	743	1411	1.112	0.527	0.520	0.525	0.494
15438	0	0	493	918	1411	1.862	0.651	0.641	0.597	0.639
15439	0	0	541	870	1411	1.608	0.617	0.575	0.556	0.573
15452	0	0	569	842	1411	1.480	0.597	0.569	0.566	0.553
15481	14	0.067478913	331	310	641	1.068	0.516	0.489	0.502	0.508
15562	0	0	408	1003	1411	2.458	0.711	0.697	0.677	0.678
15604	0	0	626	785	1411	1.254	0.556	0.515	0.524	0.518
15610	12	0.026163877	405	398	803	1.018	0.504	0.462	0.471	0.488
15611	4	0.002023839	634	618	1252	1.026	0.506	0.506	0.522	0.522
15613	3	0.001651724	654	641	1295	1.020	0.505	0.537	0.514	0.517
15614	0	0	677	734	1411	1.084	0.520	0.492	0.500	0.500
15615	0	0	694	717	1411	1.033	0.508	0.498	0.509	0.500
15619	0	0	704	707	1411	1.004	0.501	0.481	0.488	0.495
15621	3	0.001556877	641	656	1297	1.023	0.506	0.510	0.500	0.531
15623	0	0	563	848	1411	1.506	0.601	0.585	0.576	0.563
15627	0	0	422	989	1411	2.344	0.701	0.658	0.653	0.649
15675	4	0.002770083	620	637	1257	1.027	0.507	0.492	0.483	0.484
15720	4	0.002426681	635	617	1252	1.029	0.507	0.502	0.517	0.517
15744	0	0	622	789	1411	1.268	0.559	0.510	0.530	0.519
15777	0	0	535	876	1411	1.637	0.621	0.587	0.575	0.577
15790	1	0.000645188	693	681	1374	1.018	0.504	0.514	0.502	0.499
15791	0	0	406	1005	1411	2.475	0.712	0.697	0.675	0.651
15867	0	0	628	783	1411	1.247	0.555	0.529	0.488	0.479
15872	5	0.002724422	600	611	1211	1.018	0.505	0.503	0.512	0.504
15876	12	0.025499119	397	418	815	1.053	0.513	0.457	0.518	0.488
15877	11	0.027272727	439	438	877	1.002	0.501	0.487	0.497	0.531
15878	2	0.001185707	672	664	1336	1.012	0.503	0.512	0.489	0.503
15894	7	0.00577369	561	548	1109	1.024	0.506	0.480	0.498	0.526
15908	0	0	458	953	1411	2.081	0.675	0.651	0.651	0.614
15925	0	0	445	966	1411	2.171	0.685	0.664	0.643	0.619
15926	0	0	635	776	1411	1.222	0.550	0.512	0.546	0.551
15962	0	0	422	989	1411	2.344	0.701	0.696	0.670	0.679

ADE_i	iPR	CutValue	high	low	n	I	RG	Accuracy(H2010)	Accuracy(New)	Accuracy(H2010+New)
15963	0	0	499	912	1411	1.828	0.646	0.617	0.589	0.584
15965	5	0.002692258	601	609	1210	1.013	0.503	0.493	0.501	0.524
15967	0	0	592	819	1411	1.383	0.580	0.556	0.554	0.547
15970	4	0.001957631	625	629	1254	1.006	0.502	0.497	0.486	0.497
15972	5	0.003460208	613	594	1207	1.032	0.508	0.525	0.478	0.487
15974	10	0.015140742	476	460	936	1.035	0.509	0.506	0.506	0.497
15984	0	0	451	960	1411	2.129	0.680	0.670	0.654	0.634
15985	0	0	681	730	1411	1.072	0.517	0.498	0.510	0.496
15996	0	0	433	978	1411	2.259	0.693	0.657	0.653	0.661
15999	0	0	647	764	1411	1.181	0.541	0.497	0.502	0.499
16011	0	0	547	864	1411	1.580	0.612	0.577	0.582	0.565
16012	5	0.002317498	597	615	1212	1.030	0.507	0.535	0.509	0.508
16017	0	0	489	922	1411	1.885	0.653	0.623	0.586	0.613
16021	0	0	586	825	1411	1.408	0.585	0.559	0.549	0.534
16052	0	0	490	921	1411	1.880	0.653	0.620	0.604	0.600
16058	0	0	542	869	1411	1.603	0.616	0.576	0.566	0.562
16162	7	0.005552525	554	558	1112	1.007	0.502	0.511	0.505	0.521
16173	0	0	615	796	1411	1.294	0.564	0.551	0.518	0.528
16188	0	0	545	866	1411	1.589	0.614	0.566	0.580	0.561
16189	0	0	498	913	1411	1.833	0.647	0.634	0.594	0.593
16202	0	0	679	732	1411	1.078	0.519	0.524	0.510	0.521
16214	0	0	627	784	1411	1.250	0.556	0.532	0.520	0.515
16229	0	0	539	872	1411	1.618	0.618	0.595	0.544	0.554
16243	0	0	701	710	1411	1.013	0.503	0.507	0.486	0.490
16252	0	0	496	915	1411	1.845	0.648	0.634	0.598	0.608
16326	0	0	521	890	1411	1.708	0.631	0.589	0.598	0.592
16364	0	0	503	908	1411	1.805	0.644	0.604	0.614	0.601
16392	0	0	682	729	1411	1.069	0.517	0.507	0.508	0.497
16434	0	0	520	891	1411	1.713	0.631	0.599	0.594	0.594
16461	0	0	460	951	1411	2.067	0.674	0.653	0.642	0.630
16464	0	0	409	1002	1411	2.450	0.710	0.690	0.673	0.673
16465	0	0	409	1002	1411	2.450	0.710	0.700	0.653	0.663
16466	0	0	450	961	1411	2.136	0.681	0.653	0.641	0.628
16521	0	0	629	782	1411	1.243	0.554	0.546	0.540	0.551
16541	0	0	513	898	1411	1.750	0.636	0.595	0.593	0.580
16578	0	0	435	976	1411	2.244	0.692	0.680	0.664	0.650
16579	0	0	543	868	1411	1.599	0.615	0.589	0.561	0.580
16586	0	0	674	737	1411	1.093	0.522	0.488	0.510	0.509
16592	0	0	585	826	1411	1.412	0.585	0.533	0.544	0.522
16594	10	0.016666667	480	456	936	1.053	0.513	0.456	0.497	0.500
16610	5	0.003330509	601	609	1210	1.013	0.503	0.463	0.507	0.510
16627	0	0	524	887	1411	1.693	0.629	0.609	0.593	0.595
16637	0	0	542	869	1411	1.603	0.616	0.587	0.579	0.575
16677	6	0.003134439	584	577	1161	1.012	0.503	0.503	0.493	0.475
16678	0	0	456	955	1411	2.094	0.677	0.675	0.630	0.655
16689	0	0	470	941	1411	2.002	0.667	0.627	0.645	0.623
16709	0	0	481	930	1411	1.933	0.659	0.641	0.601	0.590
16743	0	0	418	993	1411	2.376	0.704	0.674	0.663	0.671
16745	0	0	676	735	1411	1.087	0.521	0.485	0.483	0.500
16747	0	0	456	955	1411	2.094	0.677	0.663	0.639	0.622
16748	0	0	553	858	1411	1.552	0.608	0.572	0.572	0.549
16749	0	0	411	1000	1411	2.433	0.709	0.697	0.694	0.676
16756	3	0.00184631	648	648	1296	1.000	0.500	0.524	0.478	0.484
16758	5	0.003622368	607	602	1209	1.008	0.502	0.492	0.496	0.493
16777	0	0	536	875	1411	1.632	0.620	0.569	0.573	0.572
16778	0	0	428	983	1411	2.297	0.697	0.677	0.640	0.641
16788	3	0.001468569	652	644	1296	1.012	0.503	0.512	0.520	0.500
16790	0	0	690	721	1411	1.045	0.511	0.473	0.465	0.482

ADE_i	iPR	CutValue	high	low	n	I	RG	Accuracy(H2010)	Accuracy(New)	Accuracy(H2010+New)
16793	3	0.001512859	650	647	1297	1.005	0.501	0.509	0.500	0.490
16804	0	0	446	965	1411	2.164	0.684	0.670	0.649	0.642
16811	0	0	472	939	1411	1.989	0.665	0.629	0.624	0.619
16815	0	0	404	1007	1411	2.493	0.714	0.668	0.658	0.663
16816	0	0	596	815	1411	1.367	0.578	0.556	0.527	0.549
16817	1	0.000719347	682	693	1375	1.016	0.504	0.496	0.505	0.506
16822	0	0	536	875	1411	1.632	0.620	0.571	0.580	0.575
16825	0	0	410	1001	1411	2.441	0.709	0.670	0.679	0.680
16831	0	0	501	910	1411	1.816	0.645	0.644	0.580	0.583
16842	1	0.000579176	686	688	1374	1.003	0.501	0.499	0.506	0.478
16845	0	0	421	990	1411	2.352	0.702	0.688	0.666	0.651
16855	0	0	664	747	1411	1.125	0.529	0.525	0.493	0.513
16857	4	0.002271366	619	637	1256	1.029	0.507	0.513	0.517	0.495
16896	0	0	583	828	1411	1.420	0.587	0.576	0.558	0.553
16940	0	0	450	961	1411	2.136	0.681	0.647	0.642	0.641
16941	0	0	413	998	1411	2.416	0.707	0.689	0.686	0.685
16944	0	0	480	931	1411	1.940	0.660	0.638	0.639	0.640
16987	12	0.021756877	397	419	816	1.055	0.513	0.526	0.517	0.530
17008	7	0.004488158	555	557	1112	1.004	0.501	0.516	0.496	0.497
17064	0	0	525	886	1411	1.688	0.628	0.610	0.571	0.586
17065	0	0	580	831	1411	1.433	0.589	0.560	0.558	0.556
17089	0	0	528	883	1411	1.672	0.626	0.588	0.576	0.580
17091	0	0	497	914	1411	1.839	0.648	0.626	0.610	0.607
17111	0	0	656	755	1411	1.151	0.535	0.519	0.524	0.534
17173	0	0	658	753	1411	1.144	0.534	0.523	0.488	0.503
17198	0	0	538	873	1411	1.623	0.619	0.600	0.585	0.569
17200	0	0	480	931	1411	1.940	0.660	0.650	0.606	0.613
17206	0	0	496	915	1411	1.845	0.648	0.627	0.611	0.609
17217	0	0	522	889	1411	1.703	0.630	0.584	0.593	0.569
17221	7	0.005429167	551	563	1114	1.022	0.505	0.518	0.523	0.495
17227	0	0	607	804	1411	1.325	0.570	0.524	0.535	0.541
17240	0	0	548	863	1411	1.575	0.612	0.593	0.578	0.568
17247	0	0	457	954	1411	2.088	0.676	0.659	0.612	0.607
17258	0	0	415	996	1411	2.400	0.706	0.678	0.663	0.650
17278	3	0.00131585	655	640	1295	1.023	0.506	0.493	0.495	0.510
17292	0	0	618	793	1411	1.283	0.562	0.541	0.531	0.537
17299	2	0.001251854	665	672	1337	1.011	0.503	0.507	0.500	0.506
17333	0	0	567	844	1411	1.489	0.598	0.572	0.545	0.539
17342	0	0	710	701	1411	1.013	0.503	0.501	0.491	0.489
17354	0	0	488	923	1411	1.891	0.654	0.634	0.611	0.606
17363	0	0	483	928	1411	1.921	0.658	0.631	0.622	0.616
17371	0	0	602	809	1411	1.344	0.573	0.557	0.532	0.544
17385	0	0	462	949	1411	2.054	0.673	0.640	0.624	0.621
17394	0	0	599	812	1411	1.356	0.575	0.549	0.530	0.535
17416	0	0	454	957	1411	2.108	0.678	0.674	0.649	0.644
17417	0	0	714	697	1411	1.024	0.506	0.476	0.500	0.521
17426	4	0.002485795	629	625	1254	1.006	0.502	0.506	0.521	0.524
17427	1	0.000603126	687	687	1374	1.000	0.500	0.503	0.477	0.482
17444	0	0	437	974	1411	2.229	0.690	0.685	0.651	0.649
17467	0	0	625	786	1411	1.258	0.557	0.547	0.524	0.533
17469	0	0	676	735	1411	1.087	0.521	0.536	0.495	0.498
17471	1	0.000605329	683	692	1375	1.013	0.503	0.495	0.495	0.513
17475	0	0	424	987	1411	2.328	0.700	0.699	0.637	0.651
17499	5	0.003267292	605	604	1209	1.002	0.500	0.505	0.511	0.517
17500	6	0.003810978	577	586	1163	1.016	0.504	0.483	0.499	0.506
17502	1	0.000620582	679	696	1375	1.025	0.506	0.481	0.492	0.483
17521	10	0.013392424	463	485	948	1.048	0.512	0.527	0.504	0.516
17522	0	0	486	925	1411	1.903	0.656	0.594	0.592	0.590

ADE_i	iPR	CutValue	high	low	n	I	RG	Accuracy(H2010)	Accuracy(New)	Accuracy(H2010+New)
17527	0	0	418	993	1411	2.376	0.704	0.703	0.654	0.678
17560	0	0	478	933	1411	1.952	0.661	0.651	0.626	0.610
17562	0	0	555	856	1411	1.542	0.607	0.578	0.564	0.563
17575	0	0	449	962	1411	2.143	0.682	0.654	0.653	0.634
17576	11	0.01537746	440	434	874	1.014	0.503	0.475	0.482	0.455
17581	1	0.000509672	688	686	1374	1.003	0.501	0.504	0.485	0.515
17593	0	0	454	957	1411	2.108	0.678	0.641	0.635	0.639
17613	0	0	413	998	1411	2.416	0.707	0.685	0.662	0.656
17629	0	0	552	859	1411	1.556	0.609	0.568	0.562	0.557
17632	0	0	423	988	1411	2.336	0.700	0.671	0.639	0.646
17640	0	0	487	924	1411	1.897	0.655	0.637	0.621	0.602
17644	0	0	547	864	1411	1.580	0.612	0.577	0.570	0.568
17656	0	0	423	988	1411	2.336	0.700	0.683	0.654	0.670
17759	0	0	712	699	1411	1.019	0.505	0.495	0.520	0.517
17773	0	0	679	732	1411	1.078	0.519	0.502	0.496	0.493
17777	0	0	491	920	1411	1.874	0.652	0.638	0.612	0.610
17782	4	0.001492686	634	618	1252	1.026	0.506	0.502	0.513	0.498
17785	0	0	476	935	1411	1.964	0.663	0.629	0.605	0.603
17796	0	0	572	839	1411	1.467	0.595	0.549	0.552	0.530
17801	0	0	627	784	1411	1.250	0.556	0.539	0.500	0.494
17826	0	0	573	838	1411	1.462	0.594	0.552	0.520	0.517
17828	0	0	618	793	1411	1.283	0.562	0.505	0.532	0.519
17842	0	0	417	994	1411	2.384	0.704	0.685	0.668	0.662
17843	11	0.019567008	431	454	885	1.053	0.513	0.499	0.516	0.514
17851	0	0	483	928	1411	1.921	0.658	0.653	0.606	0.610
17861	4	0.002733644	629	624	1253	1.008	0.502	0.477	0.493	0.511
17869	0	0	456	955	1411	2.094	0.677	0.656	0.639	0.617
17911	0	0	521	890	1411	1.708	0.631	0.604	0.585	0.590
17928	0	0	456	955	1411	2.094	0.677	0.670	0.667	0.641
17980	3	0.001356834	647	649	1296	1.003	0.501	0.509	0.485	0.477
18017	0	0	413	998	1411	2.416	0.707	0.697	0.673	0.668
18018	0	0	568	843	1411	1.484	0.597	0.576	0.549	0.534
18031	0	0	407	1004	1411	2.467	0.712	0.700	0.669	0.677
18057	0	0	560	851	1411	1.520	0.603	0.543	0.571	0.566
18067	0	0	578	833	1411	1.441	0.590	0.539	0.517	0.510
18069	0	0	672	739	1411	1.100	0.524	0.521	0.529	0.500
18070	0	0	485	926	1411	1.909	0.656	0.635	0.627	0.625
18073	0	0	457	954	1411	2.088	0.676	0.643	0.648	0.644
18075	0	0	502	909	1411	1.811	0.644	0.613	0.608	0.593
18083	0	0	588	823	1411	1.400	0.583	0.533	0.547	0.550
18088	0	0	577	834	1411	1.445	0.591	0.571	0.544	0.532
18119	0	0	689	722	1411	1.048	0.512	0.490	0.503	0.494
18128	0	0	613	798	1411	1.302	0.566	0.525	0.510	0.521
18190	0	0	700	711	1411	1.016	0.504	0.505	0.474	0.480
18217	4	0.002236683	619	637	1256	1.029	0.507	0.533	0.494	0.491
18267	0	0	479	932	1411	1.946	0.661	0.641	0.623	0.607
18268	7	0.004086312	548	568	1116	1.036	0.509	0.546	0.522	0.506
18271	11	0.017290783	434	446	880	1.028	0.507	0.501	0.524	0.500
18300	1	0.000749561	680	695	1375	1.022	0.505	0.516	0.474	0.500
18335	0	0	471	940	1411	1.996	0.666	0.656	0.629	0.629
18354	0	0	411	1000	1411	2.433	0.709	0.681	0.669	0.663
18355	0	0	584	827	1411	1.416	0.586	0.541	0.540	0.548
18379	0	0	495	916	1411	1.851	0.649	0.614	0.598	0.597
18400	0	0	515	896	1411	1.740	0.635	0.607	0.597	0.586
18412	0	0	416	995	1411	2.392	0.705	0.703	0.666	0.675
18439	0	0	476	935	1411	1.964	0.663	0.654	0.603	0.590
18441	0	0	655	756	1411	1.154	0.536	0.503	0.527	0.496
18465	0	0	615	796	1411	1.294	0.564	0.490	0.539	0.535

ADE_i	iPR	CutValue	high	low	n	I	RG	Accuracy(H2010)	Accuracy(New)	Accuracy(H2010+New)
18466	0	0	407	1004	1411	2.467	0.712	0.703	0.671	0.670
18549	0	0	409	1002	1411	2.450	0.710	0.689	0.674	0.658
18565	3	0.001270254	653	642	1295	1.017	0.504	0.483	0.496	0.499
18573	2	0.001129424	675	661	1336	1.021	0.505	0.510	0.461	0.504
18585	0	0	611	800	1411	1.309	0.567	0.510	0.517	0.517
18587	0	0	480	931	1411	1.940	0.660	0.652	0.627	0.638
18591	2	0.001292027	660	677	1337	1.026	0.506	0.514	0.475	0.491
18738	3	0.001783179	643	654	1297	1.017	0.504	0.513	0.480	0.484
18743	3	0.001893082	654	641	1295	1.020	0.505	0.495	0.495	0.484
18754	9	0.013552041	507	490	997	1.035	0.509	0.500	0.521	0.502
18793	0	0	460	951	1411	2.067	0.674	0.658	0.651	0.629
18886	0	0	684	727	1411	1.063	0.515	0.480	0.526	0.490
18965	0	0	527	884	1411	1.677	0.627	0.617	0.594	0.585
18969	9	0.007071083	496	510	1006	1.028	0.507	0.495	0.523	0.489
19027	0	0	473	938	1411	1.983	0.665	0.653	0.628	0.641
19143	0	0	609	802	1411	1.317	0.568	0.532	0.517	0.500
19204	0	0	416	995	1411	2.392	0.705	0.698	0.649	0.639
19211	0	0	431	980	1411	2.274	0.695	0.664	0.653	0.645
19269	0	0	672	739	1411	1.100	0.524	0.495	0.489	0.488
19359	0	0	475	936	1411	1.971	0.663	0.637	0.617	0.602
19371	0	0	497	914	1411	1.839	0.648	0.621	0.585	0.617
19376	0	0	601	810	1411	1.348	0.574	0.539	0.517	0.534
19379	2	0.001251669	667	669	1336	1.003	0.501	0.471	0.480	0.499
19381	2	0.00093067	660	677	1337	1.026	0.506	0.463	0.521	0.523
19384	0	0	662	749	1411	1.131	0.531	0.506	0.481	0.488
19385	0	0	595	816	1411	1.371	0.578	0.522	0.529	0.545
19396	3	0.001583347	652	643	1295	1.014	0.503	0.499	0.505	0.490
19422	5	0.003311258	604	606	1210	1.003	0.501	0.474	0.513	0.504
19487	3	0.001475265	643	654	1297	1.017	0.504	0.499	0.523	0.522
19531	9	0.010883106	502	499	1001	1.006	0.501	0.499	0.491	0.481
19533	5	0.002985911	597	615	1212	1.030	0.507	0.495	0.493	0.484
19542	2	0.001149095	676	660	1336	1.024	0.506	0.482	0.507	0.492
19546	0	0	576	835	1411	1.450	0.592	0.544	0.544	0.527
19550	1	0.000866928	680	695	1375	1.022	0.505	0.507	0.500	0.478
19631	0	0	438	973	1411	2.221	0.690	0.680	0.636	0.646
19660	14	0.058531664	328	318	646	1.031	0.508	0.453	0.467	0.480
19747	0	0	445	966	1411	2.171	0.685	0.672	0.648	0.639
19777	12	0.027902252	399	414	813	1.038	0.509	0.519	0.518	0.477
19780	10	0.015330189	464	484	948	1.043	0.511	0.534	0.531	0.526
19794	0	0	416	995	1411	2.392	0.705	0.681	0.667	0.643
19795	3	0.001577301	649	647	1296	1.003	0.501	0.498	0.498	0.508
19804	8	0.008295876	533	523	1056	1.019	0.505	0.493	0.506	0.505
19805	9	0.007555557	500	501	1001	1.002	0.500	0.495	0.502	0.488
19820	0	0	416	995	1411	2.392	0.705	0.700	0.668	0.669
19836	0	0	529	882	1411	1.667	0.625	0.629	0.595	0.576
19842	0	0	561	850	1411	1.515	0.602	0.580	0.571	0.571
19849	0	0	482	929	1411	1.927	0.658	0.631	0.624	0.610
19854	0	0	550	861	1411	1.565	0.610	0.592	0.570	0.585
19859	0	0	448	963	1411	2.150	0.682	0.650	0.641	0.639
19862	0	0	491	920	1411	1.874	0.652	0.633	0.607	0.598
19866	0	0	436	975	1411	2.236	0.691	0.665	0.650	0.639
19870	0	0	536	875	1411	1.632	0.620	0.614	0.580	0.593
19871	0	0	654	757	1411	1.157	0.536	0.522	0.498	0.490